UNIVERSITÀ DEGLI STUDI DI MILANO

Scuola di dottorato in Scienze Morfologiche, Fisiologiche e dello Sport

DOTTORATO DI RICERCA IN FISIOLOGIA
Settore scientifico/disciplinare: BIO/09
Ciclo XXVI

## Tesi di Dottorato di Ricerca

# Molecular insights in ion access, dependence and selectivity in the NSS/SLC6 transporters KAAT1 and GAT1

Dottorando:

Dott. Giovanola Matteo

Matricola: R09107

Docente guida: Prof.ssa Vellea Franca Sacchi
Tutor scientifico: Dott.ssa Michela Castagna
Dipartimento di Scienze Farmacologiche e Biomolecolari

Coordinatore: Prof. Michele Mazzanti

Anno Accademico 2012-2013

# Index

# Summary

In this thesis we have investigated some aspects of the molecular physiology of the amino acid transporter KAAT1 and of the GABA transporter GAT1 both belonging to the Neurotransmitter:Sodium Symporter (NSS) family. Wild type as well mutants of these proteins were investigated after expression in *Xenopus laevis* oocytes and functionally analyzed by radiochemical and electrophysiological assays.

In the **first chapter** a general overview of the biological importance of membrane proteins is provided jointly to a description of the *Xenopus* oocytes as expression system for this kind of proteins. The second part of the chapter is presenting the general physiological features of KAAT1 and GAT1 while the last part collects information regarding the thermodynamic aspects of secondary active transport as well as the characteristics of the bacterial amino acid transporter LeuT and of the insect dopamine transporter DAT, the two structural models of the NSS family. The last part of the chapter presents one of the most intriguing and cutting edge aspects in the field of membrane transporters: the role of symmetry in the process of ferrying substrates through the lipid bilayer.

In **chapter 2** are reported the results of our investigation of a highly conserved glycine triplet in KAAT1; this sequence is conserved at the Extracellular Loop 1 (EL1) in almost all the members of the NSS family but the data available at the beginning of our research for GAT1 and for the serotonin transporter SERT were not exhaustive and not in full agreement one to each other. We found that in KAAT1 the flexibility that these amino acids provide to the EL1 is of fundamental importance for the cation access to the extracellular vestibule of the protein. The role that we propose could justify the high degree of conservation showed by this stretch of residues in order to allow the driver ion to get access to its binding site.

Different aspects of KAAT1 molecular physiology are addressed in the **chapter 3**. With our experiments we were able to link the potassium selectivity that characterizes KAAT1 to the polarity of Na1 site and to the dimensional flexibility that is provided in Na2 site by a KAAT1 specific residue of glycine. Beside cation selectivity, we explored the weak chloride dependence of KAAT1 providing new evidences of the fact that its interaction with chloride occurs in an almost unique fashion. The analysis of the 3D homology model of KAAT1 allowed us to identify Thr67 as a residue that we proved experimentally to be a key molecular hinge for the coupling mechanism of ion and substrate flux realized by KAAT1. Furthermore this residue is involved in the initial stereochemical selection that the transporter operates on its substrates as well in the chloride dependence of the transport mechanism.

**Chapter 4** will briefly resume some preliminary data concerning the possibility to combine the insect Sf9 cell line from *Spodoptera frugiperda* with the highly efficient Baculovirus expression system with the aim of obtaining the adequate amount of purified protein for KAAT1 crystallization.

The last chapter gathers the results of our analysis regarding the influence of internal chloride in the reverse operational mode of the GABA transporter GAT1. Our results provides a link between the oscillations of the intracellular concentration of this anion with the calcium independent GABA release that is described in different pathological and physiological conditions.

**Key words**
Secondary active transporters; NSS family; structure-function studies; glycine rich domains; ion selectivity; coupling mechanism; reverse transport.

The work presented in this thesis was mainly performed at the

*Laboratory of Membrane Physiology*

Department of Pharmacological and Biomolecular Sciences
Section of Biochemistry, Biophysics, Physiology and Immunopathology
Università degli Studi di Milano
via D. Trentacoste 02, 20138, Milan, Italy.

Electrophysiological and chemiluminescence measurements were carried out in the

*Laboratory of Cellular and Molecular Physiology*

Department of Biotechnology and Life Sciences,
University of Insubria,
Via J.H. Dunant 03, I-21100, Varese, Italy.

As indicated in the text some experiments were conducted in the
laboratory headed by Professor Christine Ziegler at the

*Department of Structural Biology*

Max Planck Institute of Biophysics
Max-von-Laue-Straße 3, D-60438 Frankfürt am Main, Germany.

## List of acronyms and abbreviations used

| | |
|---|---|
| BCCT | Betaine-Carnitine-Choline Transporter (family) |
| Ac- | *Autographa californica* |
| AdiC | Arginine-agmantine antiporter |
| Ae- | *Aedes aegypti* |
| APC | Amino acid-Polyamine-organoCation (family) |
| BAC | Bacterial Artificial Chromosome |
| BetP | Betaine transporter |
| BGT | Betaine and GABA Transporter |
| CAATCH1 | Cation-Anion activated Amino acid Transporter Channel 1 |
| Cc | Carrier closed |
| Ce | Carrier open to external |
| Ci | Carrier open to internal |
| CNS | Central Nervous System |
| CSe | Carrier open to external |
| CSec | Carrier closed to external, substrate bound |
| CSi | Carrier open to internal, substrate bound |
| CSic | Carrier closed to internal, substrate bound |
| CuPh | $Cu(II)(1,10\text{-phenanthroline})_3$ |
| Cy5 | Cymal-5 (5-Cyclohexyl-1-Pentyl-β-D-Maltoside) |
| d.p.i. | Days post infection |
| DABA | Diaminobutyric acid |
| DAT | Dopamine Transporter |
| DDM | n-dodecyl-β-D-maltopyranoside |
| DM | n-decyl-β-D-maltopyranoside |
| DTT | Dithiothreitol |
| EDTA | Ethylenediaminetetraacetic acid |
| EL | External Loop |
| FCS | Fetal calf serum |
| FIRL | Five transmembrane-helix Inverted-topology Repeat, LeuT-like |
| FocA | Formate channel |
| GadC | Glutamate:γ-aminobutyric acid antiporter |
| GAT | GABA transporter |
| Glt | Glutamate transporter |
| h- | Human |
| $K_{50}X$ | Half saturation constant for X |
| KAAT1 | $K^+$-activated amino acid transporter 1 |
| KCC | $K^+/Cl^-$-cotransporter |
| LeuT | Leucine Transporter |
| m- | Mouse |

| | |
|---|---|
| m.o.i. | Multiplicity of infection |
| Mhp | Sodium coupled nucleobase symporter |
| MNPV | Nucleopolyhedrovirus |
| NAT | Nutrient Amino acid transporter |
| NET | Norepinephrine transporter |
| NSS | Neurotransmitter:Sodium Symporter |
| NTT | Neurotransmitter Transporter |
| OB | Occlusion Bodies |
| OG | n-octyl-β-D-glucopyranosyde |
| ORF | Open Reading Frame |
| p.f.u. | Plaque Forming Unit |
| Ph- | *Pyrococcus horikoshii* |
| r- | Rat |
| RT | Room Temperature |
| SDS-PAGE | Sodiumdodecylsulfate-polyacrylamide Gel |
| SERT | Serotonin Transporter |
| Sf | *Spodoptera frugiperda* |
| SGLT | Sodium/Glucose Transporter |
| SLC6 | Solute Carriers 6 |
| SSRI | Selective Serotonin Reuptake Inhibitor |
| $TCID_{50}$ | 50% Tissue Culture Infective Dose |
| TEVC | Two Electrodes Voltage Clamp |
| TM | TransMembrane domain |
| TMA | Tetramethylammonium |
| TnaT | Tryptophan transporter |
| v- | Viral |
| $V_{max\ X}$ | Maximum velocity for the process that involves X |
| WB | Western Blotting |

# Chapter 1
# General introduction

## 1.1 STUDYING STRUCTURE AND FUNCTION OF MEMBRANE PROTEINS

It is currently estimated that around the 30% of the proteome resides in the lipid bilayer that surrounds both cells and organelles. Despite this number justify *per se* the efforts in understanding how membrane proteins work, it is worth noting that the majority of the cellular, tissue, organ and organism functions rely on them. Excluding lipophilic molecule all other kind of substances require proteins to cross the membrane: channels and transporters are the key actors in these processes. Membrane proteins (receptors) are also involved in the ability of the cells "to sense" the intra- and extracellular environment and in their ability to counteract the changes modifying their metabolism. The metabolic reactions are catalyzed by the activity of a lot of enzymes harbored into the plasma membrane as well as in the membrane of highly specialized organelles like mitochondria and chloroplasts. Membrane proteins are of fundamental importance also for the intercellular communication, the keystone of the organization of multicellular organism tissues structure and function. Besides the role of membrane proteins in the Physiology of living beings, due to the over cited functions, the understanding of how membrane proteins work becomes a pillar also for Pathology and Pharmacology: to justify this statement should be enough the consideration that, to date, about the 70% of the commercial available drugs target membrane proteins.

The comprehension at the molecular level of the membrane proteins functional mechanism is the result of synergistic efforts of the application on this topic, but from the two different perspectives of Structural Biology and of Physiology. Since the first atomic determination of the structure of the photosynthetic reaction center in 1985 (Deisenhofer *et al.*, 1985) the number of unique membrane protein structures deposited in the Protein Data Bank increased exponentially (White, 2009) but at the end of 2012 only the 0.22% are membrane proteins. These data underline the most critical step in getting their structure: the difficulty to get a highly amount of stable and purified protein out from the membrane. This is mainly due to their paucity in native tissue and their poor stability outside the lipid environment. Side by side with the originally proposed X-rays crystallography, to by-pass this rate limiting step, during the last three decades, a lot of new structural techniques have been *de novo* developed or applied to the determination of the protein structure (e.g. electron microscopy, Atomic Force Microscopy, Nuclear Magnetic Resonance, lipid cubic phase crystallography). Nowadays most of these techniques are also applied to understand how these molecules work but the approach of classical site directed mutagenesis, jointly to functional assays and to the novelties in the molecular biology field are irreplaceable tools to assign a role to a specific protein structure (Guan and Kaback, 2006). Membrane proteins prediction methods (Punta *et al.*, 2007), jointly to the calculation power of a computer, allowed Bioinformatics to become a pivotal force in this field also thanks to its ability to elaborate predictions on the molecular mechanism of membrane proteins function (Shaikh *et al.*, 2013).

Great results were achieved in the field of Molecular Physiology of membrane proteins exploiting the protein expressed in "lower" organisms (not only bacteria but also small eukaryotic) in which the membrane proteins, despite distantly related to the highly investigated mammalian proteins, "*may have evolved unique features to cope with the diverse environments they encounter*" (Amara, 2007; Penmatsa and Gouaux, 2013).

## 1.2 *Xenopus laevis* OOCYTES

Almost all the experiments presented in this thesis were carried out exploiting *Xenopus* oocytes as expression system, following is a brief description of this versatile system. The expression of KAAT1 in insect cell lines presented in chapter 4 will be introduced by a brief overview also of this system. Some few experiments performed on the glycine betaine transporter BetP were carried out exploiting a particular *E. coli* strain whose properties will be briefly described in the specific chapter (3).

### 1.2.1 General characteristics

*Xenopus laevis* (Daudin, 1802) is a strictly aquatic amphibian native of South Africa with smooth skin and large clawed rear feet (is indeed also known as African clawed frog) that belongs to the *Pipidae* family. Well known as pet, for many years *X. laevis* was used as a living biological assay to establish human pregnancy status, as female *Xenopus* responds to the chorionic gonadotropin, a hormone present in pregnant women urine, by laying eggs. If the female *Xenopus* released eggs two or three days after the urine injection, then it would mean the woman was pregnant. *X. laevis* are nowadays employed in research laboratories for their oocytes, which are used in developmental biology and heterologous expression studies. The *Xenopus* oocytes and eggs can be obtained without difficulty from female animals bred in captivity in the laboratory. Eggs are obtained by deposition (following gonadotropin injection) and oocytes by means of surgery operation. Eggs are naturally deposed in unfavorable environments such as ponds or dead river arms. Probably for this reason, they are resistant cells and thus they can be easily handled in the laboratory without the necessity of a sterile bench as for canonical cell cultures. They are fully provided with all the organelles, nutrients, enzymes, and substrates required in their early stage of development following fertilization, and this total autonomy makes each oocyte an independent factory able to manufacture new proteins (Sigel and Minier, 2005). The oocyte development was divided by Dumont (1972) into six different stages, according to dimensions and pigmentation of the oocyte. In adult female, oogenesis is asynchronous and this means that all the six stages of oocyte development occur at the same time in different ovarian lobes but ovaries of adult frogs mainly contain stage V and VI oocytes (Wagner *et al.*, 2000). In the I stage oocytes have a diameter of about 35-300 µm and are transparent. In the II stage oocytes have a diameter of 300-450 µm and appear opaque, making traditional microscopy more difficult. At the III stage oocytes

have a diameter of 450-600 µm and are characterized by the onset of pigmentation, which gives them a grey color. Pigment is equally distributed in the cortex and stage III oocytes retain a non-polarized appearance. In the IV stage oocytes have a diameter of 600-1000 µm. Stage IV of oogenesis is marked by the onset of visible polarization of the oocyte along the animal-vegetative axis. During this stage, pigment (melanin) becomes unequally distributed between the cortex of the animal and vegetative hemispheres, resulting in the darkly pigmented animal hemisphere and lightly pigmented vegetal hemispheres. During stage V (1.0-1.2 mm of diameter) the animal-vegetative polarity of the oocyte continues to develop and oocytes will undergo meiotic maturation in response to progesterone. The VI stage oocyte has dimension of 1000-1200 µm and is characterized by an equatorial not pigmented band between the two poles. The animal pole contains the nucleus. The ovarian fully grown, stage VI oocyte is arrested in prophase of meiosis I. The cells surrounding the oocyte secrete progesterone, which stimulates the oocyte meiosis and undergo germinal vesicle breakdown, chromosome condensation, and assembly of the meiosis I. After a highly asymmetrical cell division that generates the first polar body, the oocyte enters meiosis II and arrests at metaphase. The meiotic maturation process takes about 5–6 hr after which the mature oocytes are ovulated into the cavity of the frog. From this cavity eggs are laid thanks to the mechanical stimulation of the male on the female abdomen. Subsequent fertilization releases the egg from its metaphase arrest and allows it to complete meiosis II and enter mitosis (Tian *et al.*, 1997). The fully grown stages V or VI oocyte are the preferred cells for expression studies. The VI stage, is the stage in which the frog leaves the eggs in the environment. This is the best moment, especially for transport experiments, as the endogenous transport activity is minimal. The oocyte is surrounded by different layers of cellular and non-cellular material. The plasma membrane of the oocyte is surrounded by the vitelline membrane, which is a non-cellular glycoprotein fibrous layer. Then, there is a layer of follicle cells electrically connected to the oocyte by gap junctions, a connective tissue layer, and an epithelial cell layer relying the ovary wall. This complete structure is called “follicle” (Orsini *et al.*, 2010).

### 1.2.2 *Xenopus* oocytes as expression system: applications, advantages and drawbacks

The oocytes and embryos of *X. laevis* are an interesting model for the study of many developmental mechanisms because of their dimensions thanks to which they can be easily manipulated in experiments. Eggs are obtained in laboratory in a controlled manner by means of injection of chorionic gonadotropin. Embryos develop rapidly after fertilization and a functional tadpole is obtained in a few days. These features made the *X. laevis* a model system for studying the early period of embryonic development. *X. laevis* oocytes are a widely employed system for the expression and functional studies of heterologous proteins demonstrated by Gurdon and coworkers in 1971. The authors found that the microinjection of mRNA coding for the human protein globin into the cytoplasm of the oocyte resulted in the synthesis of human globin. Later on it was shown that injection of the corresponding coding DNA into the nucleus also resulted in the

synthesis of human globin (Mertz and Gurdon, 1977). These studies demonstrated that transcription and translation of foreign genetic information, in this case codifying for cytosolic proteins, could be performed by the *Xenopus* oocyte. Similar results were obtained with membrane proteins. In early '80s Sumikawa and colleagues (Barnard *et al.*, 1982) showed that injection of mRNA coding for nicotinic acetylcholine receptor resulted in the formation of radioactive ligand binding sites in the oocyte surface membrane and that the oocyte plasma membrane acquired novel electrophysiological properties: they showed for the first time that was possible to get the functional expression of a foreign plasma membrane protein in *X. laevis* oocytes also underlying that the surface membrane is relatively poor in endogenous ion channels (Dascal, 1987), a property that makes the oocyte an attractive expression system for ion channels. The possibility to express foreign proteins in the *Xenopus* oocyte allows their functional characterization by means of structure-function studies. Heterologous cRNA can be easily microinjected in the oocyte cytoplasm. In a few days the protein of interest is expressed on the oocyte surface and its function can be studied. Many receptors and transporters were identified by a technique called expression cloning. In this approach a specific function observed in the oocyte, consequent to the injection of a mRNA, leads to the identification of the cRNA coding for the protein responsible for this function (Preston *et al.*, 1992; Castagna *et al.*, 1998; Meleshkevitch *et al.*, 2013). The possibility to inject directly into the cytoplasm of the oocyte the plasmid bearing the cDNA of the protein of interest jointly to the T7 RNA polymerase is another possible way to get, in a shorter way, the expression of the heterologous protein (Altafaj *et al.*, 2006). Expression of a plasma membrane protein in oocytes may also be achieved by the direct injection of the mature protein itself. Microinjection of a membrane preparation containing a receptor of interest, results in the incorporation of the protein into the surface membrane: *X. laevis* oocytes were shown to express native nicotinic acetylcholine receptors after injection with purified *Torpedo* electric plaque membrane vesicles (Marsal *et al.*, 1995). Likewise, injection of *Xenopus* oocytes with rat cortical or nigral synaptosomes resulted in the expression of γ-aminobutyric acid type A receptor-mediated $Cl^-$ currents (Sanna *et al.*, 1996). Recently *Xenopus laevis* oocytes were also successfully used as a source of eukaryotic plasma membrane samples in which, the same membrane as well as the expressed proteins of interest, can be analyzed in physiological like conditions (Fotiadis, 2012; Santacroce *et al.*, 2013). The possibility to exploit oocytes also as expression system for the quantitative purification of proteins was also explored with promising results (Bergeron *et al.*, 2011; Boggavarapu *et al.*, 2013).

Despite the highly controlled conditions in which animals are normally bred, the main drawback of this expression system is the relative seasonal variability of oocyte properties that could affect the expression level of the heterologous proteins expressed. The manual ability required for the surgery operation does normally not require any specific background in veterinarian sciences but is normally acquired by practice. Another relative limitation to the usage of *Xenopus* oocyte is the time consuming procedures normally encountered for the optimization of the common biochemical protocols in respect of

those employed for the common cell lines, as well for the time required for the expression of the protein (days).

## 1.3 THE NEUROTRANSMITTER/SODIUM SYMPORTERS FAMILY

Amino acid transport is of fundamental importance in every cell but in some tissues its significance is more complex than the simple supplying of building metabolites. In CNS it represents the way for the acquiring of neurotransmitter (or their precursors), the way by which they are accumulated into vesicles in the presynaptic terminal but also the system for their rapid wash out from the synaptic cleft after the neurotransmission event. In placenta is realized one of the quantitative highest amount of amino acid transport in human body that is also responsible of the protein production of the fetus. In kidneys and in the intestine the amino acids transport is the source by which the majority of the amino acids of the organism are reabsorbed from glomerular filtrate or absorbed from the food respectively.
The key players in these activities are integral membrane proteins that act as uniporter or cotransporter of amino acids exploiting the free energy coming from the downhill movement of ions ($Na^+$, $K^+$, $H^+$) across cell membrane. In the present thesis is manly investigated the molecular physiology of the insect secondary active transporter of neutral amino acids, the $K^+$-coupled Amino Acid Transporter 1, KAAT1, (Castagna *et al.*, 1998) that belongs to the superfamily of the Neurotransmitter:Sodium Symporters (NSS; also known as SLC6 when referred to human proteins). A chapter is also dedicated to the GABA transporter GAT1 also belonging to NSS family and few experiments were performed on the betaine transporter BetP that belongs to Betaine-Choline-Carnitine Transporter (BCCT) family whose general properties are reported in the same chapter.
NSS transporters represent, along with high affinity glutamate transporters, the major neurotransmitter transporters of the chemical synapses (Kanner and Zomot, 2008). The family groups cotransporters of substrates of different chemical nature that are accumulated against their concentration gradient exploiting the energy coming from the dissipation of a sodium gradient across membrane, but potassium can be exploited as driver by at least two members of the family (Castagna *et al.*, 2009). They are expressed both in prokaryotes (e.g *Aquifex aeolicus*, *Neisseria meningitidis*, *Haemophillus influenzae*, *Symbiobacterium thermophilum*), and in eukaryotes (the homology between the two groups ranges from 20 to 25%) and in the last ones in Vertebrates as well in Invertebrates (e.g *Manduca sexta, Drosophyla melanolaster, Aedes aegypti*). To date no NSS family members were identified in *Fungi* or in *Plantae* kingdoms. In 1990 the first member of the family was cloned from rat brain, the γ-aminobutyric acid (GABA) transporter 1 (Guastella *et al.*, 1990), whose identification opened the route to the identification of similar proteins in other cellular sources. In 2005 a milestone in the this field of research was achieved by Gouaux group who got the first crystal structure of a NSS member, the leucine transporter LeuT, from *Aquifex aeolicus* (Yamashita *et al.*,

2005). Late in 2013, the same group again pushed ahead our comprehension of the molecular physiology of NSS carriers publishing the first crystal structure of an eukaryotic transporter, the dopamine transporter ($DAT_{cryst}$) from *Drosophila melanogaster*, in complex with an antidepressant molecule and with sodium and chloride ions (Penmatsa *et al.*, 2013).

Sequence analysis showed that the highest degree of conservation is localized in TM1 and in TM4-8 while the highest variability is showed by N- and C-ends; four different glycosylation sites have been identified mainly localized in the External Loop 2 (EL2). Transport stoichiometry ranging from 1:1:1 to 1:2:1 or 3:1:1 respectively for organic substrate:Na:Cl. Originally classified as all chloride dependent, is now known that the dependence from this anion is ranging from the almost complete dependence of some transporters (typically eukaryotic ones), to the absent (for all bacterial members) passing through the weak dependence of some eukaryotic proteins (Broer, 2006; Bette *et al.*, 2008; Meleshkevitch *et al.*, 2013). LeuT, as other bacterial members of the family, shows a completely chloride independent activity thus in its structure was not possible the identification of the binding site for this anion whose site was identified in GABA and serotonin transporters some years after its crystallization (Forrest *et al.*, 2007; Zomot *et al.*, 2007). The chloride binding site is now described also from a structural point of view thanks to the crystal structure of a LeuT mutant (Kantcheva *et al.*, 2013) and much better thanks to $DAT_{cryst}$ structure (Penmatsa *et al.*, 2013) (see later chapter 3 for details). Transport is electrogenic for many members of the family and, apart from the classical transport associated currents, transient and leaky currents are also described in absence of organic transportable substrates. The molecular mechanism underlying these currents has not been fully elucidated yet but theoretical models are trying to explain them with conformational changes or with the entry of ions in the electric field of the plasma membrane (Peres *et al.*, 2004). Objections to these models also exist and rely on the observation that these currents could exist only in heterologous systems in which the proteins are overexpressed being absent *in vivo* conditions in which, so far, a clear evidence of their existence has not been gathered yet. Immediately after the first formulation of the concept of secondary active transport was clear that for the substrates the access to the transporter is never possible from both side of the membrane at the same time, but occurs alternatively from the extracellular or from intracellular side: this differentiates a transporter from a channel. NSS transporters follow this general rule and thanks to the increased results in crystallography, jointly to extensive bioinformatic analysis, in the past decade, the molecular details of this mechanism have been partially unveiled (Boudker and Verdon, 2010; Forrest, 2013). A common architectural organization, particularly in secondary active transporters, is the presence of an internal pseudo-symmetry of transmembrane domains that are organized in a mobile bundle whose structural existence was originally found in LeuT crystal structure (Yamashita *et al.*, 2005) and now confirmed also for eukaryotic members of the family (Forrest *et al.*, 2008; Penmatsa *et al.*, 2013). Based on substrate preference and on sequence homology, different subfamilies can be defined into NSS family; first of all it was defined the

subfamily of the biogenic amines transporters (dopamine, serotonin and noradrenaline), then the group of protein that are related to the GABA transporter GAT1 that comprises, beside all GABA transporters, proteins for the transport of taurine, choline, creatine, proline and glycine. Some proteins still need to be characterized but, among the most recently deorphanized carriers, of particular interest are B(0)AT (SLC6A15) expressed in human brain, NTT5 (SLC6A16) expressed in pancreas, lungs, prostate and testis (Broer, 2006) and the first eukaryotic methionine selective transporter AeNAT5 (Meleshkevitch *et al.*, 2013). Alteration of these proteins were found in many pathological conditions such as epilepsy (Richerson and Wu, 2004), schizophrenia, depression (Hahn and Blakely, 2002), obsessive compulsive disorder (Ozaki *et al.*, 2003), autism (Sutcliffe *et al.*, 2005), anxiety, anorexia, Parkinson disease, orthostatic intolerance (Shannon *et al.*, 2000), blindness due to retinal degeneration (Heller-Stilb *et al.*, 2002), cardiomyopathy, muscle-skeletal disorders, X-linked creatinine deficiency (Salomons *et al.*, 2001) and in abnormalities in kidney development. The very wide range of pathologies is the direct consequence of their wide distribution in different kind of tissues (Broer, 2006; Hahn and Blakely, 2007; Broer, 2013). Numerous drugs target NSS transporters: psychostimulants like cocaine, amphetamine and MDMA (also known as ecstasy), but also tricyclic (amitriptyline, imipramine) and heterocyclic antidepressants (desipramine, viloxazine), dopaminergic antidepressant like amineptine and Selective Serotonin Reuptake Inhibitors (SSRI) like the best seller Prozac (Fluoxetin). Antiepileptic drugs, like tiagabine, also target these proteins.

### 1.3.1 KAAT1 ($K^+$-coupled Amino Acid Transporter 1)

The main part of this thesis is regarding structure-function studies on the insect NSS transporter KAAT1 that has been exploited since its cloning, in 1998, as a tool for these kind of researches due to its almost unique physiological properties (Castagna *et al.*, 2009). It was cloned from the lepidopteran larvae *Manduca sexta* (in literature, sometimes, has also been reported as msKAAT1) where it is expressed in salivary glands and in the columnar absorptive cells of the midgut, a tissue, this last one, where potassium can move from the lumen of the organ into the cells according to its electrochemical gradient (Giordana *et al.*, 1982; Castagna *et al.*, 1998). It is composed of 634 amino acids organized in 12 TMs for 60 KDa of molecular weight; it shares a mean sequence identity with the other members of the family of about the 35%. By Fluorescent Resonance Energy Transfer (FRET) experiments was demonstrated its constitutive organization in membrane as dimers with a supramolecular organization in tetramers (or dimers of dimers); (Bossi *et al.*, 2007) retaining the functional unit only in the single monomer as also proved for many other members of NSS family (Kilic and Rudnick, 2000; Schmid *et al.*, 2001a; Schmid *et al.*, 2001b; Sorkina *et al.*, 2003; Soragna *et al.*, 2005; Mari *et al.*, 2006; Yamashita *et al.*, 2005; Bossi *et al.*, 2007). Interestingly the $DAT_{cryst}$ was found instead be monomeric both in crystal lattice and in detergent micelles (Penmatsa *et al.*, 2013). KAAT1 realizes the cotransport of neutral amino acids with both branched and

not branched side chain in adding to glycine. The stereoselectivity for L-amino acids is not fully being also able to realize the uptake of D stereoisomers. It is able to exploit as driver ion not only sodium but also potassium and, even to a lesser extent, lithium (Castagna *et al.*, 1998; Bossi *et al.*, 1999a). From the alkaline group of metal it does not accept rubidium as driver but, *in vivo,* potassium is the main ion exploited. This kind of coupling properties has rendered its cloning a turning point in the field of secondary active transport because, until then, only sodium or proton coupling mechanisms had been described. When $Na^+$ is the driver ion, threonine is the preferred substrate and then proline, methionine and leucine with this order of preference, while when the driver is $K^+$ leucine is the preferred one. The wide spectrum of transportable substrates matches the behavior of most intestinal transporters and reflects the functional role of this protein in the context in which it is expressed: in the gut its main role is to uptake as much as possible metabolites from the lumen that is, due to the vegetarian diet of the animal, normally low in amino acids and sodium content. In this scenario, the change of substrate preference according to the different driver ion suggests that the coupling properties are not due to a low ion selectivity being the protein able to modify its behavior according to a different cation. Differently from other eukaryotic NSS transporters (especially neuronal proteins) KAAT1 activity is only weakly chloride dependent (Bette *et al.*, 2008): in absence of chloride the activity is not abolished but reduced of about the 45%. The $Na^+/K^+$ selectivity is influenced by the membrane voltage, it increases with the hyperpolarization and it is particularly high *in vivo* where the voltage can reach -240 mV. Transport stoichiometry is of 2:1:1 ($K^+$ or $Na^+$:$Cl^-$:aa), the activity is influenced by the pH and the maximal level is reached in alkaline conditions (pH=10), a condition in which amino and carboxyl groups of the substrate leucine are both deprotonated (Peres and Bossi, 2000; Vincenti *et al.*, 2000). These conditions reflect those are found in the midgut of the lepidopteran larvae: in the gut of this species a peculiar tissue organization is described in which the functional absorptive unit is composed of two kind of cells, the columnar absorptive cells with their classical brush border, and the goblet cells. One of the most important characteristic of this kind of cells is the absence of the Na/K ATPase that is replaced by a V-ATPase that pumps protons to the lumen of the midgut directly in the goblet cell cavity. The activity of this pump generates a proton gradient toward the lumen and decreases the membrane voltage exporting positive charges: these cells is indeed normally deeply hyperpolarized (-240 mV) in respect of a common intestinal mammalian cell. This difference in the electric potential across the apical mucosal barrier is the main force that energizes the uptake of solutes in absorptive cells. The number of protons that are moved by the pump activity is quite low but the electric gradient is kept so big being the membrane characterized by an efficient electrical resistance which opposes the leakage of charges. In goblet cells, jointly to proton pumps, is highly expressed a $K^+/2H^+$ antiporter that, exploiting the favorable electric conditions, exports potassium recycling protons from the lumen where the pH reaches the 10.5 units. Cell membrane of columnar cells does not have a high electrical resistance as that of goblet cells and, despite are electrical connected by gap junctions, they allow the spillage of

alkaline anions drawn by the electric potential as well by the protons secreted into the lumen of the midgut. KAAT1 is expressed in the columnar absorptive cells where it imports neutral amino acids exploiting the potassium gradient; this underlies the important role of goblet cells in preparing the optimal conditions for the maximization of the amino acids uptake (see scheme in figure 1).

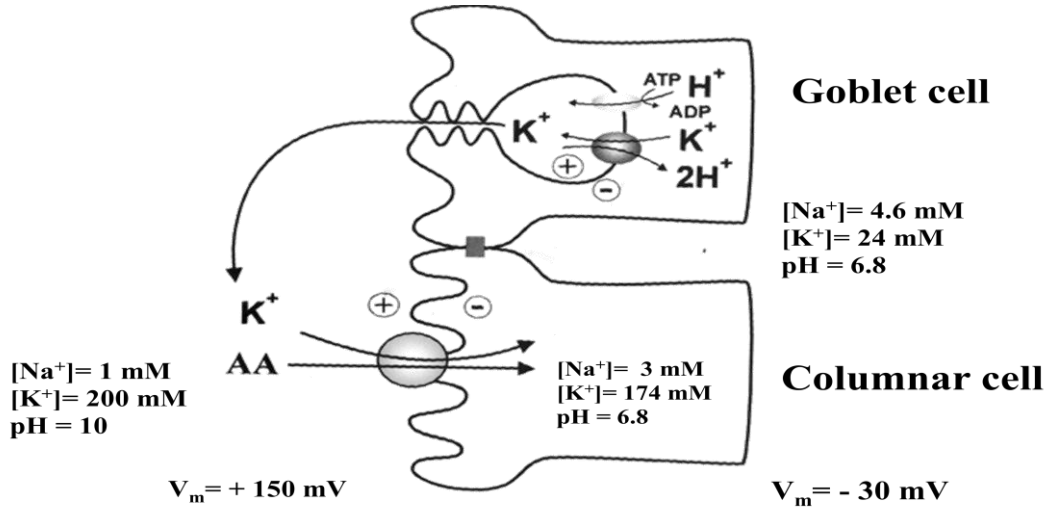


**Fig. 1** *Absorptive functional unit of Manduca sexta larvae midgut.* The goblet cell express a V-ATPase that pumps protons into the lumen and an $H^+/K^+$ antiport that exports potassium ions in the same direction. KAAT1 is expressed in the columnar absorptive cells where, exploiting the potassium gradient and driven by electrical gradient, it imports amino acids into the cell. Modified from (Castagna *et al.*, 1998).

Interestingly the affinity for sodium is 5 times higher than that of potassium (Castagna *et al.*, 1998): this seems in apparent discrepancy with the observation that KAAT1 exploits potassium in the preference of sodium as driver ion. As mentioned, the intestinal $Na^+/K^+$ ratio is extremely low (also due to the strictly phytophagus diet of the animal) and in this environment the high affinity for sodium of KAAT1 allows this transporter to function also as a sodium detector evolved to work in a context where the concentration of the ion is normally very low. The transport activity is electrogenic: beside the classical transport associate currents, it shows pre-steady state currents (also known as transient currents) and leaky currents. The amplitude of the transport associated currents is influenced both by the driver ion and by the transported amino acid (Castagna *et al.*, 1998; Liu *et al.*, 2003; Mari *et al.*, 2004; Miszner *et al.*, 2007): proline, for instance, is transportable only when the membrane is highly hyperpolarized like it has been found *in vivo* (Harvey and Wieczorek, 1997). The uncoupled currents are, as well as in other members of the family (Mager *et al.*, 1993; Mager *et al.*, 1996), particularly big and show a cation selectivity sequence of $Li^+ > Na^+ > K^+ \approx Rb^+ \approx Cs^+$ indicating that these ions interact with the protein in a specific cation binding site (Bossi *et al.*, 1999a).

KAAT1 shows the 90% of identity with the Cation-anion Activated Amino acid Channel Transporter 1, CAATCH1; (Feldman *et al.*, 2000) that is also expressed in the columnar cells of *Manduda sexta* midgut. From brush border intestinal mucosa and from brain of *Drosophila melanogaster* it has been cloned the DmNAT transporter that shows the 50%

of amino acid identity with KAAT1 and it transports mainly L-neutral amino acids with substituted lateral chain including D-isomers (Miller *et al.*, 2008). In the silkworm *Bombyx mori* an ORF has been identified coding for an intestinal amino acids transporter with a sequence identity of 60% in respect of KAAT1 that was found be responsible for the susceptibility to the *Parvovirus* like viruses that afflict this kind of insects (Ito *et al.*, 2008).

### 1.3.2 The GABA transporter GAT1

The γ-amino-butyric acid is the major inhibitory neurotransmitter in the CNS. The effect of the neurotransmitter is terminated exclusively by the activity of the neuronal and glial GABA transporters that represent the only way by which the molecule is quickly removed from the synaptic cleft. Four different GABA transporters belonging to NSS family have been cloned from mouse (mGAT1-4) and only three from rat (rGAT-1-3). mGAT2 corresponds to the GABA and betaine transporter, originally identified in dog, BGT1. In humans, so far, the homologous of rGAT-1 (hGAT1; SLC6A1), rGAT-3 (hGAT3) and of rBGT (hBGT; (Liu *et al.*, 1993; Clark and Amara, 1994) have been characterized. rGAT3 (homologous of mGAT4) is abundantly expressed in retina, but also in olfactory bulb, in hypothalamus, in medial thalamus and in the brainstem; the expression is relative low in neocortex and in hippocampus. rGAT-2 (mGAT3 homolog) (Borden *et al.*, 1992; Lopez-Corcuera *et al.*, 1992) is expressed only in pia mater and arachnoid membrane and the mRNA for betaine and GABA transporter is localized not only in CNS but also in renal tubules. GAT1 (Kanner, 2006; Kanner *et al.*, 2008) was the first member of NSS family to be cloned, firstly in rat and then in human, and is the functional prototype of the family (Guastella *et al.*, 1990; Nelson *et al.*, 1990). A chapter of this thesis is dedicated to the role of chloride in the reverse operational mode of this NSS transporter (see chapter 5). It is composed of 12 putative transmembrane domains with both intracellular N- and C- termini. Four glycosylation sites were identified in the EL2 whose role was assayed by mutagenesis evidencing the role of sugar residues in GABA transport (Liu *et al.*, 1998; Cai *et al.*, 2005). GAT1 is composed of 599 amino acids (69 kDa); the expression range comprises retina, whole brain and spinal cord with the highest levels of expression in olfactory bulb, neocortex, hippocampus and in cerebellar cortex with the exception of the GABAergic Purkinje cells that express the transporter only transiently during development (Itouji *et al.*, 1996; Yan and Ribak, 1998). The expression is not only restricted to presynaptic GABAergic neurons but also on postsynaptic glutammatergic neurons (dendrites of pyramidal neurons) and in astrocytes of rat cerebellar cortex (Augood *et al.*, 1995; Conti *et al.*, 2004). The transporter is strictly sodium and chloride dependent with a very highly turnover number (Wu *et al.*, 2006) and a local area expression of 800-1300 proteins/$\mu m^2$ in hippocampal and cerebellar interneurons (Chiu *et al.*, 2002). The membrane expression is regulated by protein kinase C (Beckman *et al.*, 1999; Quick *et al.*, 2004) that promotes its internalization, while extracellular calcium depletion or incubation with a selective and competitive inhibitor (SKF89976A) reduces

the number of GAT1 molecules available from vesicular recycling pool (Wang and Quick, 2005) but the application of extracellular GABA promotes the insertion of the molecules in membrane reducing the internalization rate. Syntaxin-1A (Wang *et al.*, 2003) is a well-known negative regulator of transport activity even though is able also to enhance the level of the expression of the same protein (Horton and Quick, 2001). The phosphorylation of some serine residues is another deeply investigated regulation way of GAT1 activity (Hu and Quick, 2008) as well as its internalization mechanism that is clathrin dependent (Deken *et al.*, 2003). As described for KAAT1, it is organized in oligomeric structure in membrane but the monomer is the minimal functional unit (Scholze *et al.*, 2002; Mari *et al.*, 2006;). As will be later discussed in major details in chapter 5, in some pathophysiological conditions the presence of specific ionic gradients could activate the transporter in the so called "reverse mode" promoting a calcium independent GABA release through GAT1 itself (Sitte *et al.*, 2002; Richerson and Wu, 2003; Wang *et al.*, 2005; Wu *et al.*, 2007). At physiological pH conditions, GABA is a zwitterionic molecule and for each transport cycle, its uptake is coupled with the transport of two sodium and one chloride ions (Mager *et al.*, 1993) rendering the mechanism electrogenic. Beside transport associated currents, transport-dependent uncoupled, leaky and transient currents have also been described (Mager *et al.*, 1993). Still open is the debate about the activation of GAT1 in the "channel mode" (Cammack *et al.*, 1994; Cammack and Schwartz, 1996; Risso *et al.*, 1996; Hilgemann and Lu, 1999; Lu and Hilgemann, 1999b). GAT1 shares with other member of the NSS family the characteristic to be permeable to water when challenged by an osmotic gradient. *Xenopus laevis* oocytes expressing GAT1 show a permeability coefficient significantly higher than those not expressing the protein and, as expected for all osmotic phenomena, the permeability coefficient is not modified by the osmotic gradient. The water movement occurs directly through the protein as proved by the ability of selective inhibitors of GABA uptake to completely abolish the water flux (Loo *et al.*, 1999; Santacroce *et al.*, 2010). The GAT1 knock-out mouse is characterized by tremors, ataxia and pathological anxiety (Chiu *et al.*, 2005). Despite 2,4-diamminobutyric (DABA) and nipecotic acid as well β-alanine inhibit the neuronal and glial GABA reuptake eliciting antiepileptic activity in different animal models, no one of these molecules is directly used in clinical protocols but some of their derivatives, like tiagabine, are now used for the treatment of some epileptic disorders.

## 1.4 MOLECULAR PHYSIOLOGY OF SECONDARY ACTIVE TRANSPORTERS

### 1.4.1 Thermodynamic aspects of the transport function in membrane proteins

The alternating access model for secondary active transporters postulates that the binding site/s for both the main substrate and driver are never accessible from the two side of the membrane at the same time (Mitchell, 1957; Jardetzky, 1966). Nowadays to this general,

and still true definition, more detailed structural and functional information have contributed to the molecular description of this mechanism highlighting also a common evolutionary functional scheme for proteins belonging to distant unrelated families (Forrest *et al.*, 2011).

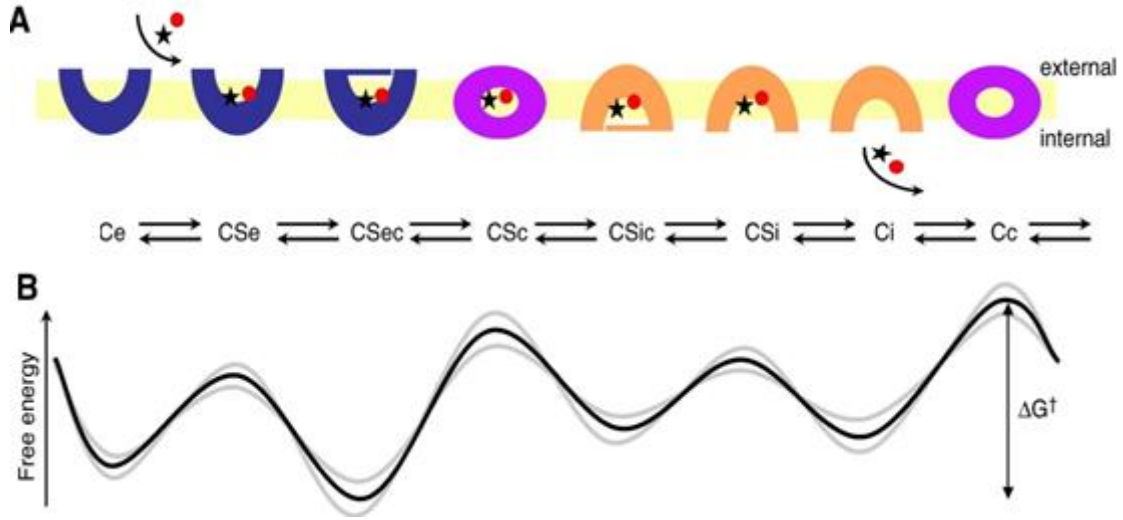


**Fig. 2** Legend: (**A**), star, red circle: substrates; Ce: externally open carrier conformation; CSe: transient substrate-bound state; CSec: occluded substrate-bound state still facing the external side of the membrane; CSic: inward-facing, occluded substrate-bound state; CSc: fully occluded, probably transient, substrate-bound intermediate state; CSi: transient substrate-bound inward-facing open conformation; Ci: inward open state; Ce: outward open state Cc: fully occluded, intermediate state Cc (for symport). (**B**), Theoretical energy profile (black) of different carrier states during catalysis, indicating minima at the gated substrate-bound states, and a putative rate-limiting barrier for the re-conversion of the empty carrier. Modified from (Forrest *et al.*, 2008).

As well for an enzyme catalyzed reaction, despite less evident, even secondary transporters rely on the thermodynamic laws that dictate the proceeding, step by step, of the transport process. What drives the process is the difference in Gibbs's free energy (ΔG) that characterizes each single step of the translocation mechanism as well as the overall ΔG of the entire process. Transporters cannot go against Thermodynamic consequently this difference must be kept negative. For a uniporter the energy liberation comes from the dissipation of the (electro)chemical gradient of the moved substrate itself. When this movement is instead endergonic, like for any uphill mechanism of transport, the coupling of the substrate flow must be coupled with the downhill movement of other ions or molecules (secondary transport) or to the hydrolysis of ATP molecules (primary active transport). Despite the differences that evolution determined in each kind of secondary transporter, the gathering of an increasing number of 3D structures, especially of bacterial proteins, showed that the alternating access model is not only shared in terms of the biochemistry of the process but is also "structurally architected". This similarity is deeply related to the internal symmetry (see next paragraph) found in the structures of these proteins that does not emerge by the simple primary sequences comparison. This internal symmetry is now proved to be the base of the molecular mechanism of membrane transporters (Forrest and Rudnick, 2009) that, jointly to numerous

biochemical and biophysical evidences, is now leading the scientific community to elaborate new common transport mechanism (Schweikhard and Ziegler, 2012) for secondary active transporters as well as a redesigned evolutionary tree for membrane proteins in which until now evolutionary distant membrane proteins, could be relocated in new common branches.

Following is the description of an attempt to generalize thermodynamic concepts of secondary transport mechanism well reviewed by Forrest *et al.* in 2011. In this analysis a prototypical series of conformational states that should characterize a transport cycle for a secondary transporter was depicted in a way that "*differentiate between substrate (or substrates) bound to an open (CSe and CSi) and an occluded form of the carrier (CSce, CSc, and CSci)*" (Fig. 2). If the carrier transports only one molecule at a time the conversion from CSec to CSic can happen in the empty form (Ci → Ce) if the protein is an uniporter, or by the involvement of a second substrate if the protein works by an antiport mechanism. For a symporter, considering the steps for co-substrate interaction and release, three other states were proposed despite the relative difficulties in their observation and analysis due to their fast transition during the transport cycle, especially CSe and CSi. The fully occluded state Csc could exist at least for some transporters.

The gates of the protein are primary actors in the molecular mechanism of carriers but the term "gate" could be referred to different concepts. First, gate (*thin* gate) is defined as the fine structure (even a single amino acid residue) that, regulating the access of the substrate/s to the binding site/s, does not direct take part to the substrate movement but the concept could has been also referred to a hole protein portion that undergoes conformational changes to allow the substrate/s movements (sometimes indicated as *thick* gate). Referring to figure 2 the thin gate act in the step between CSe and CSec and between CSi and CSic while the thick gate is responsible of the CSec to CSic conversion through the transient CSc state. Despite carriers does not covalently bind or modify substrates like enzymes usually do, the authors have elaborated the kinetic profile of the transport process taking lesson from Enzymology. When the substrate binds to the carrier the free Gibbs energy consequently released is the thermodynamic payment for the following energy demanding required to avoid, during the translocation path, low- or high-energy states (Jencks, 1989; Klingenberg, 2005) that could trap the protein in stable conformations. From this point of view the role of a gate (internal or external) is to void the kinetic equilibration between free and bound substrates. As for enzymes the binding site in the two empty conformations (Ce and Ci) does not form a perfect interaction with their substrates rendering impossible the exploitation of the free energy coming from binding. After substrate binding the protein undergoes conformational changes that could be view as a sort of preparing step in which the energy is stored in the form of conformational changes lowering the energy of the transition state. In the transition state (CSc, the occluded state) the optimal fitting is achieved but in contrast to enzymes catalysis no one chemical modification to the substrate occur. This mechanism allows the ferrying of substrates from the external, via the occluded, to the internal conformational states: the entire cycle is energized by the energy coming from "*the sequence of*

*conformational events in which the transport protein changes, upon substrate binding, between states of limited interaction with the substrate and the transition state characterized by an intimate substrate-protein interaction*" (induced transition fit mechanism; (Jencks, 1989)). According to this model a good substrate for the carrier would be that one that promotes the maximum release of energy from the generation of the occluded states. The empty carrier states are the firsts that interact with substrates but, assuming this model, is not this interaction that discriminate between "good" and "bad" substrates. In other terms, thermodynamically, is the $V_{max}$ of the protein that define its specificity rather the half-saturation constant ($K_m$); (Krupka, 1989). The foregoing also imply that an inhibitor could act on the carrier activity even if it is not structurally related to the substrate just by trapping the empty states in an energetic minimum of the energetic profile.

### 1.4.2 The structural NSS family models LeuT and DATcryst

As introduced two are the structural models of the family: the bacterial amino acid transporter LeuT (Yamashita *et al.*, 2005) and the insect dopamine transporter $DAT_{cryst}$ (Penmatsa *et al.*, 2013). Being LeuT investigated since its crystallization in 2005 the majority of information available are from different crystal structures of this bacterial transporter but the obtaining of $DAT_{cryst}$ created a new starting point being the protein from an eukaryotic source. Following is a description of the molecular physiology of LeuT and a comparison with $DAT_{cryst}$ from a structural point of view. LeuT is expressed in the prokaryotic *Aquifex aeolicus*; reconstituted in liposomes it induces a leucine uptake but is also documented its ability to transport alanine with a higher capacity than for leucine ($V_{maxLeu}$ = 343, $K_{50Leu}$ = 25 nM, $K_{50Ala}$ = 583 nM, $V_{maxAla}$ = 1730 pmol/min/mg). It transports also L-glycine, L-methionine and L-tyrosine but, to date, the preferred substrate *in vivo* is not known (Singh *et al.*, 2008). As all NSS member hydropathy models predicted before its crystallization, it is composed of 12 TMs with an α–helix topology. TM1 and 6 are the most conserved in respect to other NSS proteins and they show an interruption of the α-helix topology in the middle of the bilayer. The unwound region is bigger in TM6 with the residues of Ser256 and Gly260 that seems to act as hinges for the two part of the transmembrane domain (TM6 a/b). In crystallization cell LeuT is a dimer: the interface between the two units is partially composed by the External Loop 2 (EL2) and TM9 with TM11 and 12 that, together with the corresponding in the other monomer, create a four helix bundle. In the solved structure of the transporter was found an internal organization based on symmetry whose description and importance is highlighted in the next paragraph. $DAT_{cryst}$ was crystallized bound to the tricyclic antidepressant nortryptiline with two sodium and one chloride ions in an outward-open conformation (Cse; refers to Fig. 2). The core structure resembles that of LeuT but interesting differences were found in the periphery of the protein that could be linked to different aspects of neurotransmitter transport as well to the eukaryotic membrane localization of the protein. A sort of a kink was found in the middle of TM12, centered

on Pro572, that causes a distortion of the second half part of the transmembrane domain that is bent away from the transporter. Moreover, a latch-like domain in the C-terminus of the protein was found to cap the internal gate and a molecule of cholesterol was found wedged in a pocket bordered by TMs 1a, 5 and 7. The role of this lipid in the function of mammalian ortholog of DAT was already described (Hong and Amara, 2010) and the structure describes how this lipid acts as a stabilizer of the outward-open conformation of the transporter. Other structural aspects differentiate the two transporters that are linked to the post translational modifications that occurs only in eukaryotic organism: the presence of a disulfide bond connecting Cys148 and Cys157 in the EL2 and the glycosylation sites in the already known positions in the EL2 (Li *et al.*, 2004).

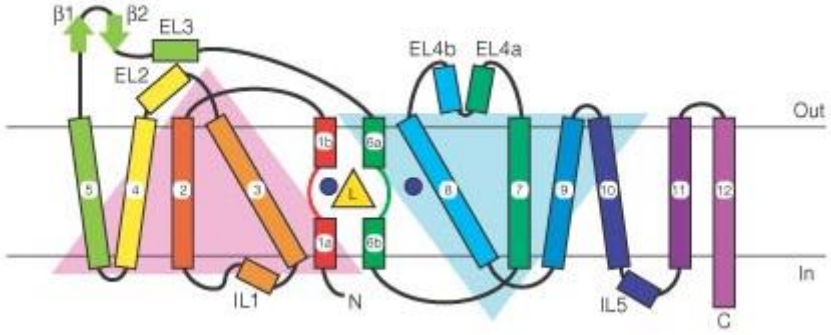


**Fig. 3** *LeuT topology*. The positions of leucine and the two sodium ions are depicted as a yellow triangle and blue circles, respectively. From (Yamashita *et al.*, 2005).

In the original structure LeuT (PDB access code 2A65) was crystallized in the closed outward facing conformation (CSce; see figure 2) with one leucine molecule and two sodium ions bound. Tyr108 and Phe253 keep the substrate and ion binding sites separated from the extracellular environment and, together with Arg30, Asp404 and part of the EL4, were proposed to create the extracellular gate. When crystallized in complex with tryptophan that acts as a competitive inhibitor of the transport, LeuT is locked in an open-to-out conformation (Singh *et al.*, 2008). This last one resulted from an outward rotation of TMs 1b and 6a, EL4 and from an increased distance between the residue Tyr108 and Phe253: all these movements widen the extracellular vestibule (a sort of foyer of the transporter in which substrates get access before reaching the binding sites) and increase the solvent accessibility to the substrates binding sites. The internal gate was proposed as the results of the dynamic interaction of Arg5 from TM1 and Asp368 of TM8 that, generating a salt bridge, hinders the substrate release jointly to the bulk action of some aromatic residues, namely Trp8, Tyr265, Tyr268 and Ser267. The primary binding site as well the residues forming the gates are conserved in $DAT_{cryst}$ in the corresponding position to those identified in LeuT. Several LeuT complexes were solved with tricyclic antidepressant, Selective Serotonin Reuptake Inhibitors and with octylglucosyde detergent: for all of them a non-competitive inhibition was proposed (Singh *et al.*, 2007; Zhou *et al.*, 2007; Quick *et al.*, 2009; Zhou *et al.*, 2009). The behavior of these drugs is different from that one exerted on mammalian biogenic amine

transporters rendering the LeuT model not exploitable for a direct pharmacological analysis. This problem has been overcome thanks to the recent synthesis of a LeuT mutant engineered to have the same pharmacological profile of mammalian proteins but with the possibility to be easily crystallized like bacterial transporters (Wang *et al.*, 2013). All these ligands were found to block the transport cycle by stabilizing the transporter in an open-to-out conformation that is also the conformation of $DAT_{cryst}$: the antidepressant molecules trap the transporter in this conformation getting access to the primary binding site of the transporter but preventing the closing of the extracellular gates (this is the first direct confirmation of this mechanism of action for the antidepressant drugs that find in DAT their target). In LeuT substrate binding site the α-amino and carboxyl groups interact with the phenolic OH group of Tyr108, one sodium ion (from Na1 site) and with amino acid residues from the unwound regions of TM1 and TM6. The stabilization of the substrate occurs via hydrogen bonds with the backbone of TM1 and 6 and with the end of the α-helices of the same transmembrane domains. The lipophilic side chain of leucine is accommodated into a nonpolar cavity lined by the side chains of residues from TM3, 6 and 8 (Fig. 4). This binding site is known as S1 site whose position and role is universally accepted for all NSS members. Beside this site a second substrate binding site (S2) has been proposed in the extracellular vestibule as a key regulator site that, once bound the substrate, would trigger the release of the substrate from the intracellular side of the membrane. A lot of confirmations as well as denials raised in recent years about this aspect and, to date, the role (and even the existence) of S2 site is still under debate (Shi *et al.*, 2008; Quick *et al.*, 2009; Piscitelli *et al.*, 2010; Reyes and Tavoulari, 2011; Quick *et al.*, 2012). Na1 site in LeuT structure hosts the sodium ion that is also coordinated by the organic substrate, specifically by its carboxyl group. Na2 is less conserved among NSS members but is highly conserved, from a structural point of view, in the FIRL fold family (Khafizov *et al.*, 2012) (see next paragraph for details). Ion binding sites are conserved in the corresponding positions also in $DAT_{cryst}$ but a fully description of them will be later provided in chapter 3 (Fig. 5).

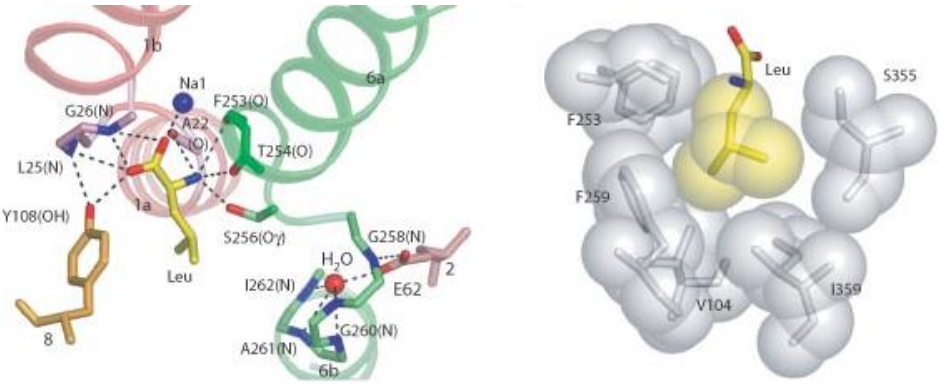


**Fig. 4** *Leucine binding pocket in LeuT* (access code: 2A65) **Left**: hydrogen bonds and ionic interactions in the leucine binding pocket. **Right**: hydrophobic interactions between the leucine and $LeuT_{Aa}$. Van der Waals surfaces for the leucine side chain and interacting residues are shown as spheres (Y108 and S256 are omitted). From (Yamashita *et al.*, 2005).

Yamashita and coworkers in 2005 proposed that sodium binds first Na1 site before substrate binds its own site (Yamashita *et al.*, 2005). Accordingly in a LeuT $Na^+$-bound substrate free crystal structure the thin extracellular gate is open while a sort of stabilizing effect was observed for TM1b and 6a whose role in substrate binding was previously demonstrated. This stabilizing effect is also extended to the extracellular gate itself whose oscillations are reduced in the open state by the sodium-protein interaction (Krishnamurthy and Gouaux, 2012). Moreover, thanks to the crystal structure of a LeuT mutant engineered to be chloride dependent (Glu290Ser), an hydrogen bond network was mapped linking chloride binding site to extracellular gate incrementing the evidences that the binding order should be: $Cl^-$ (not for prokaryotic proteins, obviously), Na ions (in Na1 site first) and then organic substrate (Kantcheva *et al.*, 2013). The isomerization of the transporter from an outward to an inward conformation is prevented only when Na is present. The stabilizing effect of sodium binding is disrupted when the organic substrate has bound the protein biasing the structure toward a closed conformational state (Focke *et al.*, 2013). Quite intriguing is the role of Na2 site in intracellular substrate releasing mechanism: some evidences supported a model in which the sodium release from this position, jointly to hinge movements of TM1b, create the conditions for subsequent substrate and ion release. In exerting this role an important function as also been assigned to the degree of hydration of the same site as was also found for one of the three sodium binding sites in the glutamate transporter GltPh (Heinzelmann *et al.*, 2013).

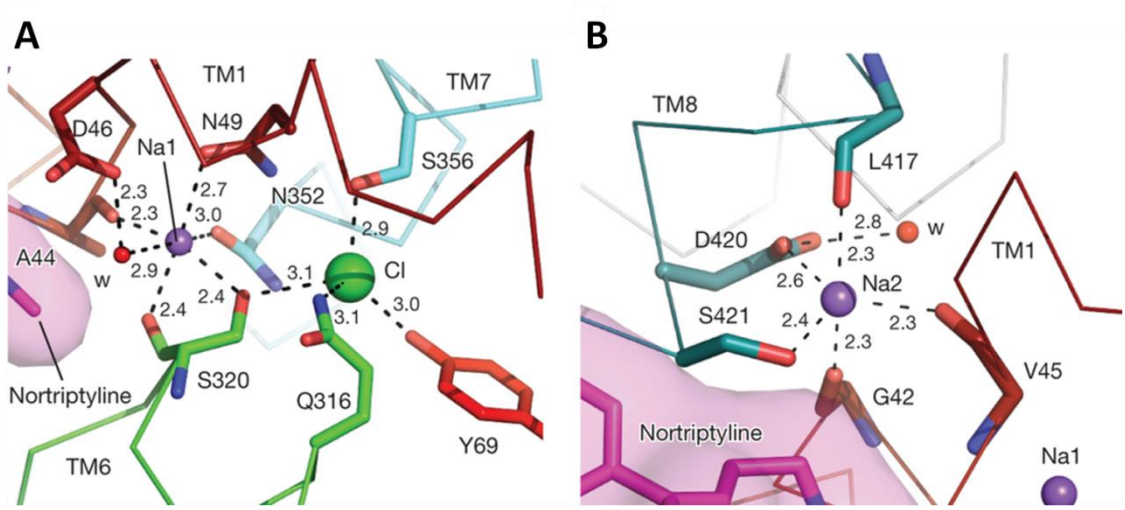


**Fig. 5** *Sodium and chloride binding sites as found in $DAT_{cryst}$ structure.*(**A**), Na1 and chloride ion binding sites. $Na^+$ is purple and $Cl^-$ is green and both are modeled as spheres. (**B**), Coordination at the Na2 site is trigonal bipyramidal with a water molecule (w, red sphere) 3.3 Å from the sodium ion. Distances are in ängstroms for residues that are in the coordination sphere and interactions are shown by dashed lines. Residues are colored according to their respective TMs. From (Penmatsa *et al.*, 2013).

### 1.4.3 The role of symmetry in the transport mechanism of FIRL folded transporters

The main drawback of protein crystallography is the absence of direct dynamic information about the functional mechanism of the proteins. The LeuT crystal structure

(Yamashita *et al.*, 2005) allowed the definition of a mechanism of function for NSS transporters, known as the rocking bundle mechanism (Forrest *et al.*, 2009), whose validity was proved for a lot of other transporters also of distant unrelated families but sharing the same fold (*five transmembrane-helix inverted-topology repeat, LeuT-like* or *FIRL* fold (Abramson and Wright, 2009; Khafizov *et al.*, 2012; Focke *et al.*, 2013).

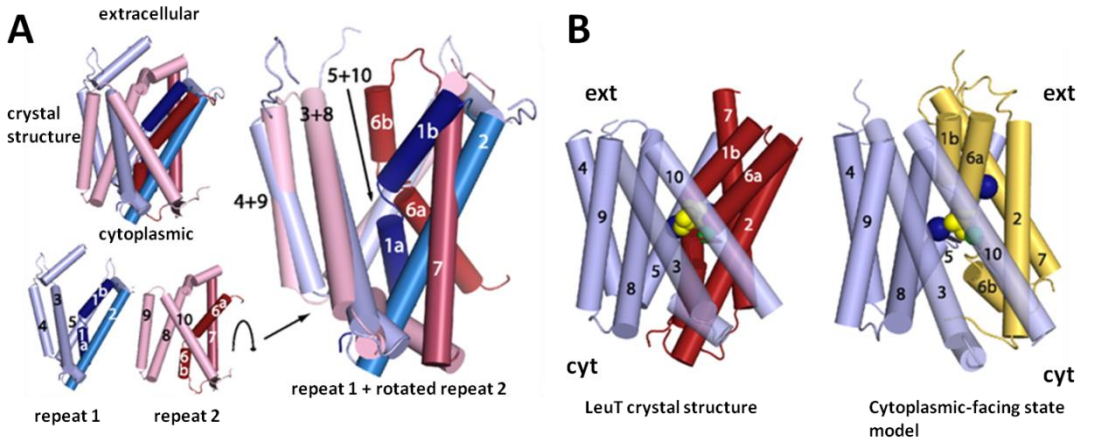


**Fig. 6** (**A**) *Structural asymmetry of repeats in LeuT*. TMs 1–10 of the LeuT crystal structure (*Upper Left*) were separated into the two structural repeats (*Lower Left*). TMs 1–2, dark blue; TMs 3–5, pale blue; TMs 6–7, dark red; TMs 8–10, pale red. Note the different orientation of the first two helices (particularly 1 and 6) in each repeat with respect to the other three helices. (**B**) *Predicted conformational change in LeuT*. The position of the four-helix bundle comprised of TMs 1–2 and 6–7 with respect to the scaffold (in blue) is shown along the plane of the membrane in red in the crystal structure and in yellow in the model of the cytoplasm-facing state. The positions of the sodium ions (blue), the leucine substrate (yellow), and the Cα-atom of S256 (green) are shown as spheres. TM11 and -12 and the extracellular loops are not shown. Adapted from (Forrest *et al.*, 2008).

In these proteins the internal pseudo-symmetry firstly described by Yamashita and coworkers in 2005, is now well proved be a facilitating structural solution for alternating access mechanism. Two observations led toward the elaboration of this model: *i*) leucine and sodium ions are bound into the protein structure, more or less, in the middle of the plane of the membrane, suggesting that the pathways from the bulk solution to the binding sites, and *vice versa*, might be symmetrical and *ii*) the existence of an unpredictable, based only on primary sequence, internal symmetry that relates TM1-5 with TM6-10 by a two-fold axis that runs normally to the plane of the membrane. In these sub-domains (*repeat A* and *B*, respectively) two out the five TMs undergo to the major conformational changes during the transport cycle, namely the TM1-2 and the TM6-7 (collectively called *rocking bundle*). It is worth noting that in the middle of TM1 and of TM6 the α–helix organization is disrupted and the unwound regions harbour residues that take part of binding sites of both leucine and sodium ions evidencing as the substrates binding sites are localized at the interface between the two repeats. Each one of these couples of helices tilt, jointly, in respect of the other transmembrane helices that behave as a sort of a rigid body, named *scaffold*. Considering the whole protein the moving of TM1-2 and of TM6-7 relatively to the scaffold open the transporter to the outward solution or to the intracellular milieu alternatively (Forrest *et al.*, 2008; Rudnick, 2011)

(Fig. 6). In this mechanism resides the power of the symmetry: two highly similar domains, just reoriented by symmetry rules, by the same movement, open and close the carrier in two opposite side of the lipid bilayer. A lot of biochemical evidences were gathered after the proposal of this model especially by accessibility studies in the serotonin transporter SERT (Forrest *et al.*, 2008) but also for the GABA transporter GAT1. In this last one, when assayed in biochemical conditions that are supposed to force the protein toward an open-to-in conformation, an aqueous route from the intracellular side to the substrate binding site was mapped lining the TM8 as predicted by the model (Ben-Yona and Kanner, 2009). Symmetry rules are nowadays also exploited to investigate these transporters by structure-function studies extending the finding for one repeat to the other one (Khafizov *et al.*, 2012). So far, no crystal structure of LeuT in inward occluded state were solved while an inward open structure was solved in 2012 (Krishnamurthy *et al.*, 2012). Interestingly the comparison between this structure with the previous ones showed that the transition between outward-open, closed and inward open conformations are not exactly corresponding to those predicted by the rocking bundle mechanism originally proposed for LeuT because the core domain does not move as a rigid body in the transition between the different structures but only a portion of the core domain moves as a single body, partially disrupting the symmetry between inward- and outward-facing conformations (Fig. 7). In LeuT, probably, local hinge movements are also responsible of the coordinated opening and closing of the gates. Surprisingly, for proteins with FIRL fold, seems, instead, that the rocking bundle mechanism strictly describes what happens during the transport cycle (Focke *et al.*, 2013). To date an increasing number of transporters where identified as FIRL folded defining an evolutionary transverse family being composed by protein quite distant from a classical phylogenetic point of view. Examples are the dopamine transporter from NSS $DAT_{cryst}$; (Penmatsa *et al.*, 2013), vSGLT1 (Faham *et al.*, 2008) of Solute Sodium Symporter family, the bacterial $Na^+$/benzyl-hidantoin cotransporter Mhp1 (Weyand *et al.*, 2008; Weyand *et al.*, 2011), from BCCT family the betaine transporter BetP (Ressl *et al.*, 2009; Perez *et al.*, 2012) and the L-carnitine-γ-butyrrobetaine antiporter CaiT (Schulze *et al.*, 2010) and members of the amino acid/polyamine/cation cotransporter APC (Lolkema and Slotboom, 2008) which include the arginine:agmatine antiporter AdiC (Fang *et al.*, 2009; Gao *et al.*, 2009) and the glutamate:γ-aminobutyric acid antiporter GadC (Ma *et al.*, 2012).

Despite with different topological orientations, structural repeats related by pseudosimmetry were identified in other secondary active carriers not belonging to the FIRL fold group. Among these, of interest is the case of the structural prototype for excitatory neurotransmitter transporters, the aspartate transporter GltPh from *Pyrococcus horikoshii* (Crisman *et al.*, 2009; Reyes *et al.*, 2009): this protein shows a very different structure from LeuT (Yernool *et al.*, 2004) but as for this latter one, the repeats "were used" to build a model in an open-to-in conformation that, as predicted, was found pseudo-symmetric to the crystal structure that was instead captured in an open-to-out configuration (Reyes *et al.*, 2009). If the rocking bundle mechanism explains the function of LeuT, the *shuttle mechanism* was instead proposed to be that one on which GltPh

rely, being provided with a shuttle domain that is able to bind, move and, at the same time, close the access to the protein as well to trig the opening of the transporter to the opposite cytosolic side.

Structural repeated elements were also found in other kind of membrane proteins, not only in secondary transporters but also in channels such as aquaporins and the formate channel FocA (Waight *et al.*, 2010). The main difference between channels and transporters is that in transporters the two halves are never exactly in the same conformation or, at least, they are characterized by some little, but crucial, differences and this is obviously related to the necessity of transporters to render impossible the free diffusion of substrate through themselves (Forrest, 2013). From an evolutionary point of view the simplest hypothesis to explain this widespread structural/functional strategy, is that all these structures have evolved from a common gene progenitor by one (or more) duplication events (and speciation, obviously, later on). This fascinating theory postulates also the existence of a common origin for all membrane carriers. The ancient progenitor was probably able to bind the substrate from one side of the primordial membrane, move and release it to the opposite side. By gene duplication, these functions were separated ad they now reside in two different structural domains, belonging to the same molecule, facing each around the substrate binding sites.

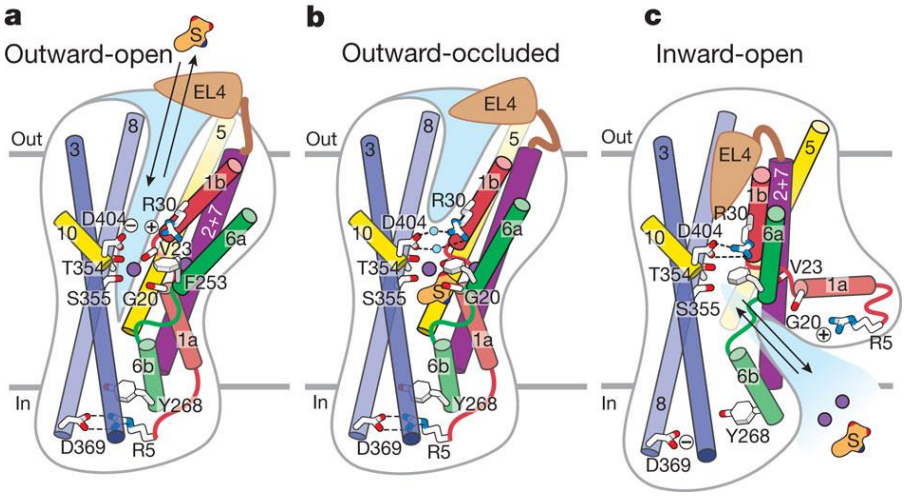


**Fig. 7** *Scheme of LeuT transport mechanism.* **a–c**, shown are structural elements and gating residues instrumental to conformational changes associated with the transition from the outward-open (**a**) to the outward-occluded state (**b**) and the inward-open state **c**, at present there is no crystal structure for an inward-occluded state and thus no schematic is provided. Drawn from (Krishnamurthy *et al.*, 2012).

# Chapter 2
# The highly conserved glycine triplet in the Extracellular Loop 1 of KAAT1 participates to cation access mechanism in the extracellular vestibule of the transporter

## 2.1 ABSTRACT[1]

As more than 80% of family members, KAAT1 shows a stretch of three glycines (G85–G87) that according to the structure of the prototype transporters LeuT and DAT, is located close to the access of the permeation pathway. In this work the role of the triplet has been investigated by alanine and cysteine scanning methods in proteins heterologously expressed in *Xenopus laevis* oocytes. All the mutants were functional but the surface expression level was reduced for G85A and G87A mutants and unaffected for G86A mutant. All presented altered amino acid uptake and transport associated currents in the presence of each of the cations ($Na^+$, $K^+$, $Li^+$) that can be exploited by the wt. G87A mutant induced increased uncoupled fluxes in the presence of all the cations and pre-steady state currents were not detectable in a $Na^+$ containing recording buffer.
Cross-linking studies, performed by the treatment of cysteine mutants with the oxidative complex Cu(II)(1,10-phenanthroline)$_3$, showed that limiting the flexibility of the region by covalent blockage of position 87, causes a significant reduction of amino acid uptake. $Na^+$ protected G87C mutant from oxidation, both directly and indirectly. The conserved glycine triplet in KAAT1 plays therefore a complex role that allows initial steps of cation interaction with the extracellular vestibule of the transporter.

[1] The work presented in this chapter has been published in (Giovanola *et al.*, 2012)

## 2.2 INTRODUCTION

KAAT1 is characterized by peculiar functional properties: an electrogenic amino acid uptake activated by $K^+$, $Na^+$ and $Li^+$ at differing extents (Castagna *et al.*, 1998; Bossi *et al.*, 1999b; Liu *et al.*, 2003) and an amino acid selectivity influenced by the driving ion (Feldman *et al.*, 2000; Liu *et al.*, 2003; Soragna *et al.*, 2004). Since its cloning the special features of KAAT1 have been exploited to investigate the structural/functional relationships within the NSS family. Sequence comparisons and site-directed mutagenesis studies have allowed the identification of the structural determinants of transport activity such as residues involved in $Na^+$ and $K^+$ interaction and in amino acids translocation (Feldman *et al.*, 2000; Castagna *et al.*, 2007; Miszner *et al.*, 2007 Castagna *et al.*, 2009).

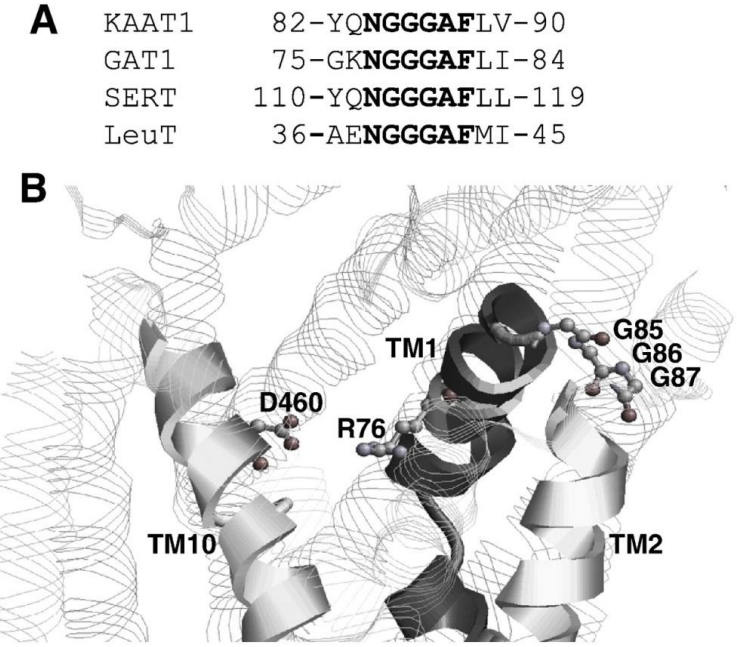


**Fig. 1.** *The highly conserved glycine triplet of NSS transporters.* (**A**): alignment of KAAT1, GAT1, SERT and LeuT sequences extending from Tyr82 to Val90 (KAAT1 numbering). (**B**): homology modeling of KAAT1 structure based on the 3D organization of LeuT. The model shows the spatial relationships of the glycine repeat with the residues forming part of the putative external gate of the transporter (Arg76 and Asp460 of KAAT1). Gly85–87, Arg76 and Asp460 are depicted as ball and stick, TM1, TM2 and TM10 as ribbons, the rest of the structure as strands.

The aim of this work has been to study the functional role of a highly conserved sequence, extending from the extracellular loop 1 (EL1) to the transmembrane domain 2 (TM2) of KAAT1 in which three consecutive glycines (Gly85–Gly87, Fig. 1A) are found. By homology modeling with LeuT and according to accessibility studies in other members of the NSS family as the serotonin transporter SERT and the GABA transporter GAT1 (Henry *et al.*, 2003; Zhou *et al.*, 2004), the glycine triplet is located at the extracellular side of the protein, close to one of the residues that participates in the external gate (Arg30 in LeuT, Arg76 in KAAT1, Fig. 1B). The degree of conservation in NSS transporters together with the structural localization suggests that the glycine triplet

plays a relevant role in transport function. This region has already been studied individually in both GAT1 and SERT (Mao *et al.*, 2008; Zhou and Kanner, 2005) with a similar approach. In GAT1, the residues between Asn77 and Ala81 (corresponding to Asn84 and Ala88 in KAAT1, Fig. 1A) have been mutated into alanine and cysteine and their accessibility has been analyzed by treatment with cysteine reactive compounds (MTS reagents), in the context of the MTS insensitive C74A mutant. The N77C mutant showed lower activity compared to the wild type protein, but was stimulated by treatment with the cysteine modifying agent [2-(trimethylammonium)ethyl]methanethiosulfonate bromide (MTSET). The G78C and G79C mutants were functional and inhibited by MTSET treatment, whereas the G80C mutant showed a complete loss of GABA uptake, but still exhibited sodium-dependent transient currents (Zhou *et al.*, 2005). The results obtained by electrophysiological analysis of this last mutant were interpreted by a model for GAT1 transport cycle, in which the transition between two outward-facing conformations of the empty transporter is impaired by the mutation of Gly80. Consequently, in the absence of $Na^+$, the transporter is locked in a conformation from which it can only be released by GABA or by depolarization.
In SERT, residues from Tyr110 through Gly115 (corresponding to Tyr82 and Gly87 in KAAT1, Fig. 1A) were replaced by cysteine residues in a mutant lacking all the native cysteines known to react with MTS reagents. The G113C mutant retained full activity, the Q111C and N112C maintained partial activity, whereas Y110C, G114C and G115C mutants were inactive. Through analysis of the cysteine modification, Mao and co-workers concluded that in SERT Gln111 and Asn112 substitution decreased the transport rate, because the residues participate in steps of the transport cycle that are subsequent to the substrate binding and that involve serotonin translocation (Mao *et al.*, 2008). Summarizing, in the two papers the role assigned to the glycine residues was different suggesting that they might have a transport-specific task in each member of NSS family, that can be related to the substrate transported. In this context, the peculiarity of KAAT1 to be able to transport a rather wide spectrum of neutral amino acids with a potency order that depends on the driver cation (Mari *et al.*, 2004; Soragna *et al.*, 2004), appears suitable to deeper investigate the role of this highly conserved sequence. In order to achieve this result the GGG sequence in KAAT1 has been analyzed by an alanine and cysteine scanning approach. Mutants were expressed in *Xenopus laevis* oocytes and functionally analyzed by radiolabeled amino acid uptake and electrophysiological measurements.

## 2.3 RESULTS

### 2.3.1 Cell surface expression of glycine mutants

To investigate the role of the highly conserved stretch of glycines, each of them was substituted with alanine, the flanking residues Asn84 and Ala88 were converted into glycine and the double mutants N84G/G87A and G85A/A88G were also synthesized in

order to obtain a shift of the entire triplet toward the N or the C terminus of the protein respectively. The mutant surface localization and the transport activity were analyzed after expression in *X. laevis* oocytes. The correct targeting to the plasma membrane of glycine mutants was determined by the single oocyte chemiluminescence (SOC) technique pioneered by Zerangue (Zerangue *et al.*, 1999). This technique allows the quantification of a tagged protein expressed at the plasma membrane.

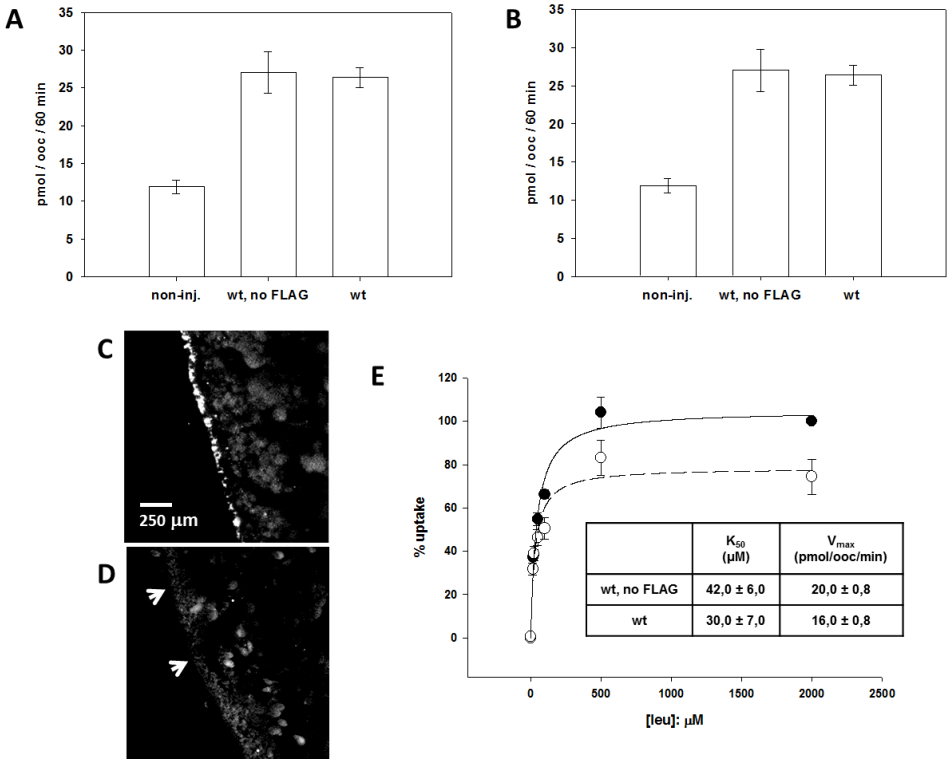


**Fig. 2.** *Functional and immunofluorecence characterization of the FLAG tagged form of KAAT1.* (**A-B**): 0,1 mM leucine uptake induced by native or FLAG tagged form of KAAT1 in presence of 100 mM NaCl (A) or 150 mM KCl (B). Data are from a representative experiment. (**C-D**): immunofluorescence against FLAG epitope for sections of oocyte expressing native (D) or tagged (C) KAAT1. Arrows in D indicate the plasma membrane surface. (**E**): kinetic analysis of leucine uptake induced in presence of 100 mM NaCl by native (●) or by the FLAG tagged protein (○). Data are shown as the relative uptake % of that induced by the native form of KAAT1 in presence of 2000 µM leucine and expressed as the means ± S.E. of at least 30 oocytes from 3 different batches.

In our experiments a functional FLAG-KAAT1 construct was used and the tagged proteins were detected by an anti-FLAG antibody. The activity of the tagged form of KAAT1 was analyzed by means of radiolabeled amino acid uptake to compare the kinetic parameters as well as the peculiar ionic selectivity to that of the untagged form: these analysis showed that the FLAG-KAAT1 protein was able to exploit both sodium and potassium as driver ion but a slight reduction in the $V_{max}$ was also measured (Fig. 2A, B, E). Immunofluorescence experiments performed on oocytes sections proved the integrity of the introduced synthetic epitope and the absence of specific signal in oocytes expressing the untagged form of KAAT1 (Fig. 2C, D). The single mutants showed a surface localization comparable to wt with the exception of G85A and G87A that were

present at the plasma membrane at a 50% level. The same level of expression was obtained also for the double mutant G85A/A88G, whereas N84G/G87A mutant was completely undetectable in the oocyte membrane.

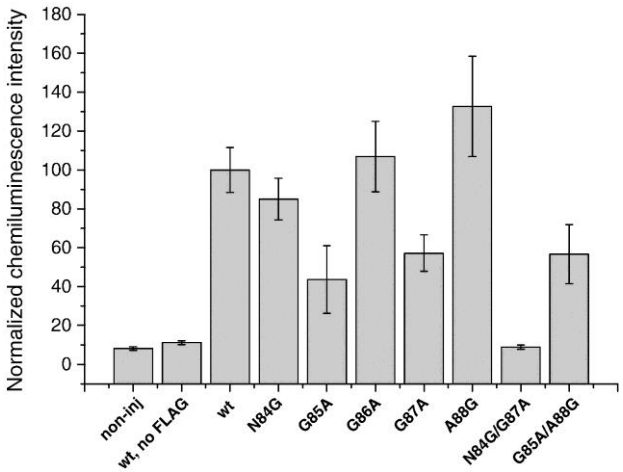


**Fig. 3**. *Membrane expression of KAAT1 wt and mutants*. The chemiluminescence detected from 20 to 40 oocytes from 5 different batches expressing the wt and the indicated mutants of KAAT1-FLAG and secondarily labeled with peroxidase-conjugated goat anti-mouse (IgG-HRP) are shown. The data were normalized to the mean value of the wild-type FLAG-KAAT1 of each batch.

### 2.3.2 Analysis of transport activity

In the presence of a $Na^+$ gradient, glycine mutants showed 0.1 mM leucine and 0.1 mM proline uptake reduced of 40–50% compared to the wild type, with the only exception of G87A that induced a comparable proline uptake (Fig. 4A and B) despite the 50% surface expression reduction (Fig. 3). The amino acid uptake reduction of G85A mutant was in agreement with its reduced surface expression. N84G mutant showed a residual transport activity that was 30% of wt whereas the activity of A88G and G85A/A88G mutants was less than 10% of wt (data not shown). The electrophysiological data here reported are different current types. First it is shown the transport associated current, that is the substrate induced current, resulting from the difference of the current in the presence and that in the absence of substrate. Next, characteristic electrical properties of the transport protein are evaluated considering two types of uncoupled current: the leak current that is a constitutive transport-independent conductance, detected only in the absence of substrate and in the presence of permeating ions and the "transport dependent"-uncoupled current that, in the experiments here reported, was seen only when proline was transported in G87A mutant. This last current is observed in the presence of both driven and driving substrates and manifests itself as a current in excess of that associated with the stoichiometric charge translocation. In general cotransporters can show one or both types of uncoupled currents (Andrini *et al.*, 2008; Perez-Siles *et al.*, 2011). The electrophysiological behavior of the glycine mutants under controlled and fixed voltage of

−60 mV confirmed the uptake results (Fig. 4C). For all the three mutants leucine application induced an inward transport current that was 20–40% of that of the wt protein; the same happened for the mutants G85A and G86A when threonine or proline were perfused, while application of these last two substrates elicited in the G87A mutant an inward current similar to that of wt or larger, mainly in the presence of proline. Investigating the electrophysiological behavior over a larger voltage range consolidated the previous results. In Fig. 5 the I–V relationships show that the transport current induced by leucine was greatly impaired in all mutants. When the substrate was threonine only the G87A presented a behavior similar to the wt, and substituting the substrate with proline increased the current generated by this mutant, as it happened at the fixed voltage experiments.

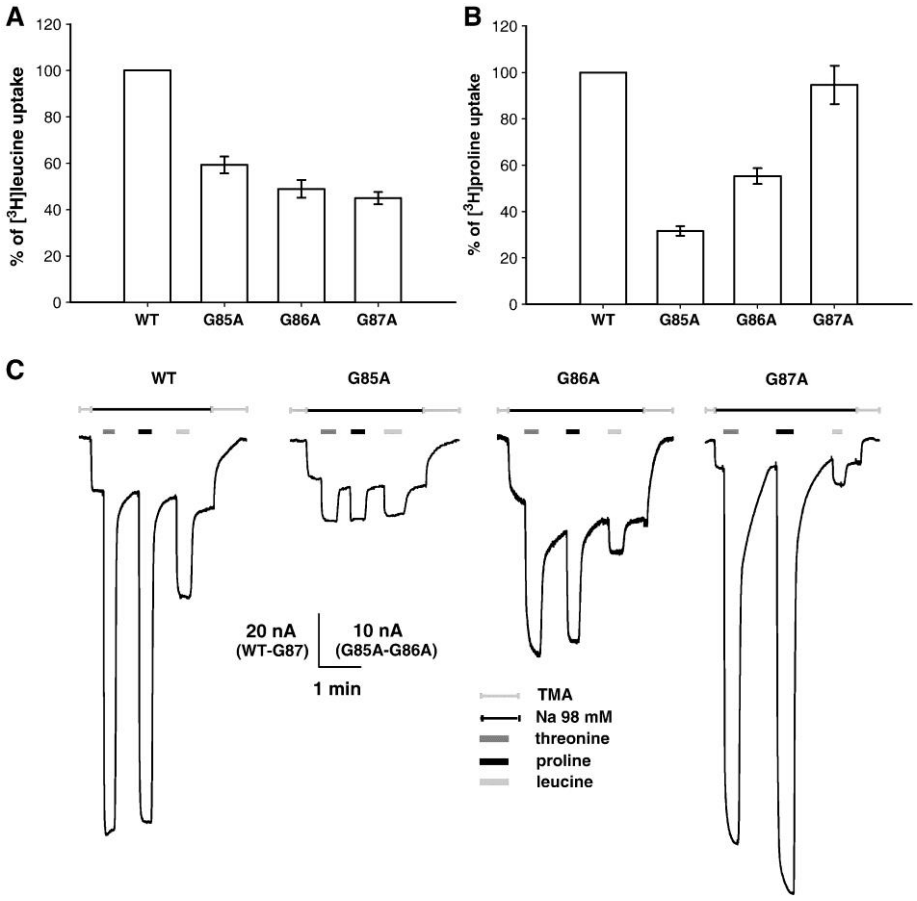


**Fig. 4**. *Amino acid uptake and transport associated currents in oocytes expressing the indicated glycine mutants in the presence of a $Na^+$ gradient.* Bars represent 0.1 mM leucine (**A**) or 0.1 mM proline (**B**) uptake expressed as percentage of wt and are means ± S.E. of at least 30 oocytes from 3 different batches. (**C**) representative oocytes expressing wild type KAAT1 and each of glycine mutants tested at the voltage to − 60 mV in TMA solution (light gray lines), then changed in Na solution (black lines). The substrates, threonine 3 mM (dark gray bars), proline 3 mM (black bars) or leucine 1 mM (light gray bars) were added after stabilization of current in sodium. Before applying the second and the third substrate, the complete recovery to the starting value of the current in sodium was waited.

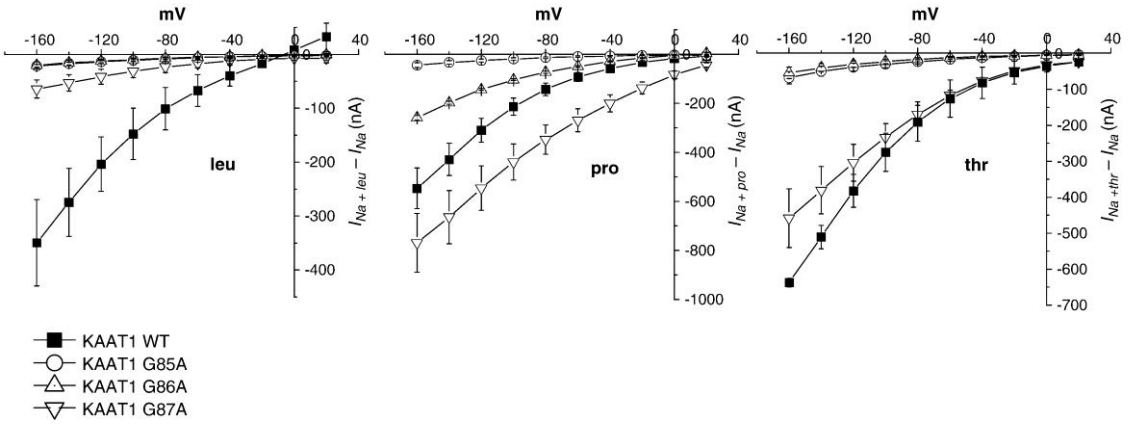


**Fig. 5.** *Current-voltage relationships from wt and mutated transporters, in the presence of $Na^+$ and the indicated amino acid.* Data were obtained by subtracting the traces recorded in the absence from those recorded in the presence of the indicated substrate (3 mM proline and threonine and 1 mM leucine). Values are means ± SE from 8 to 10 oocytes in each group.

### 2.3.3 Estimation of $Na^+$ apparent affinity

All single glycine mutants were still $Na^+$ dependent (Fig. 6) but an alteration in the affinity for this cation was also found.

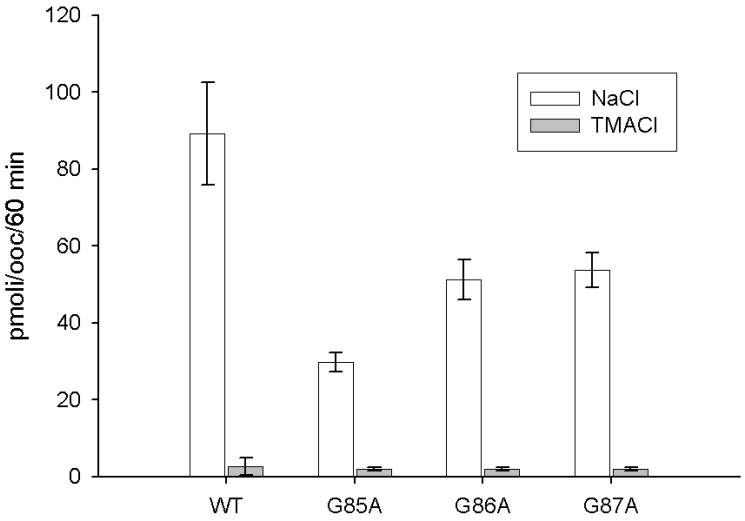


**Fig. 6** *Analysis of the $Na^+$ dependence of glycine triplet single mutants.* Bars represent the uptake induced by oocytes expressing wt or the indicated mutants in presence of 100 mM NaCl or 100 mM tetramethylammonium chloride (TMACl). Data are from a representative experiment.

The sodium transport currents in the presence of threonine were measured at − 80 mV, adding the saturating substrate (3 mM) in solutions containing $Na^+$ with increasing concentration starting from 0.3 mM. Only the G87A mutant showed transport current when the sodium was lower than 1 mM.

The data of the transport current, calculated as the difference from the current in the presence and in the absence of amino acid, were normalized to the maximal current in 98 mM $Na^+$, 3 mM Thr (relative inward (− 1) current in the graph), and fitted by Logistic equation. The values of the sodium concentrations giving rise to half of the maximal current are reported in the table inside Fig. 7. The $Na^+$ apparent affinity decreased for the G85A and G86A mutants ($K_{50}$ = 64 ± 2.2 and 62 ± 2.8 mM respectively), instead for the G87A mutant this parameter increased ($K_{50}$ = 9 ± 1.2 mM), if compared to the wild type ($K_{50}$ = 34 ± 7 mM).

The difference in the apparent affinity for sodium as well as the alteration of amino acid uptake and of the transport associated currents observed in KAAT1 mutants, prompted us to investigate if the modification in the glycine triplet could also has a role in the interaction with the other KAAT1 driving cations: $Li^+$ and $K^+$.

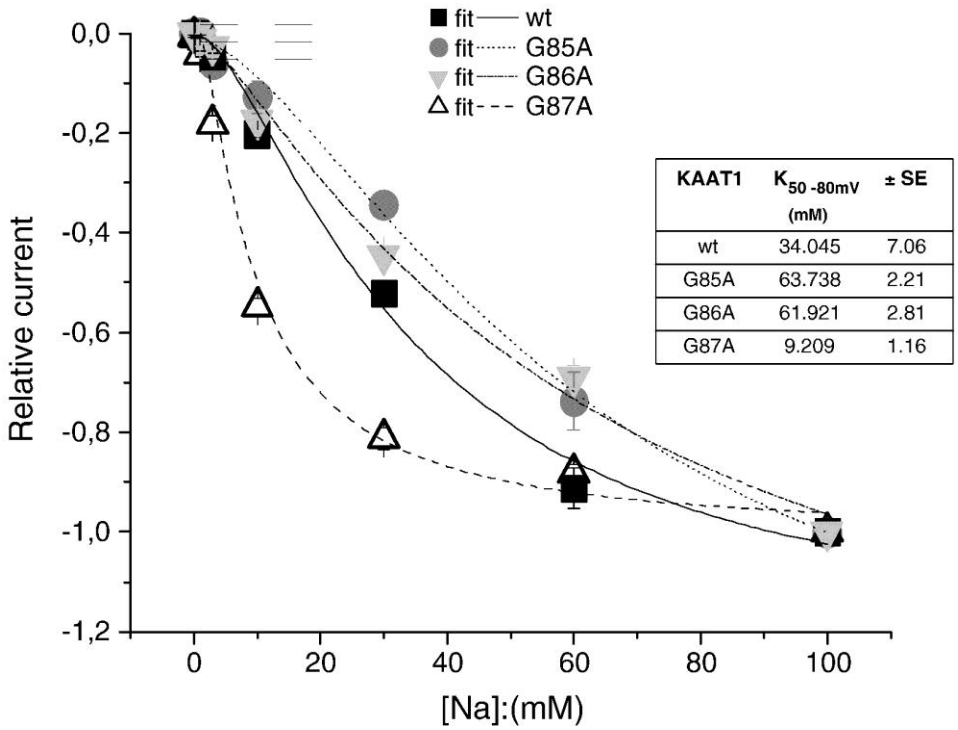


| KAAT1 | $K_{50\ -80mV}$ (mM) | ± SE |
|---|---|---|
| wt | 34.045 | 7.06 |
| G85A | 63.738 | 2.21 |
| G86A | 61.921 | 2.81 |
| G87A | 9.209 | 1.16 |

**Fig. 7.** *Measure of $Na^+$ apparent affinity.* The values of transport current at − 80 mV calculated as the difference of the steady state current in the presence and in the absence of threonine 3 mM were reported at the indicated sodium concentration. The data were normalized to the maximal current in Na 98 mM (− 1 relative current) and fitted by logistic equation. In the inset, the table reports the fitting values for the different mutants. The data were from two batches and from 4 to 12 oocytes for each $Na^+$ concentration.

### 2.3.4 Analysis of cation interaction

As shown in Fig. 8A insert, KAAT1 wt is able to transport leucine in the presence of $Li^+$ and in this condition the G87A mutant induced a comparable uptake (Fig. 8A). Nevertheless the G86A mutant exhibited a transport activity reduced to 50% of wt while the G85A mutant was inactive. To analyze the transport current in lithium, that elicits a

large leak current in the NSS transporters, it was necessary to use proline as substrate instead of leucine, with the goal to show the transport current as the difference of the current in the presence and in the absence of the substrate. In fact, as reported in (Bossi *et al.*, 2000), adding leucine to the Li solution at negative potential, switches the transporter from the leak mode to the transport mode, blocking the large leak current, so that after the subtraction the resulting transport current shows an "apparent" outward direction. With proline as substrate, the transport current is larger and the difference gives an inward transport current. The current–voltage relationships of the transport current here reported in the presence of $Li^+$ and proline confirmed the uptake data obtained in leucine (Fig. 8B): G85A was inactive, G86A was similar to the wild type and finally G87A had a larger current.

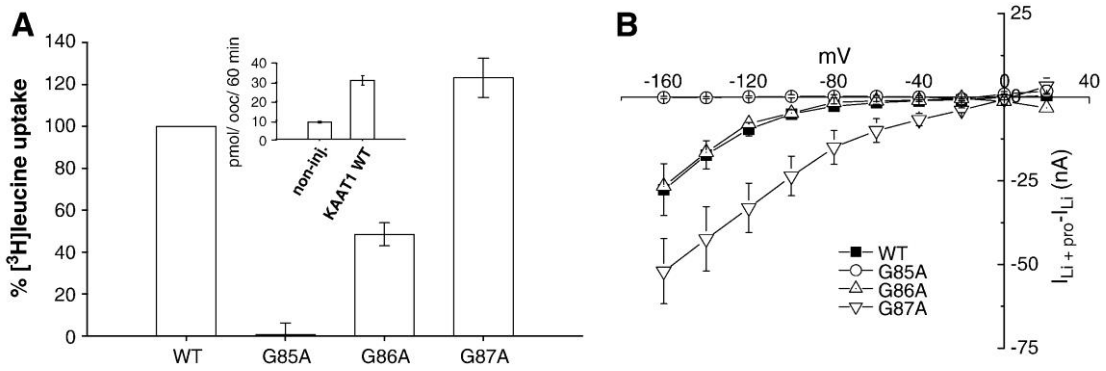


**Fig. 8**. *Amino acid uptake and transport associated currents measured in the presence of a Lihium gradient.* (**A**) Bars represent 0.1 mM leucine uptake induced by the indicated mutants in the presence of 100 mM LiCl. Data are expressed as percentage of wt and are means ± SE of 30 oocytes from 3 different batches. Inset: 0.1 mM leucine uptake measured in KAAT1 wt expressing oocytes or in non-injected oocytes as a control, in the presence of 100 mM LiCl. Data are means ± SE from 10 to 14 oocytes in a representative experiment. (**B**) Current–voltage relationships, in the presence of $Li^+$ with 3 mM proline. Data were obtained by subtracting the traces recorded in the absence from those recorded in the presence of the indicated substrate. Values are means ± SE from 4 to 6 oocytes in each group.

In the presence of high $K^+$ the G87A mutant showed a transport activity of 150% compared with wt; the G86A mutant activity was reduced to 20% and G85A mutant was inactive (Fig. 9A).

Data from electrophysiological analysis showed that in the presence of $K^+$ all three mutants exhibit a similar reduced transport current (Fig. 9B). This apparent discrepancy with the uptake data is due to the transport current estimation that is usually calculated as the difference of the current in the presence from that in the absence of the amino acid. In this case the G87A mutant has a larger leak current than the wt (Fig. 10) and this led to an underestimation of the "transport current"; it is also necessary to remember that in uptake conditions without cell potential control, the high concentration of potassium depolarizes the membrane voltage to a value around 0 mV. It is worth noting that under these unfavorable conditions the G87A mutant, which has a lower expression level than wt (Fig. 3), still exhibits a larger leucine uptake. Electrophysiological investigation of the leak currents showed two interesting aspects: the leak currents were altered, in particular

the $Li^+$ current was close to 0 in the G85A mutant, and reduced in the G86A. Furthermore, in these two mutants the $Na^+$ current was lower than in the wt. The G87A had instead the greatest uncoupled currents in all the three tested cations (Fig. 10).

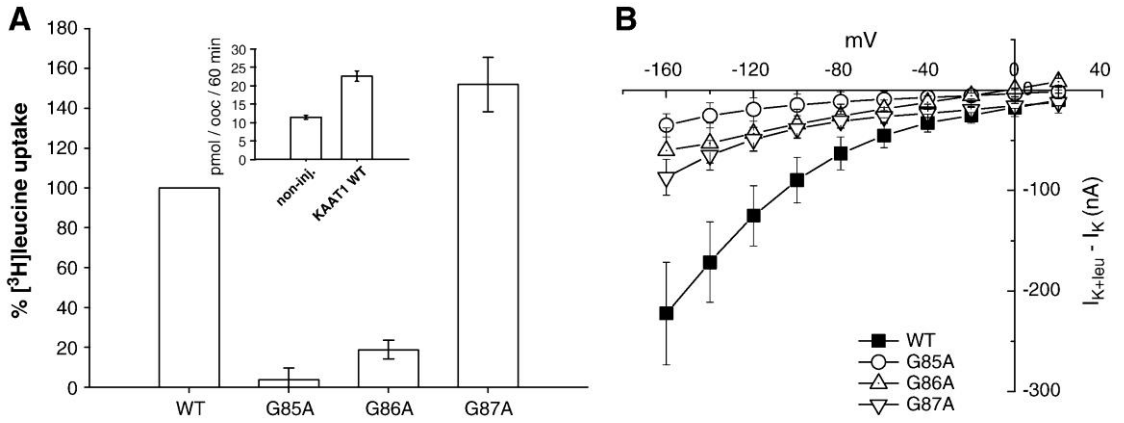


**Fig. 9.** *Amino acid uptake and transport associated currents measured in the presence of high external concentration of KCl*. (**A**) Bars represent 0.1 mM leucine uptake induced by the indicated mutants in the presence of 150 mM KCl. Data are expressed as percentage of wt and are means ± SE of 24 oocytes from 3 different batches. Inset: 0.1 mM leucine uptake measured in KAAT1 wt expressing oocytes or in non-injected oocytes as a control in the presence of 150 mM KCl. Data are means ± SE from 10 to 14 oocytes in a representative experiment. (**B**) Current–voltage relationships, in the presence of potassium solution with 1 mM leucine. Data were obtained by subtracting the traces recorded in the absence from those recorded in the presence of leucine. Values are means ± SE from 4 to 6 oocytes in each group.

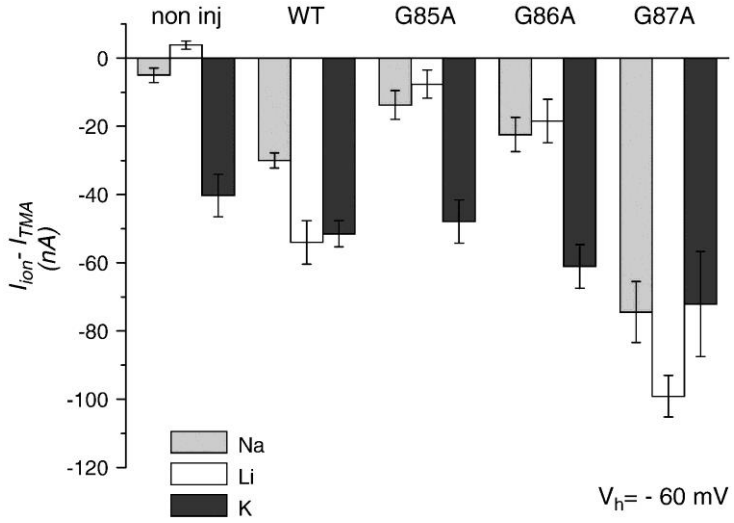


**Fig. 10.** *Leak currents elicited by KAAT1 wt and by the indicated mutants*. Leak currents were obtained by subtracting current in tetra-methyl-ammonium (TMA) solution ($I_{TMA}$) from current in ion solutions $I_{ion}$–$I_{TMA}$ containing $Na^+$ (light gray bars) or $Li^+$ (empty bars) or $K^+$ (dark gray bars) as the main cation in oocytes expressing KAAT1 wt (n = 12) or glycine mutants (G85A, G86A, G87A) (n = 14) and in non-injected oocytes (n = 7). Data represent means ± SE from 5 batches of oocytes.

The molecular origin of uncoupled currents has not been fully elucidated but there is a general agreement on the fact that some conformational changes should occur in the protein to allow this kind of charge movements.

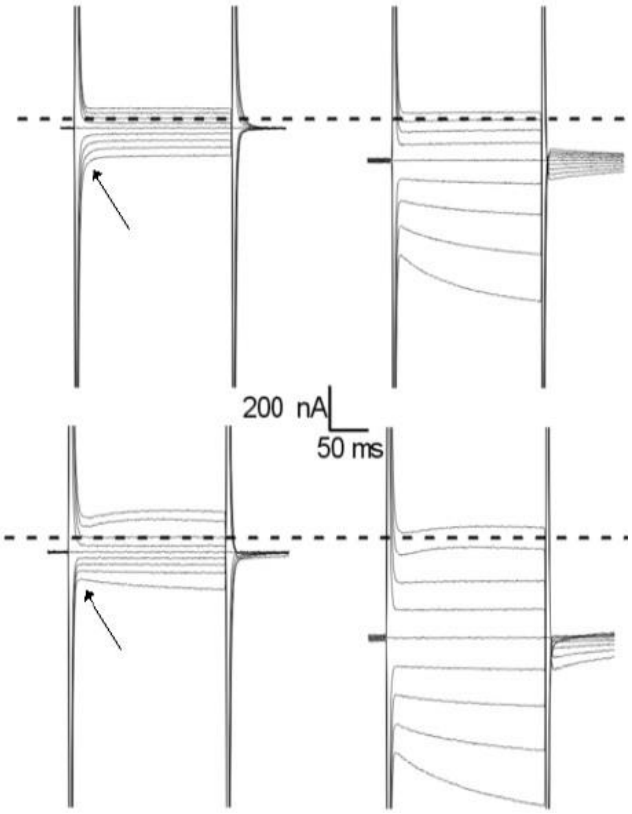


**Fig. 11**. *Investigation of cation interaction with wt and G87A KAAT1 mutant.* Pre-steady state currents (**left**) and coupled currents (**right**; 3 mM Proline), recorded for wild type KAAT1 (**upper**) or G87A mutant (**lower**) in presence of 98 mM $Na^+$. Holding potential was of –60 mV.

Beside this type of currents, SLC6 family members elicit also the so called transient currents (that should be better defined as pre-steady state currents). As for uncoupled currents the existence of this ion movements *in vivo* conditions are not yet proved and, consequently, neither a clear physiological role was, so far, proposed. The pre-steady state currents are recorded in voltage clamp conditions applying to the oocyte, expressing the proteins under investigation, an electric pulse (depolarizing or hyperpolarizing). The currents recorded as results of these jumps are generated by the holding system of the TEVC set-up and injected into the cell to keep the membrane voltage constant. If plasma membrane reacts as a pure capacitor (in other terms, in absence of transient currents) the recorded currents would be only equal in intensity, but opposite in sign, to those injected by the jump. Transient currents are instead recorded as currents with variable amplitude with a delay in reaching the voltage at which the membrane voltage is experimentally clamped (Peres *et al.*, 2004). According to a theoretical model the manifestation of transient currents is explainable with the movements of charged membrane proteins

under the initial electric pulse. Another model explain this phenomena with the entry of an ion in the magnetic field of the cellular membrane and subsequent interaction with proteins expressed in the membrane. For many secondary active transporters, to date, is known that the recording of transient currents is possible only if in the recording buffer are present ions able to interact with the protein (but not necessary exploitable as driver ion (Mager *et al.*, 1998; Zhou *et al.*, 2006). This observation justify the use of transient currents as an indirect measure of protein-ion interaction (Kanner *et al.*, 2008). Wild type KAAT1 shows Na transient currents but interestingly, among mutants of the glycine triplet, only for G87A mutant a reproducible recording following voltage jumps was possible but no transient currents were detected suggesting an alteration of the interaction properties of this mutant with sodium (Fig. 11).

### 2.3.5 Thiol cross-linking studies

Since glycine is an amino acid with no side chain, it can introduce flexibility in protein structure. Moreover, by accessibility studies, the region surrounding the glycine triplet has been shown to undergo conformational changes during the transport cycle in the glycine transporter GLYT2a and in the SERT transporter (Lopez-Corcuera *et al.*, 2001; Sato *et al.*, 2004). To verify if the flexibility of this region may influence KAAT1 activity, we tested the effect of the oxidative reagent Cu(II)(1,10-phenanthroline)$_3$ (CuPh) on the single mutants G85C, G86C and G87C and on the double mutants G85C/G87C and G86C/G87C. The rationale of this analysis is that the presence of CuPh could allow the cross-linking of cysteines by the formation of disulfide bonds thereby reducing the flexibility of the region. CuPh pre-incubations were performed in the absence or in the presence of $Na^+$ at room temperature or at 0 °C on ice (see *Materials and methods* section). G85C, G85C/G87C and G86C/G87C mutants were devoid of any leucine transport activity whereas the G86C and G87C mutants showed respectively the 25 and 40% of wt induced uptake. Incubation with 0.2 mM CuPh in the absence of $Na^+$ at room temperature caused a significant reduction of leucine transport activity only in the G87C mutant (58% of control uptake) (Fig. 12 insert). The effect of CuPh on the G87C mutant was specific and reversible as shown in Fig. 12: wt and G87A mutant were not sensitive to the oxidant and the inhibition observed for G87C mutant was significantly recovered by the treatment with the reducing agent DDT (12 mM). The effect observed in the single mutant G87C implies the formation of a disulfide bond with a native cysteine. By the analysis of the homology model of KAAT1 structure based on the LeuT crystal (PDB access code, 2A65), the only cysteine that would be at the congruent distance for the formation of a disulfide bond is Cys347. According to our hypothesis, CuPh incubation did not affect neither the double mutant G87C/C347A nor the single mutant C347A activity (Fig. 12).

The effect of CuPh on G87C mutant was also tested measuring leucine and proline uptake after 5 min of pre-incubation with the oxidant at room temperature in the presence of $Na^+$. As reported in Fig. 12 inset, in this condition G87C-induced leucine

uptake was not affected by oxidative treatment, proline uptake was 58% of control uptake after oxidative treatment in the absence of $Na^+$, and 85% of control uptake after oxidative treatment in the presence of $Na^+$. So $Na^+$ appeared to significantly prevent CuPh from exerting the transport inhibition observed in the absence of $Na^+$. We therefore tested whether the protection exerted by $Na^+$ was direct or indirect comparing the effect of the oxidative treatment in the presence of $Na^+$ at room temperature with that obtained at 0 °C. At room temperature the $Na^+$ protection could be indirectly exerted by conformational transitions, induced by $Na^+$ binding in a site different from the glycine region, hampering cysteine cross-linking; at 0 °C conformational transitions would be significantly slower and the protection observed would be therefore exerted by a direct interaction of $Na^+$ with glycines. As shown in Fig. 12 inset, in the presence of $Na^+$ and at 0 °C, leucine uptake was not affected by oxidative treatment whereas proline uptake was significantly inhibited (62% of control condition), indicating that $Na^+$ therefore protected both directly and indirectly position 87 from cross-linking.

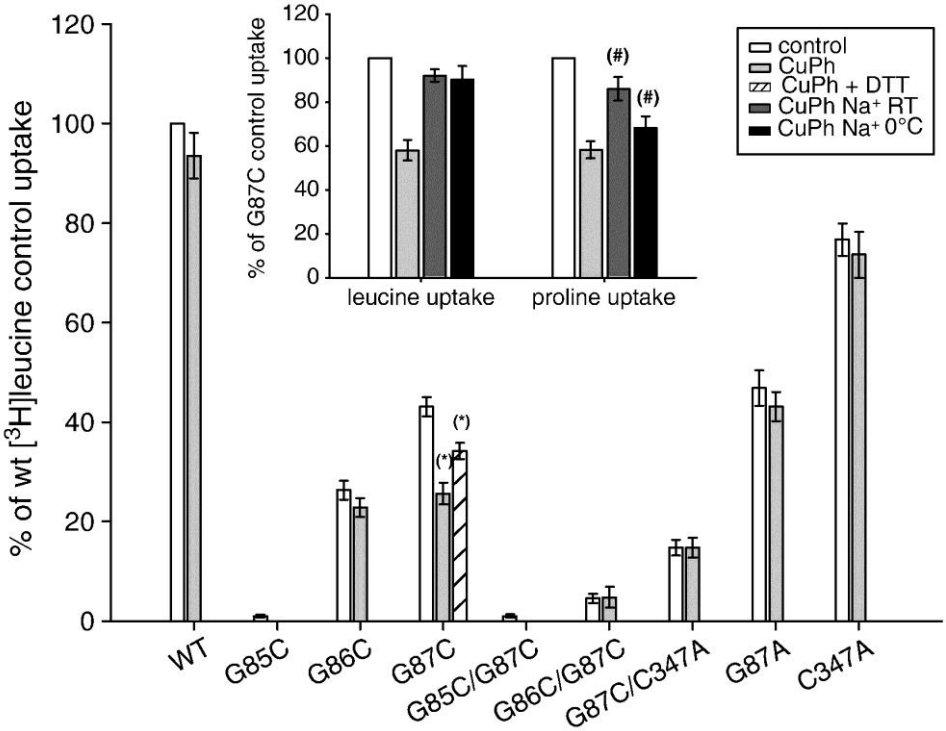


**Fig. 12.** *Effects of Cu(II)(1,10-phenanthroline)$_3$ (CuPh) on KAAT1 wt and mutants.* Bars represent 0.1 mM leucine uptake mediated by KAAT1 wt and the indicated mutants in control conditions (empty bars), after the treatment with 0.2 mM CuPh in the absence of $Na^+$ (light gray bars), after the treatment with 0.2 mM CuPh followed by incubation with 12 mM DTT (filled white bars). In the absence of $Na^+$, choline chloride substituted NaCl. Data are expressed as percentage of wt mediated uptake in control conditions and are the means ± SE of at least 30 oocytes from 3 different batches. **Inset**: $Na^+$ protection of G87C-induced leucine and proline uptake. Bars represent 0.1 mM leucine uptake and 0.1 mM proline uptake measured in control conditions (empty bars), after the treatment with 0.2 mM CuPh in the absence of $Na^+$ (light gray bars), after the treatment with 0.2 mM CuPh in the presence of $Na^+$ at RT (dark gray bars) or after the treatment with 0.2 mM CuPh in the presence of $Na^+$ at 0 °C (black bars). Data are expressed as percentage of G87C induced uptake in control conditions and are the means ± SE of 30 oocytes from 3 different batches. (*), (#): statistically different, $p < 0.05$.

## 2.4 DISCUSSION

Glycine rotates easily and adds flexibility to the protein chain because of the presence of two hydrogen atoms at the α carbon. The importance of flexibility provided by glycine is proven by the fact that $K^+$ channel activation gate involves key identified hinge glycine residues (Mathie *et al.*, 2010) and that glycine-rich elements are described in binding sites of enzymes, as protein kinases, in which the interaction with variable substrates requires the avoidance of steric restrictions at the binding site (Bossemeyer, 1994). The degree of conservation of the glycine triplet in NSS transporters suggests a common relevant role in transport function that may be related to conformational flexibility.

Data obtained from the analysis of G85, G86 and G87 mutants in KAAT1 sustain this hypothesis. The conservative mutation of each glycine into alanine did not cause an alteration of the surface localization of transporters that can fully explain the big changes observed in transport activity (Fig. 3). As in most intestinal transporters, KAAT1 shows a broad substrate specificity that, in contrast to most mammalian homologues, is influenced by the driving ion (Castagna *et al.*, 1998; Soragna *et al.*, 2004; Miszner *et al.*, 2007). A marked reduction of uptake and transport associated currents was observed for all the mutants compared with wt for all tested substrates and in the presence of each of the driver cations of KAAT1. This was especially evident for the mutation of the G85 residue that is, indeed, the most conserved among the three glycine residues. An exception was represented by the G87A mutant that although exhibited a 50% reduction of surface expression (Fig. 3), in the presence of $Na^+$ showed a proline uptake and proline and threonine transport associated currents similar or even larger than the wt, and in the presence of $Li^+$ or $K^+$ induced a leucine uptake significantly higher than wt protein (Fig. 4, 5, 8 and 9).

In all the mutants the leak currents were altered, in particular the $Li^+$ current was absent in G85A, and reduced in the G86A mutant. The G87A mutant showed instead the greatest current in all the three tested cations (Fig. 11). Not only the introduction of alanine increased the ion translocation in the absence of substrate but this substitution in the presence of proline as substrate, showed also a transport dependent uncoupled current (Fig. 5). In the presence of $K^+$ this mutant induced higher amino acid uptake than wt and reduced transport associated currents, revealing a partial uncoupling of amino acid and cation flux. Mutant transport activity was still $Na^+$ dependent but their apparent affinity for the cation was different from that of wt: it was reduced for G85A and G86A but increased for G87A mutant (Fig. 7). For all the mutants, and in particular for G87A an altered interaction with cations was therefore observed. The fact that this mutant was also void of transient currents further corroborate a model in which the mutation of the glycine triplet alters the "initial" interaction of the protein with cations. As before mentioned the "significance" of these currents has not fully yet elucidated but only explained by theoretical models. The fact that KAAT1 (as other members of the SLC6 family) shows transient currents only in presence of cation exploitable as driver ion is the main proof of the correctness of the use of these currents as a measure of the protein-ion interaction. In

this scenario the absence of these currents indicates that the interaction of KAAT1, at least with $Na^+$, is hampered by the mutation of the position 87. The application of a depolarizing pre-pulse before the voltage jumps series produced a partial recovery of the transient currents for this mutant (data not shown) similarly to what was described for G80C mutant of the GABA transporter GAT1 (Zhou *et al.*, 2005). As was proposed for GAT1 this data suggests a role for KAAT1 glycine triplet (in particular for glycine 87) of hinge whose main role is to allow a conformational transition between two empty outward facing conformation of the transporter.

The role played in KAAT1 function by the three consecutive glycines may be related to the requirement of a particular structural flexibility in this region of NSS transport proteins. Cross-linking experiments confirmed this hypothesis. The formation of a disulfide bond between pairs of cysteines engineered into the triplet was not possible since the concomitant presence of two cysteines was detrimental for transport activity, however the single mutant G87C was specifically and reversibly inhibited by 0.2 mM CuPh (Fig. 12). The inhibition was not total even at increased CuPh concentrations (data not shown) but nevertheless it indicates that position 87 of KAAT1 needs a certain degree of flexibility for an efficient transport process. It is feasible that the contiguous Gly85 and Gly86 may also participate to this flexibility. The effect of the oxidative treatment on the single mutant G87C implies the formation of a disulfide bond with a native cysteine. By the analysis of the homology model of KAAT1 structure the partner for disulfide bond formation is Cys347 and, accordingly, neither the double mutant G87C/C347A nor the single mutant C347A were affected by oxidative treatment (Fig. 9). Interestingly, Cys347 is located in KAAT1 TM 7 which we have previously demonstrated to functionally interact with TM 2, that bears at its external terminus the glycine triplet (Castagna *et al.*, 2007). The external localization of the glycine stretch, its proximity to the external gate of the transporter as well as its relevance in KAAT1 interaction with cations (Fig. 4, 5, 8, 11) suggest that the flexibility conferred by glycines may influence the conformation of the external vestibule of the transporter and alters the ions entrance. This would explain the evolutionary pressure that has determined the degree of conservation of the region.

The conservation is not only relative to the nature of the single amino acid but also for the relative position that the glycine triplet occupies in the EL1 as demonstrated by effect on transport activity produce by its shifting toward N- or C- terminus domain. The degree of conservation of the triplet could be related to requirement of flexibility of a specific region of the protein namely the extracellular vestibule to which EL1 contributes to structurally define. The analysis of LeuT, in complex with different substrates and inhibitors and computational simulations based on structural data (Yamashita *et al.*, 2005; Singh *et al.*, 2007; Zhou *et al.*, 2007; Singh *et al.*, 2008; Quick *et al.*, 2009; Zhou *et al.*, 2009) have evidenced the functional importance of the extracellular vestibule of the transporter, where substrates and inhibitors appear not only to access but also to first interact with the protein. Site-directed spin labeling and electron paramagnetic resonance have shown that $Na^+$ increments accessibility of the extracellular vestibule basically through movements of the EL4 and the TM1b segment (Claxton *et al.*, 2010). The glycine triplet flanks the

TM1b segment, and should therefore allow its movement. Accordingly, we have seen that $Na^+$ protects cysteine at position 87 from the oxidative agent CuPh (Fig. 12) but surprisingly, this protection was both directly and indirectly exerted. These results indicate that $Na^+$ interacts with KAAT1 at least in two different regions: one located at the glycine loop (direct protection) and the other that should reasonably correspond to the internal $Na^+$ binding sites and that influences the conformation of the glycine loop. In conclusion our data indicate that the glycine triplet in KAAT1 plays a multifunctional role: Gly85 and Gly87 are required for the complete surface expression of the transporter (Fig. 3), the entire region conformation is influenced by the presence of $Na^+$ and determines the access of cations to the extracellular vestibule of the transporter (Fig. 4, 8, 9, 10, 12). Data presented for G87A mutant are in agreement with observations made in GAT1 transporter (Zhou *et al.*, 2005) in which the corresponding G80A mutant shows increased apparent affinity for $Na^+$ and a reduced flexibility that, in the absence of the cation, appears to conditionally "freeze" the transporter in a state from which it cannot further proceed in the transport cycle. However, the role played by the glycine triplet in KAAT1 appears more complex than that observed in GAT1 and SERT (Zhou *et al.*, 2005; Mao *et al.*, 2008) and it might be related to the wider substrate specificity of intestinal amino acid transporters compared with neurotransmitter carriers. Our results confirm that KAAT1, with its particular functional features, represents a good model for the understanding of NSS transporter molecular physiology. The glycine triplet is surely located in a site relevant for the transport mechanism. As previously detail described in chapter 1 the integration of structural and computational analysis of LeuT has led to the conception of two different transport models, one based on a "rocking bundle" of transmembrane helices allowing the alternation of the transporter between an inward facing and an outward facing conformation (Forrest *et al.*, 2008) and the other outlining the role of an external and an internal gate in controlling the access to the central binding site (Krishnamurthy *et al.*, 2009). In the first model TM 1, 2, 6 and 7 form a *bundle* of four associated helices involved in a rocking movement relative to the other transmembrane domains (*scaffold*) that allows for conformational transitions; our findings indicate that the transport process requires reciprocal movements between TM1 and TM2 allowed by the conserved flexible glycine loop.

## 2.5 MATERIALS AND METHODS

### 2.5.1 Protein tagging

To allow optical measurements of the surface expression of the transporter proteins, a FLAG epitope ($_2$HN-DYKDDDDK-COOH) was inserted into the second extracellular loop, close to transmembrane domain 3 of KAAT1, in correspondence to the *PstI* site already present as unique cleavage site in KAAT1 sequence. Oligonucleotides encoding the FLAG epitope with the adding of two alanine residues (introduced to keep the

insertion in frame with the ORF) were ligated into the *PstI* site after annealing. Following are the sequences of the oligonucleotides used:
Forward oligonucleotide: 5'-GATTATAAAGATGATGATGATAAAGCTGCA-3'
Reverse oligonucleotide: 5'-GCTTTATCATCATCATCTTTATAATCTGCA-3'.
DNA sequencing confirmed the correct FLAG construct sequence (Primm s.r.l. laboratories, Milan, Italy).

### 2.5.2 Site-directed mutagenesis

KAAT1 mutants were obtained by PCR using high fidelity DNA polymerase *P.f.u.* (Promega). DNA sequencing (Primm s.r.l. laboratories, Milan, Italy) confirmed the mutations.

### 2.5.3 Oocyte harvesting and selection

Oocytes were obtained from adult female *X. laevis* frogs and manually defolliculated after treatment with 1 mg/ml Collagenase A (Roche, Germany) for 30–40 min at RT in $Ca^{++}$-free ORII medium (82.5 mM NaCl, 2 mM KCl, 1 mM $MgCl_2$, 5 mM HEPES/Tris, pH 7.5). Healthy V–VI stadium oocytes (Dumont, 1972) were then selected for injection and maintained at 16 °C in Barth's solution (88 mM NaCl, 1 mM KCl, 0.82 mM $MgSO_4$, 0.41 mM $CaCl_2$, 0.33 mM $Ca(NO_3)_2$, 2.4 mM $NaHCO_3$, 10 mM HEPES/Tris, pH 7.5) supplemented with 50 mg/l gentamicin sulfate and 2.5 mM sodium pyruvate.

### 2.5.4 Oocyte expression of KAAT1 wt and mutants

pSPORT-1 plasmid vector bearing KAAT1 wild type (wt) or mutants, and pAMV-PA plasmid vector for FLAG-KAAT1 wt and relative mutants were linearized by *Not1* digestion (Promega). Corresponding cRNAs were *in vitro* transcribed and capped using T7 RNA polymerase (Promega).
Defolliculated oocytes were injected with 12.5 ng of cRNA dissolved in 50 nl of RNAse-free water via a manual microinjection system (Drummond). Before use, oocytes were maintained in Barth's solution at 16 °C supplemented as described above.

### 2.5.5 Chemiluminescence

Surface expression of the tagged transporters was detected using the monoclonal primary antibody anti-FLAG M2 (Sigma F3165, 1 µg/ml) and goat anti-mouse IgG secondary antibody labeled with HRP (Jackson ImmunoResearch Laboratories). Briefly, oocytes expressing different FLAG-KAAT1 isoforms, as well as non-injected oocytes, were washed twice for 5 min in ice-cold ND96 pH 7.6 (93.5 mM NaCl, 2mM KCl, 1.8 mM

$CaCl_2$*$2H_2O$, 2 mM $MgCl_2$*$6H_2O$, 5 mM HEPES). These were then fixed with 4% paraformaldehyde in ND96 for 15 min, rinsed 3 × 5 min with equal volumes of ND96, and then incubated for 1 h in a 1% BSA-ND96 blocking solution (used in subsequent antibody incubation steps). Next the oocytes were incubated for 1 h in mouse anti-FLAG M2 1 µg/ml, washed 6 × 3 min in 1% BSA ND96, incubated for 1 h in peroxidase-conjugated goat anti-mouse IgG (HRP-IgG) 1 µg/ml, washed 6 × 3 min in 1% BSA-ND96 and then 6 × 3 min in ND96 alone. For the chemiluminescence readings, oocytes were transferred into a 96 well plate (Assay Plate White not treated flat bottom-Corning Costar) filled with 50 µl of SuperSignal Femto (Pierce). Luminescence was quantified with a Tecan Infinity 200 microplate reader. The plates were read not later than 5 min after the transfer of the first oocyte. The data were then acquired at least three times in 10 min and for each oocyte the mean of three readings was calculated. Results were normalized to the mean value of FLAG-KAAT1 wt for each batch and are plotted as relative chemiluminescence intensity.

### 2.5.6 Immunofluorescence on *Xenopus* oocytes[2]

Oocytes expressing KAAT1 wt or KAAT1-FLAG were fixed by Bouin reagent treatment for 6 hours (15 parts of aqueous saturated picric acid solution/5 parts of 40% formaldehyde solution/1 part of glacial acetic acid) before inclusion in paraffin blocks. Sections of 1,5 µM of thickness were prepared and paraffin removed by the following treatment:

| **Treatment** | Xylene | Xylene | Xylene | 100% Ethanol | 100% Ethanol | 90% Ethanol | 80% Ethanol | 70% Ethanol | Water | Distilled water |
|---|---|---|---|---|---|---|---|---|---|---|
| **Time** | 15' | 10' | 5' | 5' | 5' | 3' | 3' | 3' | Fast washing | Fast washing |

In order to obtain epitope unmasking slides were incubated in 10 mM sodium citrate pH 6 with two 750 Watt heating cycles of 5 minutes in a microwave oven separated by a 2 minutes step of recovery at RT and followed by a slow cooling in a water bath for 30 minutes. Slides were then rehydrated by applying PBS solution (137 mM NaCl, 2,7 mM KCl, 8,1 mM $Na_2HPO_4$*$2H_2O$, 1,76 mM $KH_2PO_4$, pH 7,4) for 5 minutes and then incubated for 30 minutes with the blocking solution (2% of Bovine serum albumin, 0,1% Tween-PBS). Mouse anti-FLAG M2 1 (1:150) antibody was then applied for at least two hours and the preparations were washed 3 times for 5 minutes with PBS solution. Anti-mouse secondary FITC (fluorescein isothiocyanate)-conjugated antibody in PBS solution (1:150) was then applied for 1 hour incubation far from light. Washing steps as above were then applied and anti-bleaching solution added for each slide before mounting.

[2] Oocytes inclusion in paraffin blocks, sectioning and slide preparing were made thanks to the kind collaboration of Paolo Stortini from the Department of Health, Animal Sciences and Food safety of the Università degli Studi di Milano, Milan, Italy.

Samples were analyzed by a fluorescence microscope (Axiovert; Zeiss) with a proper FITC filter ($\lambda_{excitation}$ = 496 nm, $\lambda_{emission}$ = 518 nm).

### 2.5.7 Radiolabeled amino acid uptake

Amino acid uptake was evaluated 4 days after injection. Groups of 8–10 oocytes were incubated for 60 min in 120 µl of uptake solution (100 mM NaCl, 2 mM KCl, 1 mM $CaCl_2$, 1 mM $MgCl_2$, 5 mM HEPES/NaOH, pH 8) with 0.1 mM [$^3$H]leucine (444 kBq/ml, specific activity 3.996 Tbq/mmol) or 0.1 mM [$^3$H]proline (592 kBq/ml, specific activity 2.775 TBq/mmol) (all from PerkinElmer Life Sciences). Alternatively, to evaluate uptake induced in the presence of lithium or potassium ions, NaCl was substituted by 100 mM LiCl or 150 mM KCl respectively. All uptake experiments were made at room temperature. After incubation oocytes were rinsed with ice cold wash solution (100 mM choline chloride, 2 mM KCl, 1 mM $CaCl_2$, 1 mM $MgCl_2$, 5 mM HEPES/choline hydroxide, pH 8), and dissolved in 250 µl of 10% SDS for liquid scintillation counting.
KAAT1 induced uptake was calculated as the difference between the mean uptake measured in cRNA injected oocytes and the mean uptake measured in non-injected oocytes.

### 2.5.8 Thiol cross-linking experiments

Cross linking between cysteines was obtained by oxidation treatment in the presence of Cu(II)(1,10-phenanthroline)$_3$ (CuPh). For experiments in the absence of $Na^+$, oocytes were pre-incubated for 5 min in 0.2 mM CuPh dissolved in wash solution at pH 7.5; oxidation in the presence of $Na^+$ was conducted in uptake solution (for composition see previous section). The treatments were performed at room temperature unless stated otherwise. After incubation, oocytes were rinsed with Barth's solution at RT and then tested for amino acid uptake. The CuPh stock solutions (150 mM) were freshly prepared for each assay by mixing 60 µl of 250 mM $CuSO_4$ and 40 µl of 1.25 M 1,10-phenathroline dissolved in 1:1 water–ethanol mix. For the reduction experiments, after incubation with CuPh at RT, oocytes were washed with wash solution at pH 7.5 and incubated for 5 min with freshly prepared 12 mM dithiothreitol (DTT) in wash solution at pH 7.5, then rinsed with Barth's solution at RT and tested for amino acid uptake.

### 2.5.9 Electrophysiology

Transport currents generated by the activity of the KAAT1 wt and mutants were investigated by classical two-electrode voltage clamp experiments. Intracellular glass microelectrodes were filled with 3 M KCl and had tip resistances between 0.5 and 4 MΩ. Agar bridges (3% agar in 3 M KCl) connected the bath electrodes to the experimental

chamber. The holding potential was kept at − 60 mV. Data were recorded at a fixed voltage of − 60 mV (− 80 mV for $Na^+$ dependence experiment) or applying a typical protocol consisting of 200 ms voltage pulses spanning the range from − 160 to + 20 mV in 20 mV steps. Four pulses were averaged at each potential: signals were filtered at 1 kHz and sampled at 2 kHz. Data were analyzed using Clampfit 8.2 (Axon Instruments), and figures were prepared with Origin 7.5 (Microcal Software Inc., Northampton, MA, USA). The external control solution had the following composition: 98 mM NaCl, 1 mM $MgCl_2$, 1.8 mM $CaCl_2$, 5 mM HEPES free acid; in the other solutions NaCl was replaced by LiCl, KCl or TMACl. The pH was adjusted to 7.6 by adding the corresponding hydroxide for each alkali ion or TMAOH for $TMA^+$ solution. For the sodium dose response experiment, $Na^+$ was substituted by proportional amount of tetramethylammonium (TMA), the $Na^+$ concentrations used were 0.3, 1, 3, 10, 30, 60 and 98 mM. Amino acids (leucine, threonine, proline) at the saturating concentrations (3 mM for proline and threonine, 1 mM for leucine) were added to the same solutions to induce transport-associated currents. The oocyte was perfused continuously in a rapid solution exchange chamber (Warner Instruments model RC-1Z), and the washout time was estimated to be about 1 s.

### 2.5.10 Homology modeling

Fig. 1B was prepared using RasMol program. Homology modeling of KAAT1 was based on the crystal structure of LeuT with accession code 2A65.

# Chapter 3
# Investigation of the ion selectivity and coupling mechanism in the neutral amino acid transporter KAAT1

## 3.1 ABSTRACT[3]

This chapter gathers the results of the work performed aimed to find the structural basis of cation selectivity and chloride dependence of KAAT1. We found that the potassium selectivity in Na1 site is linked to the polarity provided by the KAAT1 specific residues Ser68 and Asp338. The analysis of Na2 site highlighted instead the role of flexibility provided by the presence of KAAT1 specific Gly407 that might allow the protein to exploit drivers with a bigger ionic radius, like potassium, apart from sodium.
The weak chloride dependence of KAAT1 was investigated collecting functional evidences of the fact that chloride interacts with the protein in different fashion if compared to other eukaryotic NSS transporters. KAAT1 is indeed able to realize the transport cycle independently from the negative charge required by the orthologs with an higher efficiency.
We have also found that the residue that bridges the Na binding sites, Threonine 67, is involved in the stereoselectivity of the transporter and in the mechanism by which chloride is able to influence the transport cycle. Moreover, it acts as a molecular hinge for the coupling mechanism allowing the conformational changes that are responsible for the exploitation of the energy coming from the downhill movement of sodium gradient to drive the uptake of the amino acids.

[3] The work regarding the uptake experiments performed on BetP presented in this chapter was carried out in the laboratory of Professor Christine Ziegler at the Department of Structural Biology, Max-von-Laue-Straße 03, D-60438, Frankfürt am Main, Germany.

## 3.2 INTRODUCTION

The first part of the chapter is investigating one of the most intriguing, as well as poor understood, aspects of the molecular physiology of the NSS transporters: the ion selectivity of the transport mechanism. In particular we have here analyzed the $Na^+/K^+$ selectivity of KAAT1 from a structural point of view at both Na1 and Na2 putative cation binding sites (nomenclature according to (Yamashita *et al.*, 2005)), implementing the already known information. Moreover, we have explored the structure of the putative chloride binding site of KAAT1 being this eukaryotic transporter characterized by a peculiar dependence from this anion that cannot be fully explained by the simple sequence comparison with the other members of the family (Forrest *et al.*, 2007; Zomot *et al.*, 2007; Bettè *et al.*, 2008; Kantcheva *et al.*, 2013; Penmatsa *et al.*, 2013). The second part of the chapter will address the role of a KAAT1 specific residue in an another pivotal feature of secondary active transport, the coupling mechanism, that we found in KAAT1 rely on the residue that bridges the two sodium binding sites.

### 3.2.1 The cation interaction among NSS members is more complex than expected

As described in the *Introduction* all NSS members exploit sodium ions as driving species. Some interesting peculiarities should be pointed out. First of all NSS members KAAT1, and its homologue CAATCH1, show a unique cation selectivity being activated, apart from $Na^+$, also by $K^+$ and by $Li^+$ (Castagna *et al.*, 1998; Feldman *et al.*, 2000). The fact that lithium can replace sodium is not uncommon and proved for some secondary active transporters and, since many years, also for some epithelial channels (Palmer, 1987): this is mainly due to the high similarity between these two cations from a physical-chemical point of view. In the GABA transporter GAT1 lithium can bind Na2 site eliciting pre-steady state currents but, in any case, it is not exploitable as driver ion (Zhou *et al.*, 2006). Different is the ability to employ potassium as driver: initially identified only in the two amino acid transporters from *Manduca sexta*, it was subsequently described for others nutrient amino acid transporters (NATs) from the insect world (Boudko, 2012). On the other side channels with a low selectivity between these two metals were also described (e.g. the ionotropic receptor for acetylcholine). $K^+$ is a key player also in the activity of another deeply studied NSS member, the serotonin transporter SERT, whose reorientation from the inward facing conformation, after the substrate release into the cytoplasm, is triggered by the binding of this cation (Rudnick, 2006).
In one of the two structural prototypes of the family, the leucine transporter LeuT, two cation binding sites were identified: "*The two sodium ions have key roles in stabilizing the $LeuT_{Aa}$ core, the unwound structures of TM1 and TM6, and the bound leucine molecule. Octahedral coordination of Na1 is provided by the leucine carboxy oxygen, the carbonyl oxygens of Ala 22 (TM1) and Thr 254 (TM6), the side-chain carbonyl oxygens of Asn 27 (TM1) and Asn 286 (TM7), and the hydroxyl oxygen of Thr 254 (TM6). In the biogenic amine transporters, an aspartate residue, located at position 24 in the $LeuT_{Aa}$ sequence,*

*probably coordinates a sodium ion equivalent to Na1. Na2 is positioned between the TM1 unwound region and TM8, about 7.0 Å from Na1 and 5.9 Å from the α-carbon of bound leucine. Trigonal bi-pyramidal coordination to Na2 is achieved by carbonyl oxygens from Gly 20 and Val 23 (TM1), Ala 351 (TM8), and the hydroxyl oxygens from Thr 354 and Ser 355 (TM8). Notably, coordination for both Na1 and Na2 is accomplished by partial charges from the protein, with the carboxy group of the bound leucine being the only ligand bearing a formal charge"* (Yamashita *et al.*, 2005). In $DAT_{cryst}$ (Penmatsa *et al.*, 2013) the sodium coordination shells coincide exactly with those of LeuT but some interestingly peculiarities should be pointed out. First of all, the organic substrate does not coordinate the sodium in Na1 site due to the fact that it lacks of the carboxyl group that is instead provided by the protein itself (the natural substrate, dopamine, is indeed void of a carboxyl group that characterizes amino acidic substrates). Furthermore, a water molecule was found coordinates the ion in this site through an H-bond network starting from Asp46 ($DAT_{cryst}$ numbering) in TM1 that thus participates indirectly to the coordination if the ion.

Regarding the nature of amino acid residues Na1 is the most conserved considering all NSS members. The corresponding position to LeuT Asn27 is highly conserved while position 286 is more variable and replaced by an aspartate in KAAT1 and in CAATCH1 (see below). Four out of the five members of Na2 site are highly conserved among eukaryotic NSS transporters, the same site is also the most conserved from a structural point of view in FIRL folded proteins and, moreover, its position relative to the TMs, is conserved even in proteins that show a Na independent activity, where a positive charge residue was here identified (Khafizov *et al.*, 2012; Kalayil *et al.*, 2013). Ser355 is almost completely conserved (rarely substituted by a threonine) but Thr254 is instead frequently replaced by a serine (also alanine is found in some eukaryotic transporters). As previously mentioned, in this site the GABA transporter GAT1 is able to bind lithium: the replacement in this carrier of the residue corresponding to LeuT Thr254 with an aspartic acid residue (Asp395, GAT1 numbering) is the key difference that allows the binding of lithium (Zhou *et al.*, 2006) that is active in inducing an enhancement of the sodium-dependent uptake of GABA (MacAulay *et al.*, 2002). It has also been proposed that in this protein the affinity for sodium is greater in Na1 site where, accordingly, also the organic substrate participates to its coordination shell (at least in GABA saturating conditions). Conversely, in the Na2 site, the affinity for this cation is lower as also testified by its ability to interact with lithium.

Among NSS members variability in sodium interaction properties was also found in terms of stoichiometry: for the glycine transporter GlyT2 was proposed a $Na^+$/glycine ratio of 3:1 and not the common 2:1 (that instead characterizes the isoform GlyT1). The Na1 site is conserved in both the isoforms. Na2 site in Glyt2 is very similar to that of LeuT but in the GlyT1 isoform it is lacking of the oxygen coordinating elements corresponding of those of LeuT Thr254 is consequently and less efficient in sodium binding. The hypothesis proposed is that the third site for $Na^+$ would be also present in GlyT1 but

exploited as second site instead of the common Na2 site shared with the other members of the family (Roux and Supplisson, 2000).
The role of sodium is clear being these proteins strictly dependent on the gradient of this cation to realize the uphill transport of organic solutes but, interestingly, is known that in the serotonin transporter SERT only one of the two sodium ions is released into the cell after the translocation cycle opening questions about the role of this interaction in terms of molecular physiology (Quick, 2003). The uncoupled currents elicited by NSS members deserve to be here mentioned. As already illustrated these currents can be recorded for many NSS proteins in absence of organic transportable substrates but in presence of a cation gradient. Beside these, when the cotransport mechanism is active, a flux of cations through the protein that exceed the total amount of charge indicated by stoichiometry, can also be measured (Andrini *et al.*, 2008; Giovanola *et al.*, 2012). Of interest in this direction is also the behavior of the NSS amino acid transporter CAATCH1 that, apart to be a classical secondary active transporter, is also a cation channel regulated by amino acids (Feldman *et al.*, 2000). The structural bases for these behaviors, as well their physiological meaning, are absolutely far to be elucidated but these currents indicate that the interaction with cations for NSS members (as well for other secondary active transporters) is more complex that the simple interaction in the binding site required for the ferrying of organic substrates (De Felice *et al.*, 2008).

### 3.2.2 The betaine transporter BetP: an useful tool for secondary active transporter structural studies

The BCCT (betaine-choline-carnitine transporters) family member BetP is a secondary active transporter involved in the ability of the soil bacteria *Corynebacterium glutamicum* to tolerate hyperosmotic shock (Ziegler *et al.*, 2010). After activation by the osmotic shock it reacts importing one molecule of glycine betaine coupled with two sodium ions to restore the cell turgor (Kramer and Morbach, 2004; Kramer, 2009;). BetP is an integral membrane protein with 595 amino acids forming 12 transmembrane helices, which harbor a negatively charged N-terminal domain of approximately 62 amino acids and a positively charged C-terminal domain of about 55 amino acids, both facing the cytoplasm (Ressl *et al.*, 2009). It is organized as a stable, asymmetric trimer: this organization is of crucial importance for the regulation of BetP activity triggered by osmolarity being BetP osmosentive only in its trimeric state (Perez *et al.*, 2011). The protocols used for BetP purification from *E. coli* cells and crystallization are well established and routinely applied making BetP a useful paradigm for the study of secondary active transporters, also from different families but related by the common FIRL fold (Perez *et al.*, 2012). An example of this is the recent identification of the sodium binding sites that were definitively assigned combining bioinformatic, structural and biochemical assays (Khafizov *et al.*, 2012): interestingly a BetP structure solved with sodium bound revealed that, as in other related transporters, Na2 site is located between transmembrane helices 1 and 8 of the FIRL fold.

### 3.2.3 Chloride dependence in NSS family

The chloride binding site for the GABA transporter GAT1 and for the serotonin transporter SERT was identified in 2007 (Forrest *et al.*, 2007; Zomot *et al.*, 2007). Quite interestingly this site was found be partially superimposed on the Na1 site for sodium that, in turns, it shares some residues with the substrate binding sites highlighting that "*intimate contact enables transport*" (Kanner, 2005). According to these researches the independence from this anion is achieved in prokaryotic transporters of the family thanks to the presence of a negative charge (Glu290, LeuT numbering), near the sodium binding sites and provided by an acidic residue located in the position occupied by chloride in $Cl^-$-dependent proteins (Fig. 11A, B). Recently, a crystal structure of a LeuT mutant, jointly to the chloride binding site described in $DAT_{cryst}$, definitely confirmed this hypothesis (Kantcheva *et al.*, 2013; Penmatsa *et al.*, 2013).

It is widely accepted that the transport mechanism rely on the presence of a negative charge (alternatively provided by chloride or by the protein): in absence of chloride the activity of the $Cl^-$-dependent transporters is deeply reduced but not completely abolished (generally less than 10% of the control conditions) (Forrest *et al.*, 2007; Zomot *et al.*, 2007). This indicate that a negative charge independent mode for the coupling mechanism is possible despite with a lower efficiency to that of the classical mode (Fig. 11C). It has been also proved that for GAT1 the hyperpolarization of the cell membrane abolishes the dependence from this anion and renders chloride replaceable by an hydroxyl ion (Lu *et al.*, 1999b); other evidences were gathered supporting a model in which, during the normal transport cycle, the chloride is not transported into the cells with the other substrates but its association with the transporter might occur only transiently by an in/out movement of the ion from the bulk solution to the protein and *vice versa* (Loo *et al.*, 2000). As already described (see the *Introduction* chapter) KAAT1 chloride dependence is only partial being the protein able to work in the absence of chloride with an efficiency that is higher than the 50% of that one elicited in control conditions (Bettè *et al.*, 2008). Despite some differential results for B0AT1 transporter (Bohmer *et al.*, 2005; Camargo *et al.*, 2005) this behavior has been evidenced also for other transporters (Broer, 2006; Margheritis *et al.*, 2013; Meleshkevitch *et al.*, 2013), remarkably, all active in the absorption of amino acids from the external environment (i.e. in intestinal and renal epithelial cells) even if they are also expressed in internal districts. In KAAT1 the corresponding position of LeuT Glu290 is occupied by a neutral polar residue as found in $Cl^-$-dependent carriers. The relative dependence of KAAT1 could be attributed to the presence near the putative chloride binding site of a negatively charged amino acid (aspartate 338), which could partially contributes the required negative charge; however, other neutral amino acid transporters (mammalian B0AT1 and B0AT2, IMINO, and others), that are $Cl^-$-independent, do not appear to have such negative residue in the adjacent regions of the sequence (Fig.1). For the IMINO (proline) transporter it has been suggested, that the chloride sensitivity depends on the substrate concentration (Broer, 2006), becoming minimal in substrate saturating conditions;

alternatively, for the same proteins, a "static chloride" model in which the anion would be exploited to stabilize their structure, was also proposed (Broer, 2008).

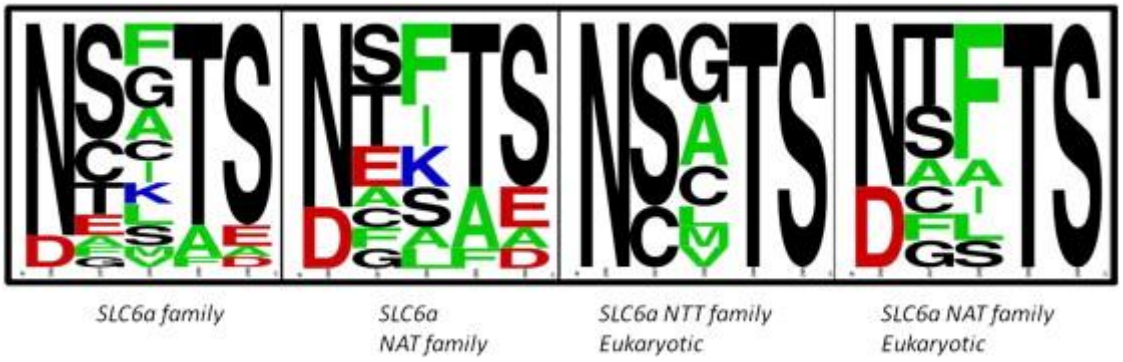


**Fig. 1** *Sequence logo representation of the chloride binding site in the SLC6A family.* The height of a given letter (amino acid residue) represents its frequency of occurrence at that particular position. The columns represent (from left to right): i) the main members of the SLC6A family from mammals, insects and bacteria, and including both neurotransmitter (NTT) and nutrient amino acid (NAT) transporters; ii) NATs from mammals, insect and bacteria; iii) eukaryotic NTT only; iv) eukaryotic NAT only. From (Margheritis *et al.*, 2013).

Trying to shed light on this articulated issue we have mutated KAAT1 putative chloride binding site looking for the structural reason of its peculiar chloride dependence and, at the same time, trying also to get more general insights into the role of this anion in the transport mechanism of NSS proteins.

## 3.3 RESULTS

### 3.3.1 An attempt to tune up the betaine transporter BetP as a structural model for KAAT1

KAAT1 and BetP belong to two different families. Despite this they should share the FIRL fold assuming that KAAT1, whose structure is unfortunately not yet known, is arranged as the NSS family models LeuT and $DAT_{cryst}$ (Yamashita *et al.*, 2005; Penmatsa *et al.*, 2013). Considering the structural conservation of the Na2 site among proteins with FIRL fold (Khafizov *et al.*, 2012), we explored the possibility to get a superimposition between the BetP Na2 site and the putative corresponding site of KAAT1. We concentrated our efforts on Na2 site considering the higher structural conservation among FIRL folded proteins. The alignment showed in Table 1 is only for the residues that define the ion binding sites in LeuT, $DAT_{cryst}$ and in KAAT1 according to the fact that in BetP these sites are located in a different position from that one predicted by LeuT model. Along years experimental data were gathered confirming that in KAAT1 ion binding sites are located in the positions predicted by comparison with LeuT crystal structure (Mari *et al.*, 2004; Castagna *et al.*, 2009).

In KAAT1 site/s sodium is better accommodated than potassium: $K_{50}$ for sodium is around 5 times lower than that for potassium (Castagna *et al.*, 1998). Another interesting

consideration about Na/K selectivity that must be considered is that the atomic radius of potassium ion is bigger than that of sodium suggesting that potassium binding sites should be bigger than those for sodium. The Na2 site is more similar between KAAT1 and BetP, especially in terms of polarity, compared to Na1 (Table 1).

| | LeuT | TM | Coordinating element | $DAT_{cryst}$ | Coordinating element | KAAT1 | BetP | Coordinating element |
|---|---|---|---|---|---|---|---|---|
| **Na1** | A22 | I | C=O(O) | A44 | C=O(O) | S68 | T426 | |
| | N27 | I | C=O(O) | N49 | R(Oδ1) | N73 | T250 | |
| | T254 | VI | R(O) | S320 | C=O(O) | S306 | F380 | |
| | N286 | VII | R(O) | N352 | R(Oδ1) | D338 | T499 | |
| | T254 | VI | R(O) | S320 | R(Oγ) | S306 | | |
| | *Leu* | *substrate* | *COOH(O)* | *D46* | *Indirect (H2O)* | | | |
| | | | | | | | | |
| **Na2** | G20 | I | C=O(O) | G42 | C=O(O) | A66 | A147 | C=O(O) |
| | V23 | I | C=O(O) | V45 | C=O(O) | V69 | M150 | C=O(O) |
| | A351 | VIII | C=O(O) | L417 | C=O(O) | L404 | F464 | C=O(O) |
| | T354 | VIII | R(O) | D420 | R(Oδ1) | G407 | T467 | R(O) |
| | S355 | VIII | R(O) | S421 | R(Oγ) | S408 | S468 | R(O) |

**Table 1:** *Amino acid residues forming Na1 and 2 ion binding sites in FIRL folded proteins LeuT, KAAT1 DAT and BetP.* Residues forming the sodium binding sites of KAAT1, DAT and LeuT are shown aligned in the corresponding position while those of BetP, not aligned with the previous ones, are reported according to (Khafizov *et al.*, 2012). Peculiar coordinating elements in each transporter are indicated in cursive. Indication of Transmembrane domains (TM) in which each residue is located as well its coordinating elements according to structures with PDB accession code 2A65 for LeuT, 4M48 for $DAT_{cryst}$ and 4AIN and 4DOJ for BetP, are also reported.

It is worth noting that while in Na2 site of $DAT_{cryst}$ the mean coordination distance fits very well with the theoretical coordination distance of 2.4 Å for sodium ion in solution, the same value in Na1 site is longer for sodium but shorter than the distance reported for $K^+$ ions (Penmatsa *et al.*, 2013). Assuming that ion coordination in KAAT1 in this site occurs as in LeuT (but the same should be true also if compared with $DAT_{cryst}$), the coordination of the ion could be realized by three carbonyl groups from the backbone of Ala66, Val69 and Ser306 and by the OH group from Ser408 with its side-chain. More difficult is the explaining of the coordinating role of G407 but, reasonably, it acts as a coordinating residue just with its carbonyl group (see later in this chapter). In BetP Na2 binding site the coordination shell is defined by three carbonyl groups (from Ala147, Met150 and Phe464) and by two lateral chains from Thr467 and Ser468, both of them bearing an OH group. As already known the mutation to Ala of these residues produces an increasing in the $K_{50}$ for sodium demonstrating their direct involvement in the coordination of the cation, as also demonstrated by structural data (Khafizov *et al.*, 2012).

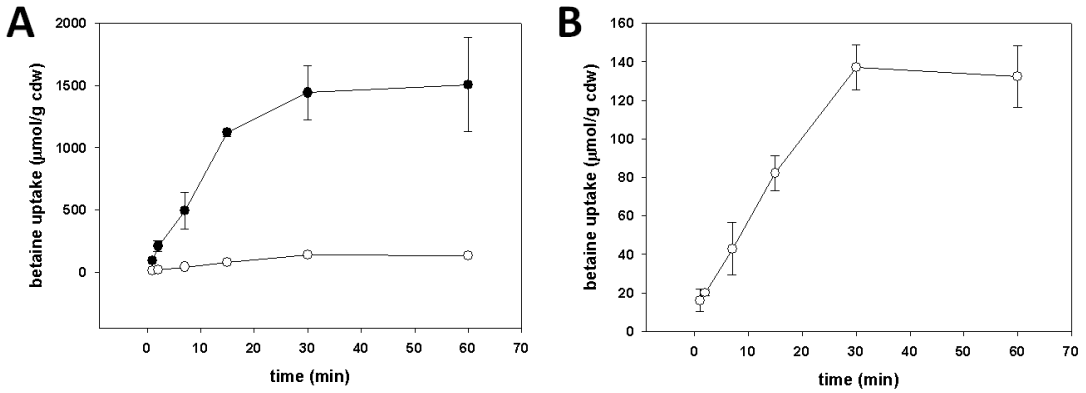


**Fig. 2**: *Betaine uptake induced by BetP T467A mutant expressed in E. coli cells.* (**A**): 500 µM [$^{14}$C]-betaine uptake induced by BetP T467A mutant expressed in *E. coli* strain MKH13 in presence of 100 mM Na (●) or K (○) chloride salt. (**B**): magnification of the uptake curve in presence of KCl curve from the plot in (A). Data are from a representative experiment and expressed as amount of betaine imported per unit of cell dry weight.

Considering the similarity between KAAT1 and BetP Na2 sites we explored the possibility to get insights into the structural determinants of potassium selectivity of KAAT1 reproducing by mutagenesis KAAT1 Na2 site in the corresponding binding site of BetP. We have tested the ability of BetP T467A, S468A and of T467A/S468A to induce betaine uptake applying high extracellular KCl in absence of sodium. The goal has been testing the possibility to gain ability to employ $K^+$ as driver ion incrementing the space in the Na binding site, as well as its hydrophobicity, to mimic the putative Na2 site of KAAT1. The activity of BetP mutants expressed in *E. coli* MKH13 strain, was tested applying 100 mM NaCl or KCl in the extracellular environment. Previous studies demonstrated that they are expressed at the same level in membrane (Khafizov *et al.*, 2012). In 7 out of the 8 independent experiments performed a betaine uptake in presence of 100 mM KCl (in absence of sodium) was observed for the T467A mutant in contrast to the wild type protein that was confirmed be completely unable to exploit potassium as driver ion. The S468A mutant, active in sodium gradient, was not active in presence of only KCl or, at least, the activity was lower than the detectable level and the double mutant was completely inactive (not shown). T467A potassium dependent betaine uptake was extremely lower if compared with that one in sodium but a curve with the classical trend of a saturable system was observed (Fig. 2B).

### 3.3.2 Mutagenesis of KAAT1 $Na^+$-binding sites

Cation selectivity of KAAT1 Na1 site was already partially investigated. This led to the identification of the Asp338 (KAAT1 numbering) that corresponds to an asparagine residue in both LeuT and $DAT_{cryst}$ Na1 site (Table 1): the mutation of this aspartate to asparagine abolishes the ability of KAAT1 to recognize potassium as driver also affecting the coupling mechanism of the transporter (Mari *et al.*, 2004). Interestingly this position

was found to interact with Lys102 in TM2 of KAAT1 (Castagna *et al.*, 2007): this interaction occurs transiently during the transport cycle (as also found in the prokaryotic transporter TnaT) and it indicates some relative movements in the TM domains of the four helix bundle that tilts relative to the rigid scaffold of transmembrane domains according to the rocking bundle mechanism proposed for FIRL folded proteins (Forrest *et al.*, 2009). In Na1 site Ser68 is not conserved among other members of the family where is normally substituted by an alanine (and, with less frequency, by serine, threonine, isoleucine or cysteine), and Ser306 is not conserved but substituted in a conservative manner (i.e, a neutral polar residue with a neutral polar residue) in the majority of the family members (in less than 10% of the eukaryotic proteins the position harbors alternatively an alanine). Looking for the structural basis of $K^+$ selectivity we mutated Ser68 to alanine and assayed its activity in presence of KCl after expression in *Xenopus laevis* oocytes. Results are shown in Fig. 3. S68A mutant showed an expression level comparable to wt (Fig.4) but around the 60% of the uptake in presence of NaCl but the activity was completely abolished when the driver ion was potassium indicating a complete impairment of the ability to recognize this ion and the involvement of Ser68 in potassium interaction at this site (Fig. 3A).

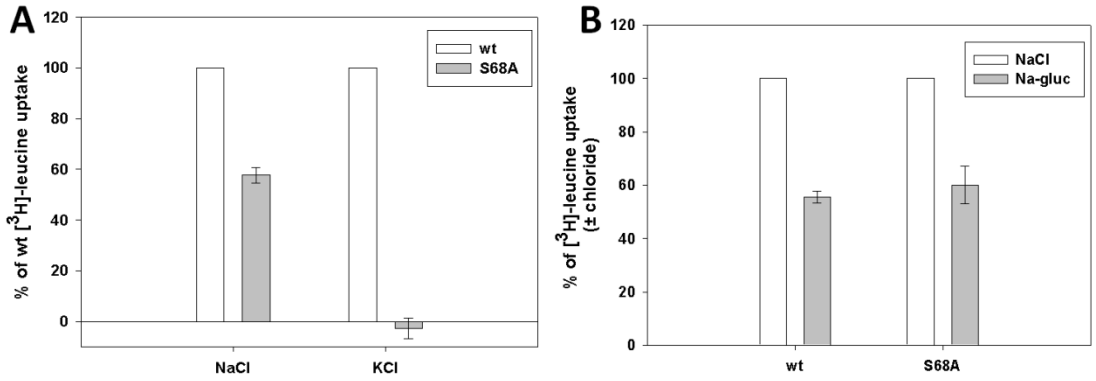


**Fig. 3.** *KAAT1 S68A mutant activity assayed in different conditions.* (**A**) 0.1 mM leucine uptake induced by KAAT1 wt (empty bars) or S68A mutant (filled bars) in presence of 100 mM NaCl or 150 mM KCl as indicated. Data are expressed as percentage ± S.E. of the uptake induced relatively to wild type protein in the same conditions from at least three independent experiments with oocytes from different batches. (**B**) Chloride dependence of KAAT1 S68A mutant compared to that of that of wt. 0.1 mM leucine uptake in absence of chloride was conducted replacing the 100 mM NaCl of control conditions (empty bars) with 100 mM of Na gluconate (filled bars). Data are expressed as percentage ± S.E. of the uptake induced in control conditions (i.e. in presence of chloride) from at least three independent experiments with oocytes from different batches.

We also built mutants of KAAT1 Na2 site that were assayed for the ability to exploit $K^+$ or $Li^+$ as driver. We have compared the sequences of KAAT1 Na2 site with other eukaryotic members of the NSS family sharing (CAATCH1) or not (GAT1, SERT, DAT and NET) its peculiar physiological features. The alignment is reported in table 2.

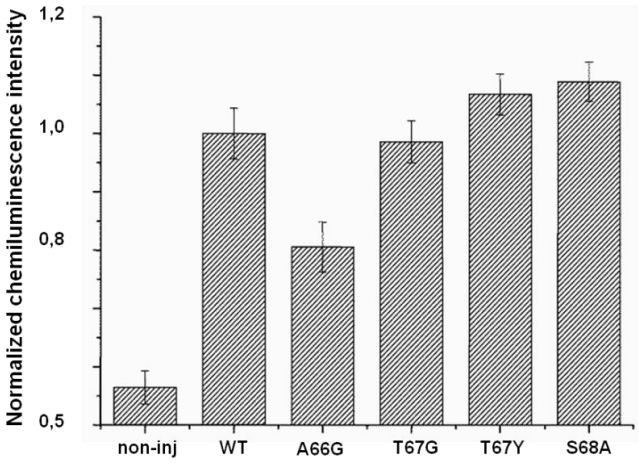


**Fig. 4** *Expression level of KAAT1 mutants of Ala66, Thr67 and Ser68.* The chemiluminescence detected from 20 to 40 oocytes from 3 different batches expressing the wt and the indicated mutants of KAAT1-FLAG and secondarily labeled with peroxidase-conjugated goat anti-mouse (IgG-HRP) are shown. The data were normalized to the mean value of the wild-type FLAG-KAAT1 of each batch of oocytes.

| KAAT1 | CAATCH1 | GAT1 | SERT | DAT | NET |
|---|---|---|---|---|---|
| **A66** | A66 | G59 | G94 | G42 | G71 |
| V69 | V69 | I62 | V23 | V45 | V74 |
| L404 | L404 | L392 | A351 | L417 | L415 |
| **G407** | G407 | D395 | T354 | D420 | D418 |
| S408 | S408 | S396 | S355 | S421 | S419 |

**Table 2.** *Residues forming Na2 binding sites in some eukaryotic insect and mammalian NSS family members.* DAT: dopamine transporter from *Drosophila melanogaster*; NET noradrenalin transporter.

From the alignment was immediately clear that two were the less conserved residues, namely the Ala66 and the Gly407. Also for these positions mutants were built and their cation selectivity functionally investigated in *Xenopus laevis* oocytes.

KAAT1 A66G was the first synthesized to evaluate the effect of lateral chain absence in this position as found in eukaryotic transporters (table 2) as well in other members of the family (glycine in this position is found in almost the 90% of NSS members). No significant effect of the mutation was found for A66G mutant neither for the expression levels nor for the activity being fully able to exploit $Na^+$ or $K^+$ as driver (Fig. 4, 5A).

The mutations against alanine, serine or threonine were instead created for Gly407 incrementing both polarity and dimension of the lateral chain of the residue in this position with the aim to assay the effect of these two parameters on the cation selectivity of Na2 site: position 407 (KAAT1 numbering) is indeed less conserved than 66 among NSS proteins.

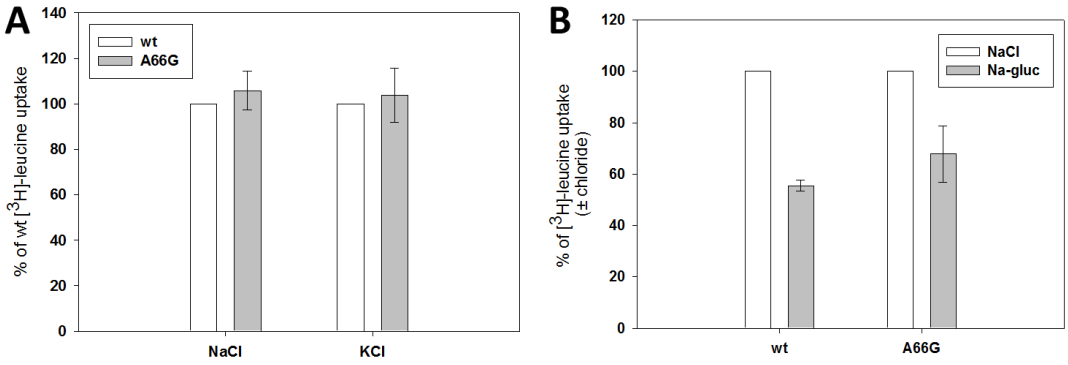


**Fig. 5.** *KAAT1 A66G mutant activity assayed in different conditions.* (**A**) 0.1 mM leucine uptake induced by KAAT1 wt (empty bars) or A66G mutant (filled bars) in presence of 100 mM NaCl or 150 mM KCl as indicated. Data are expressed as percentage ± S.E. of the uptake induced relatively to wild type protein in the same conditions from at least three independent experiments with oocytes from different batches. (**B**) Chloride dependence of KAAT1 A66G mutant compared to that of wt. 0.1 mM leucine uptake in absence of chloride was conducted replacing the 100 mM NaCl of control conditions (empty bars) with 100 mM of Na gluconate (filled bars). Data are expressed as percentage ± S.E. of the uptake induced in control conditions (i.e. in presence of chloride) and from at least three independent experiments with oocytes from different batches.

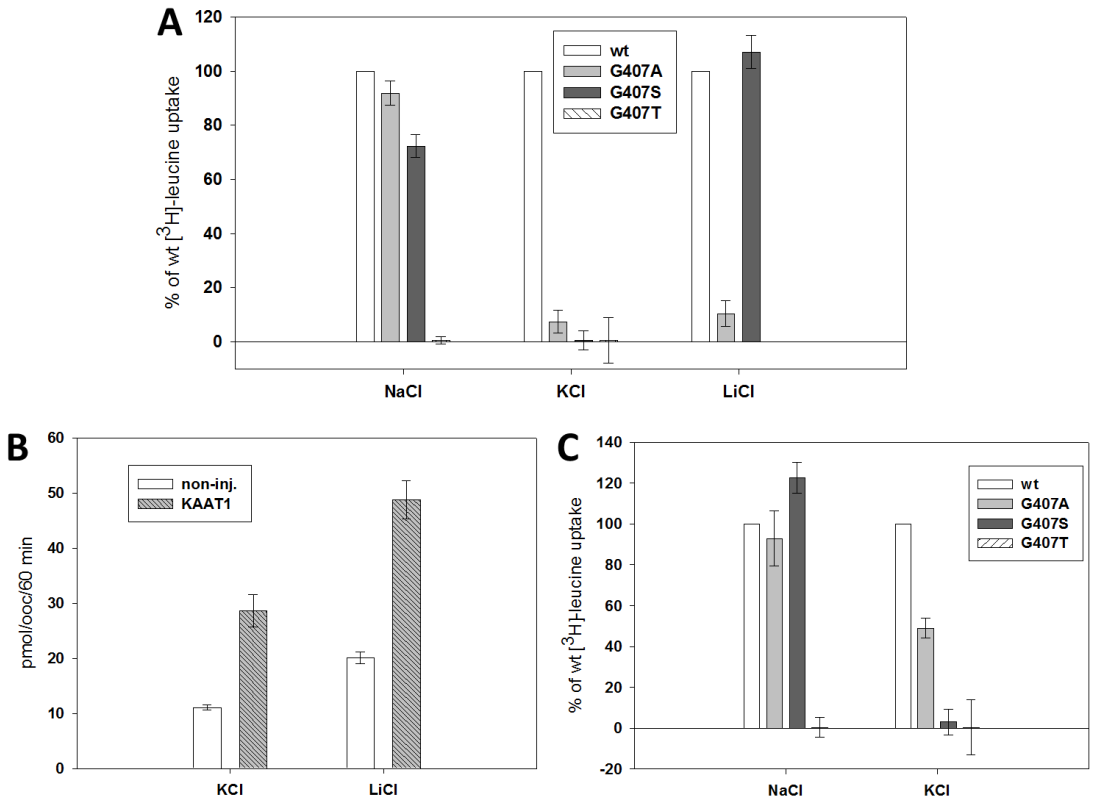


**Fig. 6.** *KAAT1 G407 mutants activity assayed in presence of $Na^+$, $K^+$ or $Li^+$ chloride salt.* 0.1 mM (**A**) or 1 mM (**C**) leucine uptake induced by KAAT1 wt, G407 mutants in presence of 100 mM NaCl or LiCl or 150 mM KCl as indicated. Data are expressed as the mean percentage ± S.E. of the uptake induced relatively to wild type protein in the same conditions from at least three independent experiments with oocytes from different batches. (**B**) 0.1 mM leucine uptake measured in KAAT1 wt expressing oocytes or in non-injected oocytes as a control, in the presence of 100 mM LiCl or 150 mM KCl. Data are means ± SE from 10 to 14 oocytes in a representative experiment.

In presence of 100 mM NaCl leucine uptake was slightly reduced to 90% and 70% of wt activity for G407A and G407S respectively (Fig. 6A). G407T mutant was void of transport activity even when substrate concentration was raised up to 1 mM (Fig. 6C). We therefore undertaken experiments aimed to verify the ability of the mutants to exploit $K^+$ and/or $Li^+$ as driver like known for the wild type. Mutants were assayed for leucine transport in presence of high extracellular $K^+$ and results are shown in figure 6A and C. Should be noted that the high extracellular KCl concentration has a depolarizing effect on oocytes counteracting the uptake of the amino acid. Despite this fact, in this condition KAAT1 is able to induce a significant amino acid uptake (Fig. 6B).
When the 0,1 mM leucine uptake was measured in presence of 150 mM KCl G407A and G407S activity was, respectively, lower than the 10% (compared to wt) or unappreciable, indicating that the mutations impaired the ability of the transporter to exploit potassium as driver (Fig. 6A). The inactivity of G407T mutant was again confirmed even in this case indicating a severe impairment of transporter function by this mutation. The enhancement of leucine concentration up to 1 mM in presence of KCl (Fig. 6C) significantly recovered the activity of G407A mutant but not for G407S mutant whose inactivity underlies the severe alteration of $K^+$ interaction at Na2 site. Moreover, the rescue of activity for the G407A mutant by the enhancement of organic substrate concentration also indicates an alteration of the kinetic parameters induced by the mutation. A kinetic measurement aimed to estimate $K_{50}$ and $V_{max}$ for substrate for this mutant will be the way to get confirmation (or not) to this hypothesis. The activity of mutants in presence of LiCl is also reported: G407A mutant showed a deeply reduced activity in presence of 100 mM LiCl but in the same conditions G407S mutant retained a full activity level.

### 3.3.3 Mutagenesis of KAAT1 $Cl^-$-binding site

Table 3 shows the alignment of KAAT1 residues forming the putative chloride binding site aligned with both chloride dependent (SERT and GAT1) and independent (LeuT and TnaT) proteins (according to (Forrest *et al.*, 2007) and (Zomot *et al.*, 2007)) for which this binding site has been already analyzed by mutagenesis. It should be noted that positions corresponding to KAAT1 Asp338 and Thr339 were differentially found to be chloride coordinating elements in the previous mentioned mutagenesis studies. This is the reason because their role has been investigated also in KAAT1 chloride dependence but, being the characterized $Cl^-$-binding site in LeuT E2920S mutant (Kantcheva *et al.*, 2013) an "artificial" site created by mutagenesis, the only native coordination shell for chloride, so far known, is that one described for $DAT_{cryst}$ (Penmatsa *et al.*, 2013). In $DAT_{cryst}$ a tetragonal coordination occurs to allocate the anion that comprises Tyr69, Gln316, Ser320 and Ser356 from TM2, 6 AND 7. In KAAT1 three out of the four positions (Table 3) are transversally conserved in the position corresponding to the

putative chloride binding site among proteins with a different dependence from this anion.

| KAAT1 | SERT | GAT1 | DAT | LeuT | TnaT |
|---|---|---|---|---|---|
| Y93 | Y121 | Y86 | Y69(OH) | Y47 | Y46 |
| Q302 | Q332 | Q291 | Q316(Nε) | Q250 | Q228 |
| S306 | S336 | S295 | S320(Oγ) | T254 | S332 |
| **D338** | N368 | N327 | *N352* | N286 | N264 |
| **T339** | C369 | S328 | *S353* | E287 | S265 |
| **S342** | S372 | S331 | S356(Oγ) | E290 | D268 |

**Table 3.** *Representative alignment of residues of chloride binding site in NSS family members.* Residues forming the chloride binding site in the chloride dependent transporter GAT1, SERT and DAT are shown aligned with the corresponding positions in the bacterial proteins LeuT and TnaT and with the putative chloride binding site of KAAT1. Investigated position are shown in bold letters. Non-coordinating residues in $DAT_{cryst}$ are reported in black cursive (see text for details) and coordinating atoms in $DAT_{cryst}$ are also provided (red).

In strictly agreement with the proposed model for chloride interaction among NSS proteins, KAAT1 should be chloride dependent bearing in the fourth position a neutral amino acid (Ser342) that corresponds to LeuT Glu290 (Table 3). This has not been verified from experiments (Bettè *et al.*, 2008) and the first hypothesis suggested a replacement role for the acidic position of KAAT1 (Asp338) that is only four position (one α-helix turn) before Ser342. With the aim to verify this hypothesis we introduced a negative charge in position 342 (S343E mutant) but we also tested the effect of the removing of the negative charge in position 338 of KAAT1 (D338N mutant). The goal was to get a protein fully chloride independent or dependent, respectively, to identify the structural reason of the weak chloride dependence that characterizes wild type KAAT1 challenging the functional model for the other transporters of the family. We have also mutated Thr339 against cysteine, glutamate or serine. The activity of these mutants as well the chloride dependence of some of them is showed in figure 7. The activity of the mutants ranged from the inactive S342E mutant to the two fold higher activity of T339C mutant. Apart from these cases the impact of the mutagenesis of the putative chloride binding site reduced the activity of the protein from the 50% to the 90% if compared to that of the wt protein. When gluconate replaced chloride (Fig. 7B) more interestingly results were observed but, unfortunately, due to the low activity level showed by some mutants (namely T339E, S342A, D338N/T339E and D338N/S342E), not all could be tested for the chloride dependence. The main finding was that the deletion of the negative charge in position 338 in D338N mutant did not alter the chloride dependence of KAAT1 allowing us to reject the hypothesis of a chloride vicarious role for this position and suggesting the existence of a transport scheme that does not rely on a negative charge whose more detailed description will be later provided in the final discussion.

Unfortunately the S342E mutant was inactive and this prevented us to assay the effect of the introduction of a negative charge in this position. Even when this serine was substituted with an alanine the activity was too low to be further investigated (indicating that this serine might exerts an important role in KAAT1 activity); the introduction of a cysteine gave instead an active mutant with a reduction of the chloride dependence (but not fully independent).

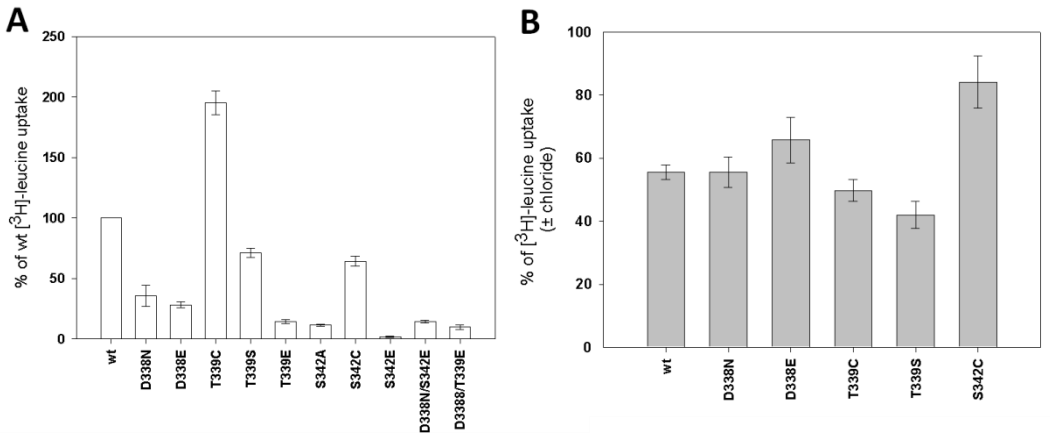


**Fig. 7.** *Activity and chloride dependence of KAAT1 mutants.* (**A**) 0.1 mM leucine uptake induced by KAAT1 wt and indicated mutants in presence of 100 mM NaCl. Data are expressed as percentage ± S.E. of the uptake induced by the wild type protein in the same conditions from at least three independent experiments with oocytes from different batches. (**B**) Chloride dependence of KAAT1 wt and mutants. 0.1 mM leucine uptake in absence of chloride was conducted replacing the 100 mM NaCl of control conditions with 100 mM of Na gluconate. Data are expressed as percentage ± S.E. of the uptake induced in control conditions (i.e. in presence of chloride) and from at least three independent experiments with oocytes from different batches.

Thr339 was investigated because the corresponding position in LeuT was originally proposed as alternative site able to provide a negative charge to the protein (Zomot *et al.*, 2007). It was mutated against cysteine and serine as found in the almost completely chloride dependent transporters GAT1 and SERT (see table 3) but also introducing a negative charge (with glutamate) as found in LeuT (Glu286; this residue, due to its higher pKa than that of Glu290, seems to be protonated at pH=7 and, consequently, probably not directly involved in providing the independence from $Cl^-$ ion, (Forrest *et al.*, 2007)). Glutamate introduction impaired the activity of the protein at a level that rendered the further step not investigable and T339C and T339S mutants did not show any alteration in the chloride dependence. We have also tried to measure the effect of the moving of the negative charge of Asp338 to Thr339 and Ser342 positions. The low activity of the two double mutants D338N/T339E and D338N/S342E unfortunately prevented us to test their $Cl^-$-dependence.

### 3.3.4 Threonine 67 is a key player in the coupling mechanism

Despite the increasing number of solved 3D structures, one of the less understood aspect, beside ion selectivity and dependence, is the coupling mechanism. Thr67 was identified

analyzing the ion binding sites in KAAT1 because of two main reasons: *i*) the degree of conservation and *ii*) its position in the 3D structure of KAAT1 according to model of the transporter built exploiting LeuT structure (PDB access code 2A65; (Yamashita *et al.*, 2005)) as template.

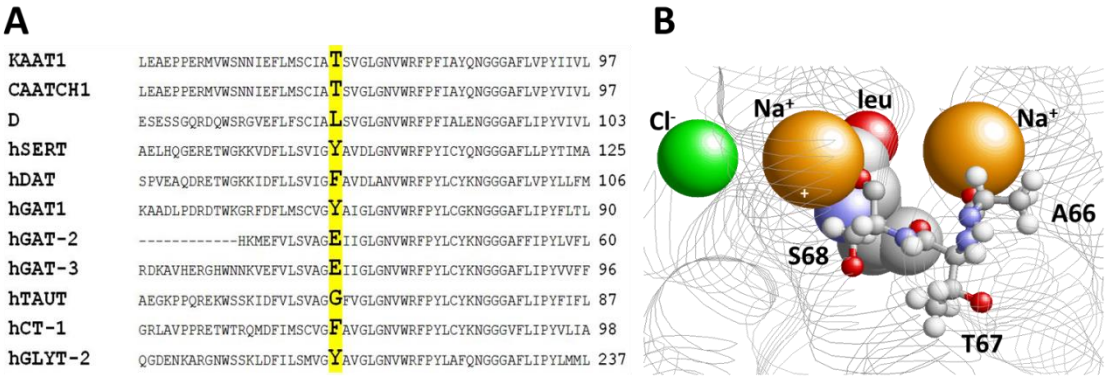


**Fig. 8.** (**A**) *Alignment of transmembrane domain I of some NSS members in the corresponding position of KAAT1 threonine 67 and the corresponding* (**B**) *3D model.* Sodium, leucine and chloride are shown in their putative binding sites. Ala66, Thr67 and Ser68 are shown as ball and stick representation. Please note the participation of Ser68 and Ala66 to Na1 and Na2 binding site respectively. $Cl^-$ is located in its putative chloride binding site according to (Forrest *et al.*, 2007; Zomot *et al.*, 2007). The 3D model of KAAT1 has been built basing the modeling on LeuT structure with PDB access code 2A65 (Yamashita *et al.*, 2005).

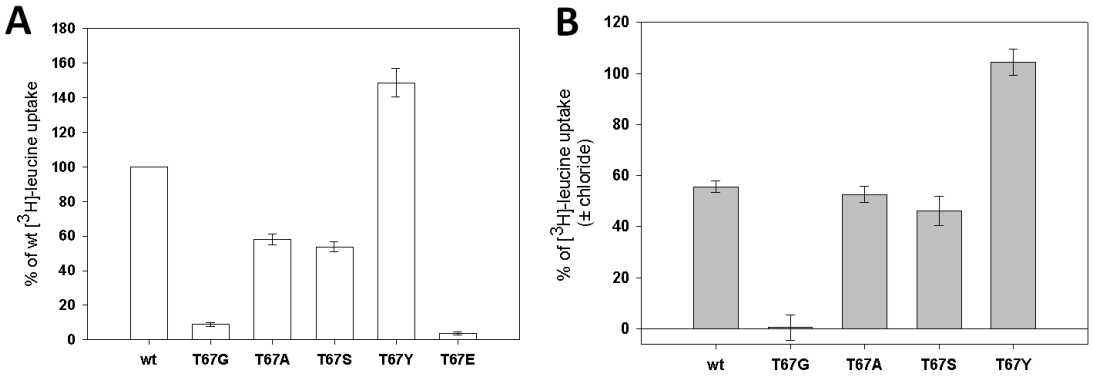


**Fig. 9.** *Activity and chloride dependence of KAAT1 threonine 67 mutants.* (**A**) 0.1 mM leucine uptake induced by KAAT1 wt and indicated mutants in presence of 100 mM NaCl. Data are expressed as percentage ± S.E. of the uptake induced relatively to wild type protein in the same conditions from at least three independent experiments with oocytes from different batches. (**B**) Chloride dependence of KAAT1 wt and mutants. 0.1 mM leucine uptake in absence of chloride was conducted replacing the 100 mM NaCl of control conditions with 100 mM of Na gluconate. Data are expressed as percentage ± S.E. of the uptake induced in control conditions (i.e. in presence of chloride) and from at least three independent experiments with oocytes from different batches.

The positions corresponding to Thr67 is not conserved among NSS members but, interestingly, is conserved as threonine only in 2 out of 250 analyzed NSS sequences that share some uniqueness in terms of molecular physiology, KAAT1 and CAATCH1 (Castagna *et al.*, 2009). More interestingly, when the position of Thr67 was investigated in the 3D model it was found to be in a keystone zone being the bridging position between the two sodium binding sites (Fig. 8) and, at the same time, a coordinator point for the

organic substrate. We therefore undertaken extensive mutagenesis studies aimed to clarify the role of Thr67 in KAAT1 transport activity. Position 67 was modified removing the later chain (T67G), substituting the native with a smaller one, both apolar (T67A) or polar (T67S), or bigger (T67Y) but was also tested the effect of the introduction of a negative (potentially formal) charge (T67E). The activity of the mutants is reported in Fig. 9A and the expression level of T67G and T67Y mutants is showed in Fig.4. The removing of the lateral chain as well the introduction of a glutamate residue had the major impact on the functionality of the transporter being the residual activity reduced of about the 90% and 95% of the wt activity respectively. The activity was reduced of the half for T67A and T67S mutants but, surprisingly, increased of almost 1.5 times for the mutant in which the threonine was substituted by a tyrosine. T67Y was the mutant in which we have mostly performed the studies to address the role of Thr67. Despite out of the putative binding site for chloride but considering that CAATCH1, that shares Thr67 with KAAT1, is also weak chloride dependent (Bettè *et al.*, 2008), we firstly challenged the mutants in absence of chloride finding very interesting result (Fig. 9B). The presence of the lateral chain in position 67 is required for the activity of KAAT1 in absence of chloride being T67G mutant completely inactive in this condition. The dependence was not modified for T67A and T67S but completely abolished introducing a bulkier, neutral, polar residue like the aromatic tyrosine in T67Y mutant. Considering the physical-chemical properties of the lateral chain of the native threonine, the modulation of the chloride dependence seems therefore to be related to the dimension of the lateral chain. In fact, reducing the dimension of the lateral chain with (T67A) or without (T67S) modifying its polarity did not affect the chloride dependence but removing it (T67G) or introducing in its stead a bigger, polar and neutral (only slightly more acidic) residue (T67Y) the protein was able to work in a chloride dependent or independent fashion respectively.

Being also the Thr67 flanking positions, Ala66 and Ser68, peculiar of KAAT1 and CAATCH1 (see previous section) we have also tested a possible role of these positions in the weak chloride dependence that characterizes the two insect transporters. Neither S68A nor A66G mutant showed altered chloride dependence (Fig. 3B, 5B).

Prompted by these results we have further investigated the role of Thr67 exploiting the high activity of T67Y mutant. Chemiluminescence analysis (Fig. 4) revealed that was expressed at the same level of wt in plasma membrane indicating, assuming the same number of active form of the protein *per* surface area unit, an increased activity of the mutant itself. This activity was still sodium dependent (Fig. 10B) and higher then that one of wild type even when KCl replaced NaCl (Fig. 10A) indicating that the ability to exploit potassium is not affected by the mutation and that the presence of the cation is required for the activation of the transport mechanism. No significant differences were found in the affinity for sodium between KAAT1 wt and T67Y indicating the structural integrity of the sodium binding sites but a lowering of the affinity for the cation was measured in absence of chloride for both proteins (Fig. 10C, D). Surprisingly, when the transport activity of T67Y mutant was assayed by electrophysiology we found clear evidences of an uncoupling effect of the mutation. As illustrated in the tape in Fig. 11A, the coupled

current elicited by this mutant was only the 20% of that one induced by the wild type in presence of NaCl despite the amount of amino acid transported (assayed by radiochemical assay, Fig. 9A) was higher than that of the wt. Also the uncoupled currents of the mutant were affected: as reported in Fig. 11C a consistent lithium and potassium leak currents were measured for KAAT1 wt but not for T67Y mutant indicating a severe impairment of the leakage pathway of the native transporter.

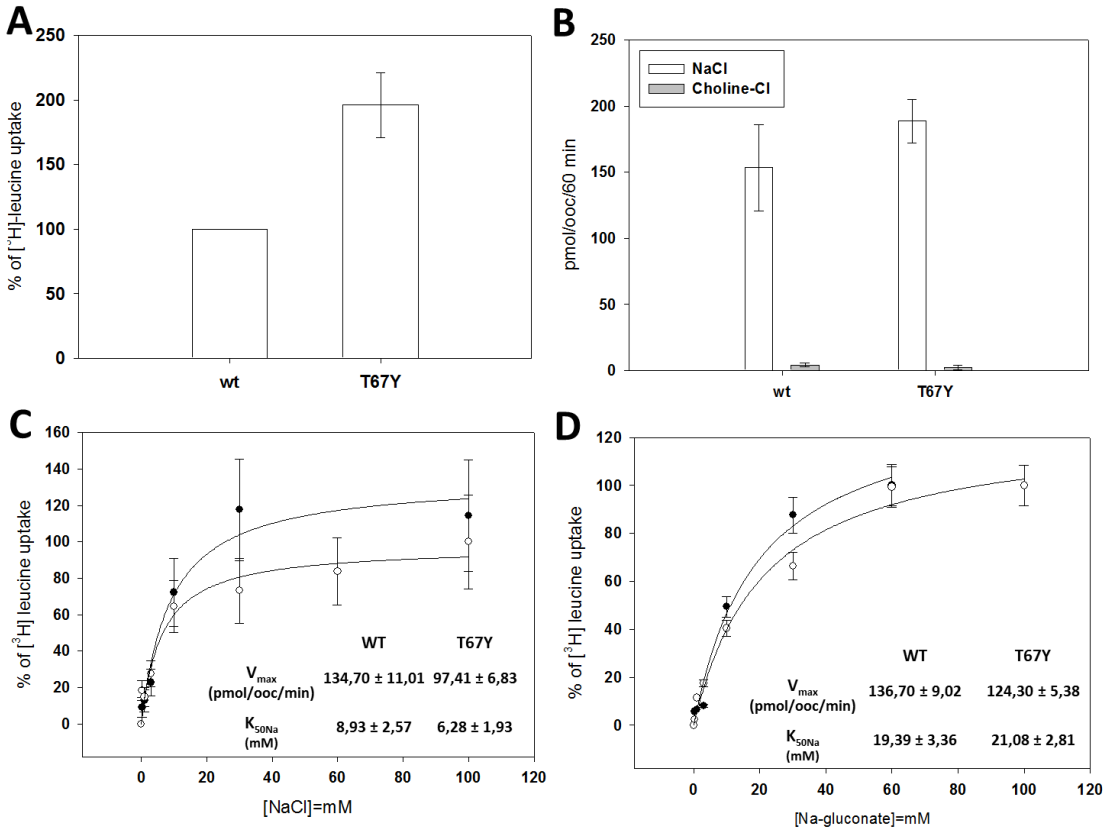


**Fig. 10.** *Characterization of KAAT1 T67Y mutant activity.* (**A**) 0.1 mM leucine uptake induced by KAAT1 wt and T67Y mutant in presence of 150 mM KCl. Data are expressed as percentage ± S.E. of the uptake induced relatively to wild type protein in the same conditions from at least three independent experiments with oocytes from different batches. (**B**) Sodium dependence of KAAT1 wt and T67Y mutant. 0.1 mM leucine uptake in presence 100 mM NaCl or 100 mM of choline chloride measured in oocytes for 60 minutes in the indicated conditions. Data are means ± SE from 10 to 14 oocytes in a representative experiment. (**C**, **D**) Measurement of sodium affinity for KAAT1 wt (●) and T67Y (○) in presence (C) or in absence (D) of chloride. The uptake of 0.1 mM leucine was measured in presence of increasing NaCl or Na-gluconate concentrations respectively. Data are expressed as percentage of uptake induced by the wild type in presence of 100 mM Na-salt for 5 minutes and expressed as percentage ± S.E.. Data are from a representative experiment.

From literature is known that the residue corresponding to Thr67 in KAAT1 is the Tyr95 in the serotonin transporter SERT. It has been previously reported that mutation of Tyr95 increased the ability of the protein to discriminate between R- and S-citalopram indicating a role in substrate selection for this residue (Henry *et al.*, 2006). Many insect transporters can transport, beside proteinogenic L-amino acids, their corresponding D-enantiomers (Geer, 1966; Miller *et al.*, 2008). KAAT1 is not fully stereoselective for L-amino acids. We have therefore performed a competition uptake experiment in which

the uptake of 0,1 mM [$^3$H]-L-leucine in presence of 100 mM NaCl was challenged applying unlabeled 4 mM D-leucine. In these conditions the activity of the wild type protein has been lowered of about the 80% but not completely abolished (as expected) and shown in figure 12. Of major interest was the result obtained for T67Y mutant whose activity was found be significantly less sensitive to the effect of D-leucine application. The inhibitory effect was, in fact, only of the 40% indicating that the mutation introduced an increasing in the stereoselectivity of the transport process.

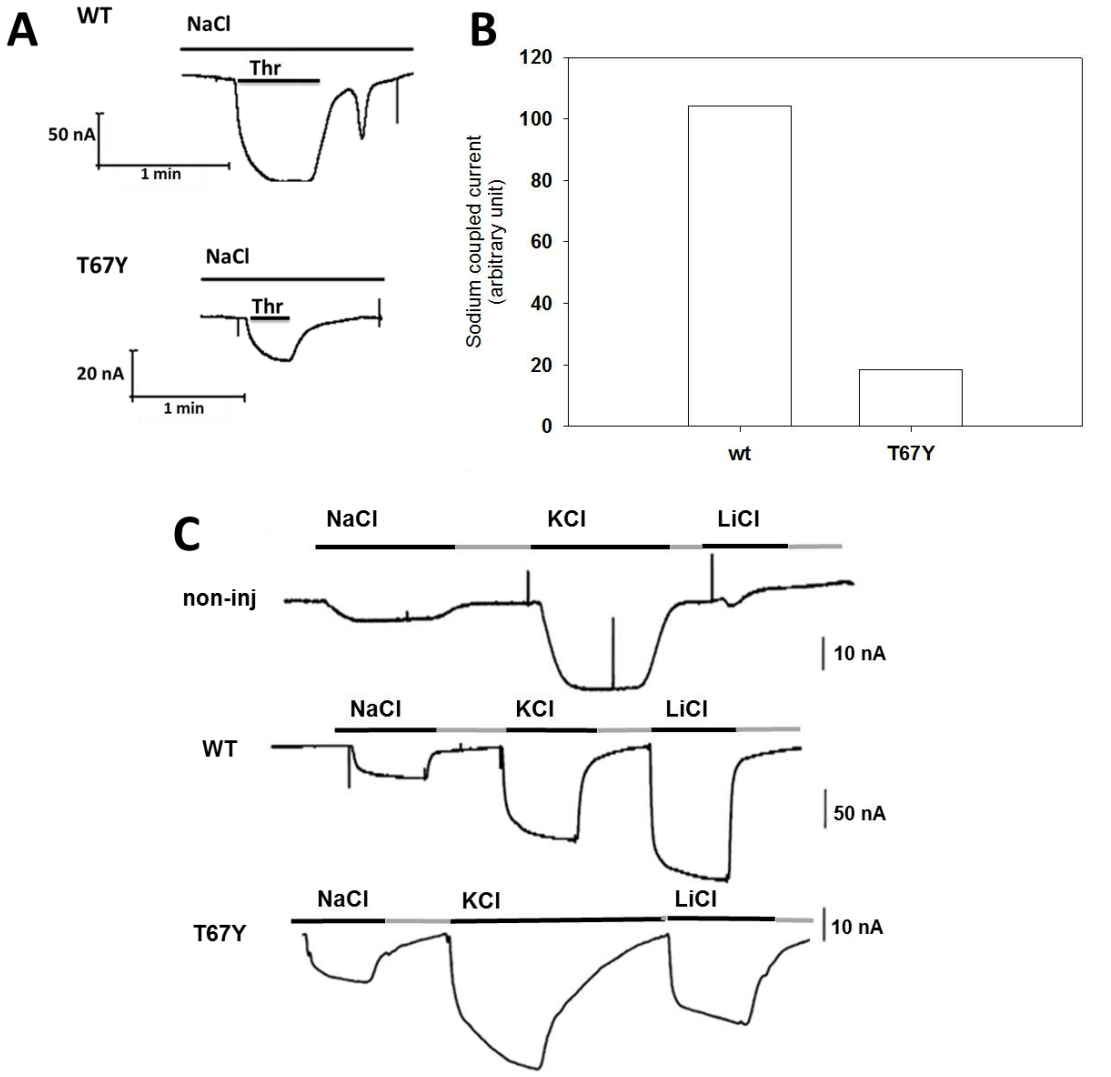


**Fig. 11.** *Recording of currents elicited by KAAT1 T67Y mutant.* The tapes are from a representative oocyte expressing wild type KAAT1 or T67Y mutant tested for the coupled (**A**) or uncoupled (**C**) currents. In (A) measurements were performed at the voltage to − 60 mV in a NaCl solution (upper line); the substrate, 3 mM threonine (lower bar), were added after stabilization of the current in sodium. (**B**) Quantification of the coupled currents from the tape in (A). Leak currents (B) were obtained by subtracting current in tetra-methyl-ammonium (TMA) solution from current in ion solutions containing $Na^+$, $Li^+$ or $K^+$ as the main cation in oocytes expressing KAAT1 wt or mutant. The difference in amplitude of the currents should be noted by the different reference value of the scale bar.

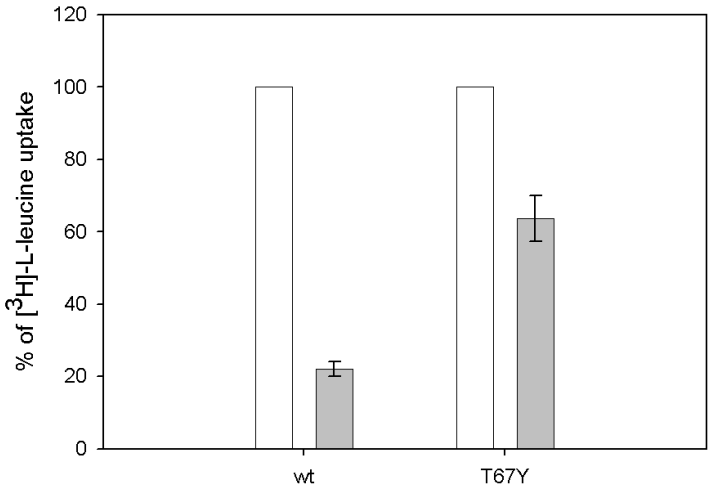


**Fig. 12.** *Stereoselectivity of KAAT1 T67Y mutant* 0.1 mM [$^3$H]-L-leucine uptake induced by KAAT1 wt and T67Y mutant in 100 mM NaCl in presence (filled bars) or not (empty bars) of 4 mM D-leucine. Data are expressed as percentage ± S.E. of the uptake induced relatively to wild type protein in absence of D-leucine from at least three independent experiments with oocytes from different batches.

## 3.4 DISCUSSION AND FUTURE INVESTIGATIONS

The indication of activity in presence of potassium chloride of T467A BetP mutant need to be further confirmed by means of different techniques exploiting the purified form of the protein. The measure of the $K_{50}$ was impaired by the low activity but the reconstitution in liposome should make its measuring easier. Soaking technique with rubidium as potassium tracer could allow getting structural information about the coordination of this cation. The structural evidence of rubidium coordination in BetP would be, jointly to the functional data, the only certain proof of a real coupling with potassium in this BetP mutant: the radiolabeled uptake of betaine performed in cells could be affected by the membrane depolarization imposed by potassium flux into the cells during uptake experiments, but also by the fact that the increased amount of intracellular potassium concentration into the cell could led to an indirect activation of BetP by the potassium flowed into the cell during the incubation (Ochrombel *et al.*, 2011).

The interaction of potassium with the Na1 site of KAAT1 was previously proved by mutagenesis (Mari *et al.*, 2004). Regarding the main differences in Na1 site between KAAT1 and the other NSS members these are linked to the presence of Asp338 and Ser68. Ser306 is also not conserved but is normally mutated in a conservative way (threonine instead of serine). The role of Asp338 was already illustrated (Mari *et al.*, 2004): an acidic amino acid is found in the 40% of prokaryotic NSS proteins (Beuming *et al.*, 2006) but the majority (especially eukaryotic ones) harbor in this position a neutral residue of asparagine. Confirming the importance of this site in potassium interaction we found that the elimination of the OH group of Ser68 completely impaired KAAT1

activity in presence of $K^+$ (Fig. 3A). Again, in almost all the members of the family this position is not polar as found in KAAT1, but substituted by an alanine (even though few of these proteins show a polar residue in this position like serine or cysteine). Taken together these data indicate that the potassium selectivity in KAAT1 Na1 site rely on the global polarity of the site provided by the concomitant presence of Asp338 and Ser68: when polarity is reduced by mutagenesis the protein loses the ability to exploit potassium but the use of sodium, despite reduced, is not completely abolished. A new interesting aspect of cation coordination was got from $DAT_{cryst}$ in which, as already described, a water molecule was found coordinates sodium in Na1 site being part of an hydrogen bond network that involves the Asp46 in TM1 of the transporter (Penmatsa *et al.*, 2013). In the corresponding position of DAT Asp46 KAAT1, interestingly, shows a glycine (Gly70) that is chemically unable to create this sort of interaction. The functional characterization of the reciprocal mutants could reveals new insight in cation selectivity of the two proteins. Data gathered on the activity of Na2 binding site mutants indicated that potassium binds also this site and this allows, for the first time, the inference that the stoichiometry of 2:1 cation:amino acid measured for $Na^+$ (Bossi *et al.*, 2000), is also true for potassium. The inactivity of G407T mutant could be explained in, at least, two ways: i) the introduction of a threonine in this position could impairs the interaction with the metal ion, regardless of its nature (sodium or potassium) or ii) the mutation disrupts the protein fold at a level that prevents the surface expression of the protein. In any case, considering the fact that the corresponding position in the majority of the bacterial NSS members is occupied by a threonine, the effect on KAAT1 activity highlights the importance of a glycine in this position of the Na2 site. An aspartate occupies this position in more than the half part of eukaryotic members, a glycine is found in around the 25% and, in a lower percentage of cases, is also replaced by a serine. Moreover, if the expression of this mutant in membrane will be confirmed this could suggest a hierarchy of importance between the two ion binding sites: in fact in G407T mutant, the unmodified Na1 site is alone unable to allow the cotransport process probably indicating that both the sites need to be functional for the transport activity or, in other terms, that Na1 site is not able to sustain KAAT1 transport activity. The modification of position 407 also deeply impaired the possibility to exploit potassium indicating the importance of the native glycine in determining the this unique feature of KAAT1 (Fig. 6A). The recovery of the activity observed for G407A mutant by enhancing the concentration of the leucine (Fig. 6C) could be explained with an effect of the mutation on the kinetic parameters ($V_{max}$ and/or $K_{50}$) for the substrate also indicating an effect of cation binding on the substrate interaction with KAAT1. This is also what was found in $DAT_{cryst}$ where a communication route was found exactly between Na2 site and the substrate binding site (see later). Glycine 407 appears to be the key residue that determine the cation selectivity in Na2 site of KAAT1. The mutation of the other less conserved Na2 residue (only the 5% eukaryotic NSS members show an alanine in this position), Ala66, did not modify the possibility to exploit potassium. The properties of lateral chain of position 407 influences the possibility to exploit a specific driver ion: the absence of the lateral chain in the native protein could allow the

accommodation of all the alkaline metals exploitable for coupling but when a apolar residue (alanine) is introduced the interaction with sodium is still possible but the activation by $K^+$ or by $Li^+$ is significantly reduced. When is also modified the polarity of the lateral chain introducing an hydroxyl group (serine instead of alanine) the interaction with potassium is completely impaired but is preserved the possibility to function with sodium or with lithium as well (Fig. 6A, C). LeuT Thr254 (table 1), that corresponds to KAAT1 Gly407, coordinates the $Na^+$ ion (and the substrate leucine) by means of its hydroxyl group on the lateral chain and by its backbone. Lacking of the lateral chain in position 407 of KAAT1 suggests that probably this glycine coordinates the ions by the oxygen atom of the carbonyl group but, introducing amino acids with a lateral chain, this role could be influenced by the dimensions and by the polarity of the same lateral chain (alanine substitution) or demanded to its coordinating atoms (for serine or threonine). These data suggest that the presence of a glycine in Na2 site of KAAT1 being void of the side-chain, could allow the protein to exploit drivers with a bigger ionic radius like potassium (lithium is indeed smaller than sodium) but the investigation deserve more attention. The membrane expression level of each mutant must be analyzed especially for the inactive G407T mutant. A full electrophysiological analysis of pre-steady state and uncoupled currents for all the cations tested is necessary to better define the type of alteration in cation interaction with the protein. Would be also interesting the building of reciprocal mutants in other members of the family trying to export some KAAT1 features into them as confirmation of data obtained for KAAT1. For instance, the substitution of the aspartate 395 with a glycine in the GABA transporter GAT1 (corresponding to Gly407 of KAAT1) could transfer the possibility to exploit potassium also in this protein.
The goal to identify the structural reasons of the weakly chloride dependence of KAAT1 was not reached. As already proved the interaction between KAAT1 and chloride occurs in a different fashion if compared to what occurs in the other eukaryotic proteins (Bettè *et al.*, 2008) despite the four coordinating positions found in the binding site of $DAT_{cryst}$ are identically conserved also in KAAT1 (Table 3) (Penmatsa *et al.*, 2013). As already reported in the absence of chloride the activity of $Cl^-$-dependent transporters is not completely abolished but only deeply reduced. This allows us to say that, apart from the classical coupling scheme reported in Fig. 13A and C (left), also a different modality is possible that coexists in the same protein with the classical one (named *chloride assisted mode*), that we can define as *negative charge independent mode* (Fig. 13C, right). Our investigation of the putative chloride binding site, allows us to extend this conclusion also at the structural level. In fact, as indicated by the results plotted in graphs of figure 7, we found that the negative charge of Asp338 is not able to replace the negative charge of chloride as occurs in bacterial proteins indicating that the negative charge independent mode is possible also for KAAT1. This is in full agreement with the fact that Asn352 of $DAT_{cryst,}$ the corresponding of KAAT1 Asp338 (Table 3) does not participate in chloride coordination (Penmatsa *et al.*, 2013). The main difference between KAAT1 and the other eukaryotic members of the family resides in the relative efficiency of the two kind of transport cycle modalities: assuming as reference the chloride assisted mode, the relative

efficiency of the alternative mode is for the chloride dependent proteins less than the 10% while in KAAT1 it reaches the 55% highlighting again that in KAAT1 the interaction with chloride occurs through different modalities. The role of chloride in the coupling mechanism of NSS proteins has not been fully elucidated yet. The most reasonable hypothesis indicates for this halide a role in the partial neutralization of the positive charge of sodium allowing an increase in the coupling rate for the transporter. Besides this, for the localization/movement of the ion, once bound the protein, some hypothesis has been already proposed and previously described in this thesis (see the *Introduction* of this chapter). As reported the weak chloride dependence (or the complete independence of some insect eukaryotic members (Boudko, 2012) and of all prokaryotic proteins) seems to be linked to the facing of the protein to the extracellular environment. For these proteins the role of chloride in the transport cycle is not easily explainable. For the neurotransmitter transporters (GAT1, SERT and DAT) the proposed model of chloride binding site as a site for the neutralization of the positive charge of sodium is, at least partially, able to explain the role of chloride in their molecular physiology. We can speculate that prokaryotic transporters did not evolve this dependence being these proteins counteracting an environment not always constant in its composition, in which the dependence from the availability of another ion, apart from sodium that is necessary for the activation of the transport, could be a disadvantage in terms of competition for nutrients. The solution was found in keeping the required negative charge constantly associated to the transporter (and varying its protonation state according to the different step of transport cycle (Zomot *et al.*, 2007). Evolution probably allowed the loosing of this adaptation in mammalian transporters being these proteins harbored in a system that steadily bath cells membrane with a fluid in which the chloride concentration is never limiting. Still open is the question regarding the evolutionary advantage gained by these molecules in acquiring the dependence from this anion (or, in other terms, why they have loose the negative charge reasonably present in their prokaryotic ancestor). More complicated is the case of proteins that face the extracellular environment in eukaryotic organisms that have evolved a similar or identical structure, in the putative chloride binding site, to those of mammalian strictly chloride dependent proteins but also a behavior that, somehow, is superimposable to that of bacterial members of the family. We can again speculate that this could be an evolutionary adaptation. It is easy to think to a common origin for eukaryotic NSSs. Those that are active in apical membranes of renal or intestinal epithelia are devoted to uptake their substrates in conditions not highly controlled as found by their homologues in the internal environment of the organisms. The loosing of chloride dependence could be a sort of exit strategy to renders the uptake less susceptible of variation of the environmental conditions. For some of these mammalian chloride independent proteins the absence of chloride do not modify the uptake capacity while for insect amino acid transporters the activity in absence of chloride is only the half part of that one in presence of the anion indicating a more complex role for this halide.

The role of threonine 67 in KAAT1 is quite intriguing because it seems to act as a sort of a molecular hinge for the coupling mechanism. The TM1 was found be involved in the switching between leak and coupling mode in the GABA transporter GAT1 (Kanner, 2003) and in this carrier mutants of the corresponding residue, Tyr60, were previously described: the reverse mutation to KAAT1 T67Y in GAT1 (Y60T mutant) induced an increasing in lithium leak current and in sodium dependence of the coupled currents (Kanner, 2003). In KAAT1, mutating this residue, we were able to influence the majority of the aspects of the transport mechanism. The mutation of the residue against tyrosine did not modify the sodium binding sites indeed the affinity for the ion was not modified (Fig. 10C, D). Interestingly the protein was fully active both in presence of sodium or in presence of potassium at least when assayed by radiochemical assays that measure the flux of the amino acid through the protein (Fig. 9A, 10A). When the currents associated to the transport process were measured by electrophysiological meanings, a deep dissection of the coupling mechanism was found (Fig. 11). T67Y mutant showed a flux of amino acid even higher of the wild type but only the 20% of this flux was coupled to sodium movement indicating that in the protein exist, at the same time, two ways by which the substrate could flow through the transporter. Around the 20% of the amino acid flows in the classic, weakly chloride dependent mode (data not shown) as for the native protein. The majority of the substrate amount pass instead through the protein by a mechanism that is uncoupled from the metal ion flux and not influenced by the presence of chloride (Fig. 9B, 13D). This anion was able to enhance T67Y mutant affinity for sodium but the same effect was found also for the wt protein (Fig. 10C, D). Interestingly in this mutant the relative efficiency of the negative charge independent mode has been raised up to the same level of the chloride assisted mode indicating an unbalancing effect of the mutation between the two transport modalities. Moreover, the uncoupled amino acid flux was strictly sodium dependent being completely abolished when choline replaced sodium in the uptake solution (Fig. 10B). This data suggests that in the mutant the acquiring of the conformation able to induce this amino acid flux is reachable only in presence of sodium. The mutation of Thr67 to Tyrosine altered also the conformation of the transporter that is active in allowing the passage of cations in absence of transportable organic substrates (uncoupled currents; see Fig. 11C) and, accordingly, the reciprocal mutant in the GABA transporter (GAT1 Y60T mutant) was previously found be characterized by increased uncoupled currents (Kanner, 2003). According to LeuT and DAT crystal structure Tyr67 should be involved in the organic substrate coordination: as already described for the serotonin transporter SERT (Henry *et al.*, 2006) the residue is involved in the optical selection that the protein operates on its substrates. The corresponding residue in $DAT_{cryst}$ is Phe43 that is involved with its carbonyl oxygen in a H-bond with the amino group of the bound nortriptyline (Penmatsa *et al.*, 2013). While for the serotonin transporter and for $DAT_{cryst}$ this is relevant especially for the interaction with unnatural ligands (drugs), for KAAT1 the significant of this result is different being the protein able to translocate also D-amino acids (Castagna *et al.*, 1998). Thr67 is a player in determining the balance between the preference of the transporter for the L- or D-stereoisomers. The

physiological significant of the ability of KAAT1 to import D-amino acid is not known but it is not uncommon for insects realize this kind of uptake and also to exploit D-amino acids as regulatory molecules (as also found in mammals).

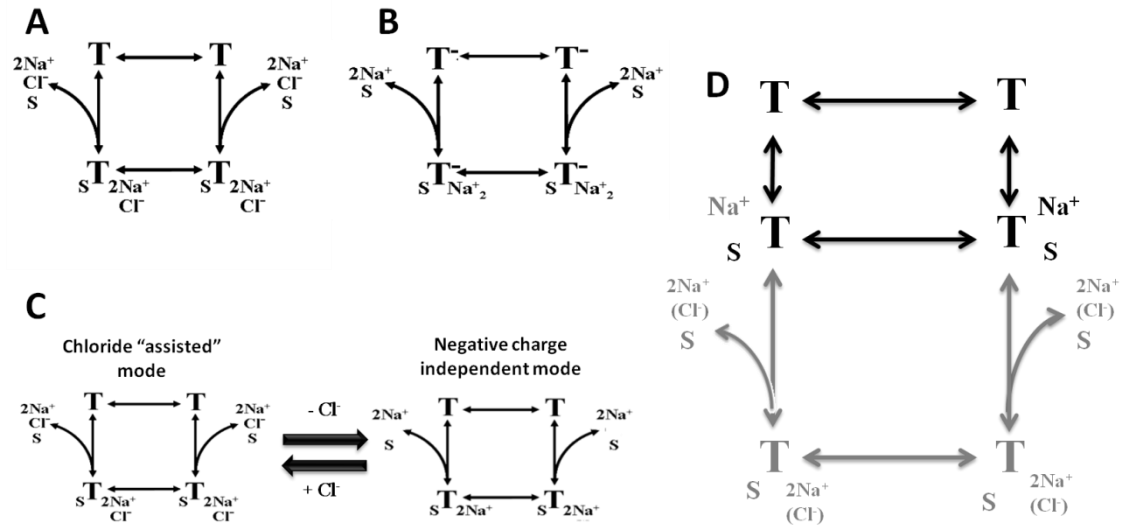


**Fig. 13.** *Coupling schemes for wt and mutant NSS mutants.* Schematic coupling scheme for a strictly chloride dependent (**A**) or independent (**B**) NSS transporter. Adapted from (Zomot *et al.*, 2007). Proposed alternative transport cycle modalities for KAAT1 wt (**C**) or T67Y (**D**) mutant. Legend: T, transporter; T-, transporter with formal negative charge; S, organic substrate. Brackets indicate the fact that what is indicated could be present or not without differences. The representation in grey indicates a branch of the pathway with smaller capacity in terms of total amount of transported amino acid. See text for details.

Our data support a model that assign a central role to threonine 67 in KAAT1 transport mechanism: this residue reasonably, acts as a coordinating point that allows, at a molecular level, the coupled transport at different stages of the translocation mechanism as well in the poor understood mechanism of the uncoupled cation flux through the transporter. In absence of organic substrates Thr67 participates to conformational changes that allow the cation leak through the protein: when it is substituted by a Tyrosine, somehow, the passage of cation closes almost completely. In a normal transport cycle, instead, this residue should be involved in the substrate recognition when it get access to its binding site but also in the mechanism that realizes the coupling between driven and driver fluxes and in the influence that $Cl^-$ exerts on the transport mechanism. The recently solved structure of $DAT_{cryst}$ showed us also how this could be possible. Phe43 (corresponding to KAAT1 Tyr47) is a member of a H-bond network that links the substrate binding site occupied by the drug, and the Na2 site. In particular Ser421 (KAAT1 Ser408), member of the Na2 site, is 3.5 Å from the propylamine group of nortryptilne and also forms an hydrogen bond with the carbonyl of Phe43. If this network exists also in KAAT1 this would involve Ser408 from Na2 site, Thr67, and, eventually, the substrate present in its binding pocket. We can therefore hypothesize that the effects that we saw mutating Thr67 could be attributed to the modification of this crosstalk also in KAAT1.

## 3.5 MATERIAL AND METHODS

### 3.5.1 Mutagenesis

Mutation in wt BetP were introduced by PCR with QuikChange® Site-Directed Mutagenesis kit according to manufacturer instructions on *strep*-BetP in pASK-IBA vector. Full sequencing of the gene confirmed the mutation.
KAAT1 mutants were obtained by PCR using high fidelity DNA polymerase *P.f.u.* (Promega). DNA sequencing (Primm s.r.l. laboratories, Milan, Italy) confirmed the mutations.

### 3.5.2 Oocyte harvesting and selection

Oocytes were obtained from adult female *X. laevis* frogs and manually defolliculated after treatment with 1 mg/ml Collagenase A (Roche, Germany) for 30–40 min at RT in $Ca^{++}$-free ORII medium (82.5 mM NaCl, 2 mM KCl, 1 mM $MgCl_2$, 5 mM HEPES/Tris, pH 7.5). Healthy V–VI stadium oocytes (Dumont, 1972) were then selected for injection and maintained at 16 °C in Barth's solution (88 mM NaCl, 1 mM KCl, 0.82 mM $MgSO_4$, 0.41 mM $CaCl_2$, 0.33 mM $Ca(NO_3)_2$, 2.4 mM $NaHCO_3$, 10 mM HEPES/Tris, pH 7.5) supplemented with 50 mg/l gentamicin sulfate and 2.5 mM sodium pyruvate.

### 3.5.3 Oocyte expression of KAAT1 wt and mutants

pSPORT-1 plasmid vector bearing KAAT1 wild type (wt) or the relative mutants were linearized by *Not1* digestion (Promega). Corresponding cRNAs were *in vitro* transcribed and capped using T7 RNA polymerase (Promega). Defolliculated oocytes were injected with 12.5 ng of cRNA dissolved in 50 nl of RNAse-free water via a manual microinjection system (Drummond). Before use, oocytes were maintained in Barth's solution at 16 °C supplemented as above described.

### 3.5.4 Uptake measurements for BetP

Uptake of [$^{14}$C]-betaine was measured in *E. coli* MKH13 cells. This strain has been engineered to be unable to uptake choline by BetT transporter, unable to synthesize glycine betaine (*betBA* gene deletion) and is also deleted for the genes *ProU*, *ProP* and *PutP* deputy to the uptake of compatible solutes. Cells expressing the strep-BetP mutants were cultivated at 37 °C in LB medium added with 50 µg/ml carbenecillin. The expression of BetP was induced at an OD of 0.5 adding 200 µg/l anhydrotetracycline to the cultures. After two hours cells were harvested by centrifugation and resuspended in resuspension buffer (50 mM TRIS pH 7,5, 40 mM glucose). For uptake measurements cells were incubated in the uptake buffers for 3 minutes at 37 °C before the addition of

[$^{14}$C]-betaine. Uptake experiments were performed in the following buffer: 100 mM NaCl or KCl, 25 mM TRIS pH 7,5, 20 mM glucose; final osmolarity 270,5 mOsm, 500 µM betaine. Cell samples were picked up at different time points, passed through a glass fiber filter (Millipore, Schwalbach, Germany) and washed twice with 0.6 M. KPi buffer. Filters where then collected and radioactivity retained counted by liquid scintillation counting.

### 3.5.5 Radiolabeled amino acid uptake in *Xenopus* oocytes

Amino acid uptake was evaluated 3 days after cRNA injection. Groups of 8–10 oocytes were incubated for 60 min in 120 µl of uptake solution (100 mM NaCl, 2 mM KCl, 1 mM $CaCl_2$, 1 mM $MgCl_2$, 5 mM HEPES/NaOH, pH 8) with 0.1 or 1 mM [$^3$H]-leucine. Alternatively, to evaluate uptake induced in the presence of lithium or potassium ions, NaCl was substituted by 100 mM LiCl or 150 mM KCl respectively. The affinity for $Na^+$ was estimated by measuring the uptake activity induced by KAAT1 wt or mutants for 5 minutes in presence of 0,1 mM [$^3$H]-leucine in the above indicated uptake solution with increasing concentration of NaCl or Na-gluconate (for experiments in absence of chloride). Uptake experiments were made at room temperature. After incubation oocytes were rinsed with ice cold wash solution (100 mM choline chloride, 2 mM KCl, 1 mM $CaCl_2$, 1 mM $MgCl_2$, 5 mM HEPES/choline hydroxide, pH 8), and dissolved in 250 µl of 10% SDS for liquid scintillation counting.
KAAT1 induced uptake was calculated as the difference between the mean uptake measured in cRNA injected oocytes and the mean uptake measured in non-injected oocytes.

### 3.5.6 Electrophysiological experiments

Transport currents generated by the activity of the KAAT1 wt and mutants were investigated by classical two-electrode voltage clamp experiments. Detailed procedure has been already described in chapter 2, *Materials and Methods* section. Briefly, data were recorded at a fixed voltage of − 60 mV. The external control solution had the following composition: 98 mM NaCl, 1 mM $MgCl_2$, 1.8 mM $CaCl_2$, 5 mM HEPES free acid; in the other solutions NaCl was replaced by LiCl, KCl or TMACl. The pH was adjusted to 7.6 by adding the corresponding hydroxide for each alkali ion or TMAOH for $TMA^+$ solution.

### 3.5.7 Chemiluminescence

Surface expression of the tagged transporters was detected using the monoclonal primary antibody anti-FLAG M2 (Sigma F3165, 1 µg/ml) and goat anti-mouse IgG secondary antibody labeled with HRP (Jackson ImmunoResearch Laboratories). Briefly, oocytes

expressing different FLAG-KAAT1 isoforms, as well as non-injected oocytes, were washed twice for 5 min in ice-cold ND96 (93.5 mM NaCl, 2mM KCl, 1.8 mM $CaCl_2{}^*2H_2O$, 2 mM $MgCl_2{}^*6H_2O$, 5 mM HEPES) pH 7.6. These were then fixed with 4% paraformaldehyde in ND96 for 15 min, rinsed 3 × 5 min with equal volumes of ND96, and then incubated for 1 h in a 1% BSA-ND96 blocking solution (used in subsequent antibody incubation steps). Next the oocytes were incubated for 1 h in mouse anti-FLAG M2 1 µg/ml, washed 6 × 3 min in 1% BSA ND96, incubated for 1 h in peroxidase-conjugated goat anti-mouse IgG (HRP-IgG) 1 µg/ml, washed 6 × 3 min in 1% BSA-ND96 and then 6 × 3 min in ND96 alone. For the chemiluminescence readings, oocytes were transferred into a 96 well plate (Assay Plate White not treated flat bottom-Corning Costar) filled with 50 µl of SuperSignal Femto (Pierce). Luminescence was quantified with a Tecan Infinity 200 microplate reader. The plates were read not later than 5 min after the transfer of the first oocyte. The data were then acquired at least three times in 10 min and for each oocyte the mean of three readings was calculated. Results were normalized to the mean value of FLAG-KAAT1 wt for each batch and are plotted as relative chemiluminescence intensity.

### 3.5.8 Homology modeling

Fig. 9B was prepared using RasMol program. Homology modeling of KAAT1 was based on the crystal structure of LeuT with accession code 2A65.

# Chapter 4
# Preliminary investigation of Baculovirus expression system as a candidate for KAAT1 expression and purification from insect Sf9 cell line

## 4.1 ABSTRACT[4]

In this chapter is described the first attempt to find a suitable eukaryotic expression system for KAAT1 aimed to get it in a purified, stable and active form in enough amount to perform structural studies. Being KAAT1 expressed in lepidopteran cells we exploited the Baculovirus expression system and insect Sf9 cell line to express two differently tagged form of KAAT1 (with FLAG and His tags) whose expression was obtained at promising level. Despite not completely exhaustive, exploiting the introduced tags some further steps for its purification from Sf9 membranes were carried out whose results indicated the feasibility of this production and purification approach for this NSS transporter.

[4] The work here presented was carried out in the laboratory of Professor Christine Ziegler at the Department of Structural Biology, Max-von-Laue-Straße 03, D-60438, Frankfürt am Main, Germany.

## 4.2 INTRODUCTION[5]

### 4.2.1 Overview on Baculovirus expression system

Baculoviruses are viruses that exploit insect cells for their replication, specifically their life cycle takes place in ovarian tissue of lepidopteran larvae. A recombinant baculovirus used for protein expression is a baculovirus that has been genetically modified to bear a foreign gene that can be expressed in insect cell lines under the control of a virus gene promoter (Smith *et al.*, 1983). The most common used cell lines are Sf21 and its derived clone Sf9 that were derived from *Spodoptera frugiperda*. We used a system based on *Autographa californica* nucleopolyhedrovirus (AcMNPV; FlahBAC system, *Oxford Expression Technologies*). AcMNPV (Ayres *et al.*, 1994) has a circular double stranded DNA genome (134 Kbp) packaged in a rod shaped nucleocapsid whose volume can be easily enhanced to accommodate a bigger genome. The life cycle of the virus is phased in two stages in which viruses can be found as budded virus (BV) or as occlusion derived virus (ODV). BVs are exploited as carrier for the expression of the foreign genes being thousand times more infectious for cultured cells (Volkman and Summers, 1977). A lot of occlusion bodies (OB) are normally found in late stages of infection that are also known as polyhedra. These structures are got from the aggregation of OBs enclosed in an envelope, acquired *de novo* in the nucleus, and embedded within the para-crystalline matrix of the OB/polyhedra. The major component of the OB matrix is polyhedrin (Rohrmann, 1986), a protein that is produced by the powerful transcriptional activity of the polyhedrin gene (*polh*) promoter[6]. OBs protect the virus in the passage between different hosts and within the environment. In most of the Baculovirus based expression systems the *polh* gene is deleted and this makes virus unable to survive out from the cell cultures. The strong *pohl* promoter is instead maintained in the recombinant virus to drive the expression of the foreign gene.

Advantages over bacterial expression system include the safety of usage, the possibility to get the expression of genes independently from their dimensions under the control of a very strong promoter. Being insect cells eukaryotic the proteins expressed are commonly properly folded and functional bearing all the post translational modifications whose introduction is not possible in prokaryotic system. The labour-intensive and technically demanding steps needed to produce and maintain recombinant virus stocks are the main drawbacks of this system.

The baculovirus genome is too large to directly allocate the insertion of a foreign gene. Instead the foreign gene is cloned into a transfer vector, which contains sequences that flank the polyhedrin gene in the virus genome. The virus genome and the transfer vector are introduced into the host insect cells and homologous recombination, between the flanking sequences common to both DNA molecules, effects the insertion of the foreign

[5] The Introduction of this chapter has been summarized from the usage guidelines provided with flashBAC™ kit purchased from *Oxford Expression Technologies* where more detailed information are available (www.oetltd.com).

[6] Patent applications EP1144666, WO0112829, AU6460800.

gene into the virus genome, resulting in a recombinant virus genome. The genome then replicates to produce recombinant virus (BV phenotype only, as the polyhedrin gene is no longer functional), which can be harvested from the culture medium.

### 4.2.2 The flashBAC™ system (Oxford Expression Technologies)

FlashBAC™ system[7] has been specifically designed to remove the need to separate recombinant virus from parental virus by plaque purification or any other means (necessary for the first systems that exploited Baculoviruses). The production of recombinant virus has been reduced to a one-step procedure in insect cells and is thus fully amenable to high throughput and automated production systems. The AcMNPV genome exploited in this system lacks part of an essential gene (ORF 1629; (Possee and Howard, 1987)) but it contains a bacterial artificial chromosome (BAC) at the polyhedrin gene locus, replacing the polyhedrin coding region. The essential gene deletion prevents virus replication within insect cells but the BAC allows the viral DNA to be maintained and propagated, as a circular genome, within bacterial cells. A recombinant baculovirus is produced by simply transfecting insect cells with flashBAC DNA and a transfer vector containing the gene of interest. Homologous recombination within the insect cells restores the function of the essential gene allowing the virus DNA to replicate and produce virus particles and simultaneously inserts the foreign gene under the control of the polyhedrin gene promoter removing the BAC sequence. The recombinant virus genome, with the restored essential gene, replicates to produce BV that can be harvested from the culture medium of the transfected insect cells. As it is not possible for non-recombinant virus to replicate there is no need for any selection system. The flashBAC system also facilitates membrane protein targeting. Baculovirus genome contains several auxiliary genes, which are non-essential for replication in insect cell cultures. One of these is chitinase (*chiA*), which encodes an enzyme with exo- and endochitinase activity (Hawtin *et al.*, 1995). Deletion of *chiA* from flashBAC has improved the efficacy of the secretory pathway and resulted in a greatly enhanced (up to 60-fold in some instances) yield of membrane targeted recombinant proteins (in comparison with recombinant viruses that synthesize chitinase).
The main bottleneck in the obtaining of structural data for eukaryotic proteins is the high number of difficulties that prevent the obtaining of enough amount of purified protein. The choice of the best expression system in of extreme importance to achieve this result. Being KAAT1 cloned from insect cells of *Manduca sexta* larvae (Castagna *et al.*, 1998) we though to exploit the excellent properties of Baculovirus expression system to heterologously express KAAT1 in *Spodoptera frugiperda* cell line (Sf9). We also carried out some preliminary analysis to investigate the possibility to get KAAT1 out from Sf9 membranes for further steps of purification.

[7] Patent applications EP1144666, WO0112829, AU6460800.

## 4.3 RESULTS

### 4.3.1 KAAT1 expression in Sf9 cell line

Two different tagged form of KAAT1 were generated to create a protein that could be purified from cell membranes using commercial available tools, namely the Ni-NTA column and/or the anti-FLAG column. The FLAG-tagged form of KAAT1 described in chapter 2 was cloned in pVL1393 vector to get a double tagged construct with the FLAG epitope in the second extracellular loop and with a 7-histidine tag at the C-terminus (KAAT1-FH). KAAT1-CFH was instead generated cloning KAAT1 into the pVL-FH vector obtaining at the same time the introduction of both FLAG and a 8-histidine tag at the C-terminus domain of the protein.

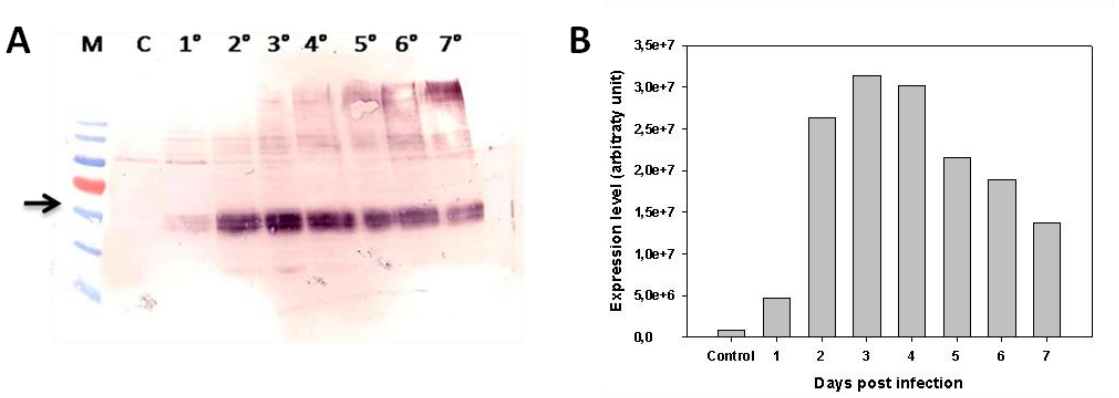


**Fig. 1**: *Expression test for KAAT1-FH in Sf9 cells.* **(A)**: WB against FLAG epitope. M: molecular weight marker. C: non infected cells. Numbers indicate the day of cell collection after infection. Arrow corresponds to a MW of 60 kDa. **(B)**: quantification of Western blot band intensity.

Sf9 cells were infected in an adherent monolayer culture with a multiplicity of infection of 10 with the Baculoviruses bearing the genes for KAAT1-FH or for KAAT1-CFH and collected each 24 hours for seven days after infection. KAAT1 expression was evaluated by means of Western blot analysis applied on cells lysed with SDS (see *Materials and methods* section). The results are shown in figure 1 and 2 for KAAT1-FH and -CFH respectively.

WB qualitative analysis indicated that both KAAT1 constructs were expressed by Sf9 cells at good levels. The protein (molecular weight of about 60 kDa) was detected since the first day post infection (d.p.i) for KAAT1-FH and from the third d.p.i for KAAT1-CFH. The highest expression level was at the third and at the fifth d.p.i for KAAT1-FH and CFH respectively. No significant aggregated forms of the proteins were detected. Bands of lower molecular weight than expected for KAAT1 were detected in each d.p.i for CFH construct in a relative intensity comparable to that of the protein, probably due to a more susceptibility to degradation of this construct compared to KAAT1-FH.

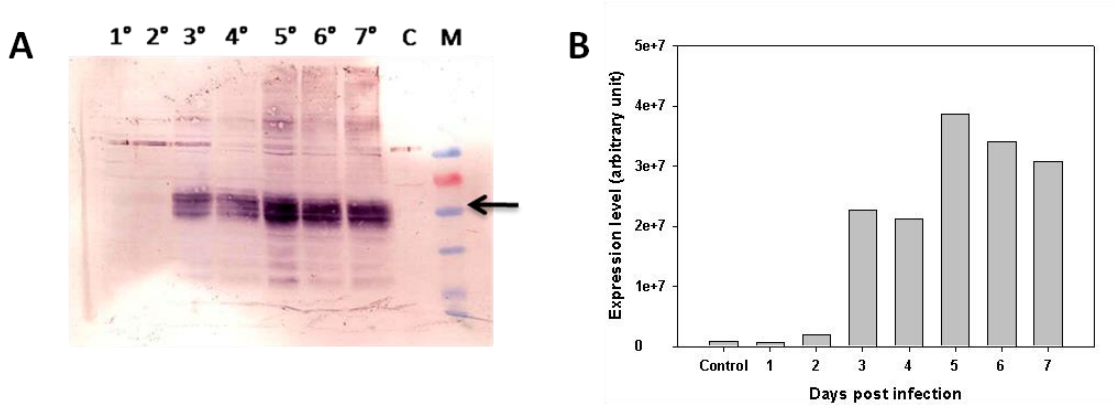


Fig. 2: *Expression test for KAAT1-CFH in Sf9 cells.* (A): WB against FLAG epitope. M: molecular weight marker. C: non infected cells. Numbers indicate the day of cell collection after infection. Arrow corresponds to a MW of 60 kDa. (**B**): quantification of band intensity.

### 4.3.2 Detergent screening

For this test we choose KAAT1-FH construct instead of KAAT1-CFH because characterized by a lower evidence of protein degradation. The productive culture production gave a concentration of 10 mg/ml of proteins in membrane preparations after the preparation procedure describe in *Materials and Methods* section. To get membrane proteins out from the membrane in a folded and stable conformation, the choice of a proper detergent is of pivotal importance. We applied the most common mild detergents used for membrane protein purification and/or crystallization to membrane samples got from a shaking culture of Sf9 cells expressing KAAT-FH at the third d.p.i. After solubilization trial supernatant and pellet of non-solubilized material were both analyzed by WB to explore the ability of the detergent to extract the protein completely out from the membrane (Fig. 3).

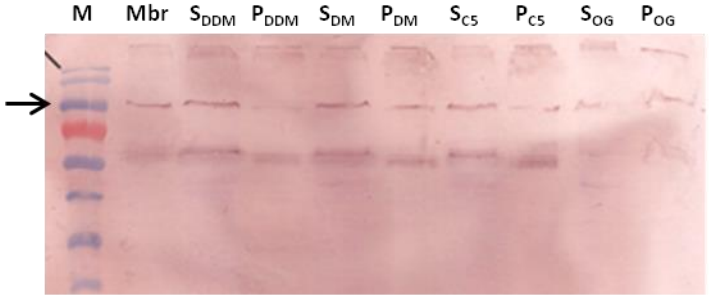


**Fig. 3.** *Solubilization test for Sf9 cell membranes expressing KAAT1-FH.* The result of the WB analysis after solubilization is shown for each detergent used. M: molecular weight marker; Mbr: not solubilized membrane expressing KAAT1-FH. After solubilization in a solution of 2% of each of the indicated detergents, solubilized (S) and pellet material (P) got after solubilization were loaded on 12.5% PAA gel and analyzed afterwards by WB using an antibody against FLAG epitope. Arrow corresponds to a MW of 60 kDa. Legend: DM (n-decyl-β-D-maltopyranoside), DDM (n-dodecyl-β-D-maltopyranoside), C5 (Cymal-5; 5-Cyclohexyl-1-Pentyl-β-D-Maltoside) and OG (n-octyl-β-D-glucopyranosyde).

Three out of the four detergents screened worked as solubilizing agent for KAAT-FH, namely DDM, DM and Cymal-5. The signal from the sample for the solubilization test carried out with OG did not get any result. DM and DDM worked better than Cymal-5. DDM seems had worked better than others being the signal at the correct molecular weight concentrated only in the solubilized fraction but no further conclusions could be gathered due to a low KAAT1-FH expression in the cell batch: this was not comparable to that one got from the expression test due to a wrong estimation of the virus titer of the stock used for the infection of productive cultures.

### 4.3.3 Purification trial

On the same batch of membranes used for detergent screening we applied 2% DDM for 1 hour at 4°C with the aim to get the protein completely out from the membranes and apply a little scale purification test. To do so (see *Materials and Methods* section for details) after solubilization the non-solubilized material was removed by centrifugation and the supernatant applied to a Ni-NTA column. Protein elution was monitored by Bradford assay and positive fractions were pulled together and applied again on an anti-FLAG column. The positive fractions, despite the protein concentration was very low, were collected and concentrated by centrifugation with Amicon Ultra-0.5 mL Centrifugal Filters. Flowthrough (fraction got after the loading of anti-FLAG material incubated with the sample in the column), washing fraction and elution fractions after concentration, were loaded on SDS-PAGE and following analyzed by WB analysis. Results are shown in figure 4.

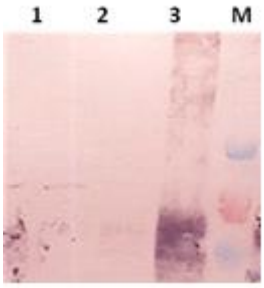


**Fig. 4.** *Purification trial for KAAT1-FH from Sf9 cell membrane.* WB against FLAG epitope. M: molecular weight marker. 1: flowthrought; 2: washing; 3: fraction of purified and concentrated KAAT1-FH protein after two purification steps, namely a Ni-NTA and an anti-FLAG column (see text for details).

The quality of the SDS-PAGE as the efficiency of blotting were very bad. Despite this fact no signals was detected in flowthrought and in the washing step from the anti-FLAG column but a signal at the correct molecular weight was got after elution from the anti-FLAG column and concentration. Due to the low expression level the gel was analyzed by WB instead of Coomassie blue staining preventing the possibility to get information about the purity of the protein after the purification.

## 4.4 DISCUSSION AND OUTLOOKS

The explorative trial to purify KAAT1 was only partially carried out.
The Baculovirus system has proved to be a good expression system for the expression of KAAT1 as demonstrated by the results of the expression tests (Fig. 1, 2). Both the constructs conceived and built for its purification were expressed at qualitatively good levels but at a different time points, namely 3 an 5 d.p.i. for KAAT1-FH and KAAT1-CFH respectively. No evidence of protein aggregation was detected and only a slight signal of degradation was revealed for KAAT1-CFH (Fig. 2) but the signal of the protein at the expected molecular weight was always the predominant signal in each lane corresponding to different d.p.i.. An immunofluorescence analysis to check the proper insertion of KAAT1-FH in plasma membrane should be performed according to the fact that the expression test was conducted on the whole cell lysate.
The low expression level in the productive cultures unfortunately impaired the possibility to get further indications from the subsequent steps. As explained this was due to an incorrect virus stock titration that led to an infection at an m.o.i. lower than the theoretical of 10 that should have been properly used for the expression test. In spite of this some positive clues for the purification of KAAT1 were anyway gathered. The possibility to find a good detergent for KAAT1 solubilization from plasma membranes of Sf9 cells and the positive signal after two affinity purification steps indicates the feasibility of KAAT1 purification exploiting this system.
To develop this system as a system for higher scale KAAT1 production and purification for structural studies it is necessary a further analysis aimed to find the best detergent in which KAAT1 should be not only completely solubilized from the membrane but also in which the protein could be purified in high amount in a stable, folded and active form. Should be noted that some unidentified protein material at lower MW than expected was observed in the WB for the solubilization test that requires further investigations to clarify its nature. After this step an assay to test the functionality of the purified protein should be also performed before proceeding with the scaling up of the procedure aimed to the structural investigation of the protein structure.

## 4.5 MATERIAL AND METHODS

### 4.5.1 KAAT1 cloning and tagging

KAAT1 FH: the coding sequence of KAAT1 tagged with FLAG epitope in the second extracellular loop was amplified by PCR from pSPORT vector adding the restriction sites for the endonucleases BamHI and NotI at the 5'- and 3'-end respectively. With the same primers a 7-histidine tag was also added to the C-terminus of the protein. After digestion with endonucleases the PCR product was cloned into pVL1393 vector (kindly gift of Gabriele Maul from the Molecular Membrane Biology Department, Max Planck Institute of Biophysics, Frankfürt am Main, Germany).
The primer used were the following:

forward:
5'-GCATCAGGATCCATGAATGACGGCCAAGTGAACG-3'
reverse:
5'-CATAGATGCGGCCGCTTAGTGATGGTGATGGTGATGGTGCTTATTAATATTACGCCTGTAAGC-3'.
KAAT1 CFH: wild type KAAT1 coding sequence was amplified from pSPORT vector adding the restriction site for the endonucleases BglII and BamHI at the 5'- and 3'-end respectively. After restriction digestion the PCR product was cloned in the vector pVL-FH (*AB Vector*) obtaining a DNA coding for KAAT1 double tagged at the C-terminus with FLAG epitope and with a 8-histidine tag. The primer used are following listed:
forward: 5'-GACATATTGTGAGATCTATGAATGACGGCCAAGTGAAC-3'
reverse: 5'-AGTCAGTAGGATCCCTTATTAATATTACGCCTGTAAGC-3'.
Gene sequencing confirmed the proper insertion of the tags and the cloning of the gene in frame under the control of the *polh* promoter.

### 4.5.2 Cell line and maintenance

Sf9 cell line (kindly gift of Gabriele Maul from the Molecular Membrane Biology Department, Max Planck Institute of Biophysics, Frankfürt am Main, Germany) was maintained in TNM-FH medium without glutamine supplemented with 5% Fetal Calf Serum (FCS), 50 µg/ml gentamycin, 2% L-glutamine, 0.01 µg/ml vitamin B12 (complete medium). 0.1% Pluronic® 68 was also added to maintain cells in shaking cultures. Growing temperature was of 27°C in an incubator without $CO_2$ supplying; a 125 rpm shaking was also provided for shaking cultures. Changing in medium composition were used for specific purposes during the production of Baculoviruses (see *Recombinant Baculovirus production* section).

### 4.5.3 Recombinant Baculovirus production

$1.28*10^6$ healthy and log phase growing cells from a monolayer culture were seeded in one well of a 6 multiwell plate for each of kind of virus. Cells were allowed to adhere after seeding for 30 minutes at RT and then washed 4 times, each 10 minutes, with complete medium without FCS. After the last washing, 1 ml of complete medium without FCS was dropwise applied to the monolayer mixed with 50 µL of the transfection mixture. This was prepared right before the usage incubating for 15 minutes at RT the following mix: 500 ng of pVL1393 vector bearing KAAT1-FH or pVL-FH vector bearing KAAT1-CFH, 100 ng of FlashBAC transfer vector (*Oxford Expression Technologies*) and 30 µl of Lipofectamine® (*Invitrogen*) in a final volume of 50 µl of bi-distilled sterile water. Cell were incubated at 27°C in a close box with wet paper for 22 hours and then 1 ml of complete medium with 10% FCS was applied to each well. Incubation was then prolonged up to 7 days when cells were checked to verify the cytopathic effect due to virus replication. The supernatant was then sterilely collected and cells eliminated by

centrifugation at 6000 rpm for 10' at RT. This master stock of virus was then used to amplify the virus batch. Otherwise was conserved and store far from light at 4°C.

### 4.5.4 Virus amplification

From the master virus stock the F1 generation of Baculovirus was produced. 50 ml cultures of Sf9 cells were started with $5*10^6$ cells/ml and infected with 1 ml of the master stock virus got from the plate (see previous section). After 6 days of culturing cells were collected by centrifugation (6000 rpm, 10 minutes, RT) and discharged; supernatant containing the viruses was collected and used for the production of the F2 virus generation starting a new culture of 500 ml of Sf9 cells as described and infected with an multiplicity of infection (m.o.i) of 0.01 assuming a F1 virus titer of $1*10^7$ p.f.u. (plaque/forming/unit)/ml. Viruses were collected after 6 days as described. Both F1 and F2 virus stocks were titered and stored at 4°C far from light. From F1 stocks aliquots of viruses were stored at -80°C as a virus reference stock.

### 4.5.5 Virus stock titration

Virus titer in each stock was determined by end point dilution assay. For each virus stock each well of a 96 multiwell plate were seeded with $1*10^5$ healthy Sf9 cells from a monolayer culture in 100 µl of complete medium. After cell attaching 10 µl of virus stock dilution (diluted with the complete medium) were applied in each well according to the following scheme: 3 wells with $10^{-2}$ and $10^{-3}$ dilutions and 4 wells for $10^{-4}$ virus dilution. 12 wells for each dilution from $10^{-5}$ up to $10^{-9}$ were also infected. At least 2 wells were used as a negative control seeded only with cells without infection. Plates were incubated in a box with wet paper at 27°C until the $6^{th}$ day after infection. Cytopathic effect was evaluated in each one of the wells by direct observation under light microscope for three days, namely from the $6^{th}$ until the $8^{th}$ day post infection. Positive wells were assigned if cells were infected otherwise wells were considered negative. The data gathered were then used for the determination of the virus titer according to the following calculation: for each dilution the number of positive and negative wells were counted; the Δ (delta) of infection was calculated for both positive and negative wells, for each virus dilution. The positive wells were summed from the highest to the lowest dilution assuming that wells positive at higher dilution were also positive at lower dilution. Conversely, the negative wells were summed from the lowest dilution to the highest dilution assuming that the non-infected wells at lower dilution were also negative at higher dilution. With positive and negative Δs of each dilution the Δ percentage of positive wells for each dilution was calculated to determine the *a* parameter as the first Δ percentage of positive well over 50, and *b*, as the first Δ percentage lower than 50. The following scheme of calculation were applied to get the virus titer: the PD parameter was firstly determined applying $(a-50)/(a-b)$. This allowed the calculation of the Tissue Culture Infection Dose 50 ($TCID_{50}$) considering that

$logTCID_{50}$ = dilution corresponding to *a* – PD. The virus titer in 10 µl of virus stock corresponds to $1/10^{logTCID_{50}}$. From this the calculation of the number of virus particles in 1 ml was easily got considering the dilution factor of 100. The Plaque Forming Unit (p.f.u.)/ml were then calculated considering that p.f.u./ml corresponds to $logTCID_{50}$*0.69.

### 4.5.6 Expression test

To test the expression of KAAT1 for each construct 7 wells from 6 well plates were seeded with $1.28*10^6$ cell from a log phase growing culture and infected with an m.o.i. of 10 with viruses from the stocks. Each 24 hours cells from one well were collected and stored for each type of virus. Non infected cells were considered as a control. From each time point $6*10^5$ cells were harvested, collected by centrifugation (6000 rpm, 10 minutes, 4° C) and dried by supernatant removing. Cell pellet were resuspended with 80.5 µl of benzonase buffer (50 mM Tris-HCl, 1.5 mM $MgCl_2$, 1% SDS), 1.2 µL protease inhibitor cocktail (Complete EDTA free protease inhibitor cocktail (*Roche*): 1 tablet dissolved in 2 ml of water with 100 mM EDTA), 1.2 µL 100 mM phenylmethanesulfonylfluoride and 2 µL Benzonase (3 U/µL). After resuspension cell lysates were incubated on ice for 60 minutes and then 1.2 µL 100 mM phenylmethanesulfonylfluoride were added before analysis by SDS-PAGE.

### 4.5.7 Productive cultures

Cultures for quantitative protein expression were started with cells from log growing phase culture, collected by centrifugation (1000g, 10 minutes, RT) and resuspended with complete medium to get a final cell density of $2.5*10^6$ cells/ml. To this culture a proper volume of virus stock was added to have an m.o.i. of 10.

### 4.5.8 Cell harvesting and membrane preparation

At the 3rd day after infection cells expressing KAAT1-FH were collected by centrifugation (6000 rpm, 10 minutes, 4°C) and cells resuspended with ice cold buffer A (50 mM TRIS pH 7.5, 8.6% glycerol, 200 mM NaCl) with Complete EDTA free protease inhibitor cocktail, *Roche*) to have a final cell density of $5*10^6$ cells/ml. Cellular suspensions were then applied to Cell Parr Bomb set up for 500 psi for 20 minutes *per* cycle to get cells broken for more than 90%. Low speed centrifugation was applied (1000g, 10 minutes, 4°C) to remove the unbroken cells and membranes from the supernatant were collected for ultracentrifugation. The latter was performed with the following parameters: 45000 rpm, 60 minutes, 4°C. The membranes, got as a pellet, were then resuspended in ice cold buffer A and homogenized manually by means of a Dounce until the disappearance of visible clumps. Membranes not immediately used were stored at -80°C until use.

### 4.5.9 Detergent screening

For solubilization test 20 µl of membrane preparation were incubated for 60 minutes on ice with 2% of each of the tested detergent: DM (n-decyl-β-D-maltopyranoside), DDM (n-dodecyl-β-D-maltopyranoside), Cymal-5 (5-Cyclohexyl-1-Pentyl-β-D-Maltoside) and OG (n-octyl-β-D-glucopyranosyde). After incubation non solubilized material was collected by centrifugation (14000 rpm, 30 minutes, 4°C) and the supernatant got was collected. Pellet was resuspended in 1% SDS page buffer before loading on SDS-PAGE together with the relative supernatant.

### 4.5.10 Purification test

Membrane were solubilized adding 2% DDM for 1.5 hours by shaking at 4°C and then centrifuged for 60 minutes, 14000 rpm, 4°C. Ni-NTA resin was washed with distilled water and, after equilibration with buffer A with 5 mM imidazole and 0.1% DDM, was mixed with the supernatant by shaking for 30 minutes at 4°C. The material was then applied to the column and leave standing until the complete sedimentation of the material. After washing with equilibration buffer, elution was realized applying fractions of 400 µl of elution buffer (buffer A with 250 mM imidazole and 0.1% DDM). Elution was qualitatively monitored by Bradford assay applied on each of the elution fractions. Positive fractions were pulled together and mixed to anti-FLAG resin material previously equilibrated with 0.1% DDM in buffer A. After 30 minutes of mixing at 4°C the mixing was applied to the column and left standing to get a complete sedimentation. After a washing step with the equilibration buffer the elution was realized with 400 µl/fraction of elution buffer (0.1% DDM buffer A added with 100 µg/ml FLAG peptide). The Bradford positive fractions were then pulled together and concentrated by centrifugation with *Amicon* Ultra-0.5 mL Centrifugal Filters for Protein (MW cut off: 100000).

### 4.5.11 SDS-PAGE and Western-blot analysis

12.5% polyacrylamide gels were used for all the analysis performed. After running proteins were transferred from gel on polyvinylidene fluoride (PVDF) membrane (*Immobilion® -P*) previously activated by methanol, by applying a voltage of 18V for 35 minutes. For Western blotting blocking was realized incubating the PVDF membrane for at least 60 minutes at RT with 5% milk powder solution in TBS buffer (200 mM Tris-HCl pH 7,5, 1,5 mM NaCl). Primary antibody was a mouse anti-FLAG (1:1000, *Sigma*); incubation was conducted o/n at 4°C. After three washing steps with TBS buffer the secondary antibody was applied for at least 2 hours at RT (anti mouse tagged with Alkaline phosphatase, *Sigma*). Revealing was performed employing *Sigma FAST™ BCIP®/NBT* system. Gel images were analyzed by *ImageJ* software from NCBI.

# Chapter 5
# Role of intracellular chloride in the reverse operational mode of the GABA transporter GAT1 investigated by radiochemical assays

## 5.1 ABSTRACT[8]

We have investigated the effect of intracellular chloride depletion on the GABA efflux mediated by the neuronal cotransporter GAT1 expressed in *Xenopus* oocytes. By means of [$^{3}$H]-GABA efflux determination we found that the reverse operational mode of GAT1 depends on the presence of intracellular chloride. Remarkably the co-expression of the $K^+/Cl^-$ cotransporter (KCC2) was able to reduce the GABA efflux by GAT1 suggesting that in particular physiological conditions, like during the development, the activity of KCC2 could affect the GABAergic transmission by influencing the intracellular concentration of this anion.

[8] The results of the presented analysis were published in (Bertram *et al.*, 2011).

## 5.2 INTRODUCTION

The reverse transport of neurotransmitter by transporters, normally deputy to uptake it into the cells, has been so far identified as a phenomena that could occur in physiological and pathological conditions, both in adult organism and during development. For the main inhibitory neurotransmitter of mammalian CNS, GABA, this kind of transport was already described (Cammack *et al.*, 1994; Lu and Hilgemann, 1999a; Lu *et al.*, 1999b). A non-vesicular, calcium independent, GABA release from neurons is the main actor in the tonic inhibition of CNS regulating the brain excitability and was reported in different pathological conditions including epilepsy (Richerson *et al.*, 2003; Richerson *et al.*, 2004). Night to day variations in internal chloride are observed in the suprachiasmatic neurons and are believed to be involved in the regulation of the circadian cycle, again via effects on GABA receptors (Wagner *et al.*, 1997; Wagner *et al.*, 2001). The role exert by chloride is also relevant during the development. During neuronal development big changes in the internal chloride concentration were described whose effects are mainly evident on the switching between excitatory and inhibitory activity of the same GABA. It is well known that in adult mammalian cells the electrochemical gradient of chloride across cell membranes is almost null, in other terms, when the permeability of membrane is increased (e.g, by the opening of a $Cl^-$-channel) the movement of chloride does not modify significantly the membrane voltage. In neonatal neurons the internal chloride concentration is higher than outside consequently the activation of $GABA_A$ receptors lead to depolarization of the cell in which are expressed (Yuste and Katz, 1991; Ben-Ari *et al.*, 1989; Cherubini *et al.*, 1991; LoTurco *et al.*, 1995; Ben-Ari, 2002). The lowering internal concentration is due to the temporized expression of KCC2 (K/Cl cotransporter 2) whose expression, low during initial phases, increases progressively during development. Accordingly, KCC2 deprivation causes hyperexcitability and epileptic seizures in mice (Woo *et al.*, 2002) and an unbalance between $Na^+/K^+/Cl^-$ cotransporter (NKCC2)/KCC2 expression profile decreases GABAergic inhibition in the human peritumoral epileptic cortex (Conti *et al.*, 2011). The intracellular concentration of chloride decreases parallel to the increasing of active forms of KCC2 expressed in the plasma membrane (Rivera *et al.*, 1999; Ben-Ari, 2002).

It is already known that extracellular $Na^+$ and intracellular $Cl^-$ bind the cotransporter GAT1 in a mutually excluding way. Intracellular chloride could sequester the protein in the inward faced conformation being proved that the binding of the anion to the cytoplasmic side of the protein precede the binding of sodium and of the neurotransmitter itself (Cammack *et al.*, 1994; Lu *et al.*, 1999a; Lu *et al.*, 1999b). The binding of intracellular chloride also reduces the GABA uptake from the extracellular environment being the carrier not available for the binding of $Na^+$ (Loo *et al.*, 2000). In this scenario fluctuations in the intracellular chloride concentration could affect both the rate of GABA uptake and its outflow from the same cells.

We performed radiochemical experiments to test the effect of the intracellular chloride concentration variations on the reverse GABA transport mediated by GAT1. This

analysis was done in the context of a bigger project, running in the laboratory of Cellular and Molecular Physiology headed by Professor Antonio Peres (University of Insubria, Varese), aimed to investigate the role of the intracellular chloride in the GABA efflux induced by the cotransporter GAT1.

## 5.3 RESULTS

### 5.3.1 Measure of GABA efflux from *Xenopus* oocytes expressing GAT1

The proper expression of GAT1 in *Xenopus* oocytes was verified by the uptake of radiolabeled GABA induced in GAT1 expressing oocytes compared to that in non-injected oocytes before each efflux experiment.

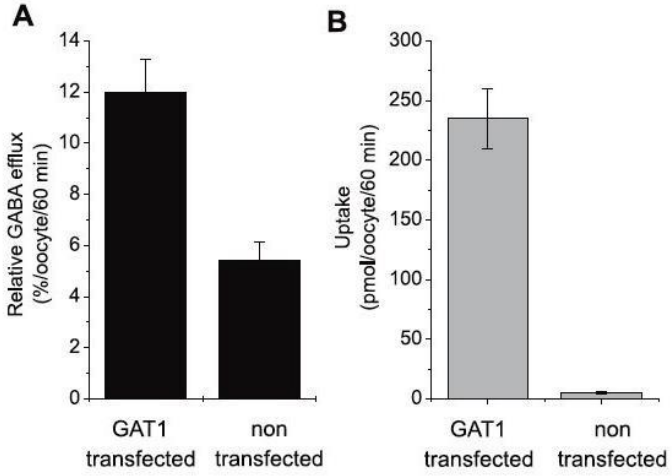


**Fig. 2**: *Radioactive GABA fluxes* (**A**): GABA efflux after injection of 100 mM radioactive GABA (final concentration 10 mM) in the oocytes. Bars represent the GABA efflux expressed as percentage of the total injected radioactive GABA and are means ± SE of groups of 20–25 oocytes in triplicate from different batches. (**B**): uptake of 0.1 mM GABA measured in GAT1 transfected oocytes and in non-transfected oocytes as controls. Bars are means SE of groups of 8–10 oocytes in a representative experiment.

GABA efflux was tested injecting oocytes with 10 mM (final) radiolabeled GABA and incubating oocytes for 60 minutes in a solution containing alternatively 98 mM KCl or NaCl. Only in presence of depolarizing conditions, i.e. in presence of high extracellular KCl, a 2.4 times higher GABA efflux was seen from oocytes expressing GAT1 if compared to that got from control oocytes (Fig. 1A).

### 5.3.2 Effect of internal chloride depletion on GABA efflux

The activity of the cotransporter GAT1 is strictly chloride dependent (Zomot *et al.*, 2007). To test the role of intracellular chloride in the reverse mode of the transporter the intracellular chloride concentration was reduced by means of three different methods as described in *Materials and Methods* section. Even in these cases the expression of GAT1

was verified by the uptake of 0,1 mM GABA: no one of the conditions used to produce the intracellular chloride depletion produced a significant reduction of the activity of GAT1 rendering the oocytes treated by three different methods directly comparable (Fig. 2B). The expression of KCC2 was instead directly evaluated by electrophysiological measurements in the laboratory of Professor A. Peres.

The GABA efflux was reduced from oocytes depleted of intracellular chloride by means of all the three methods used if compared to control oocytes (Fig. 2A). In particular, in oocytes expressing KCC2 and incubated o/n in the hypotonic chloride free solution, the GABA efflux induced by GAT1 was completely abolished being the efflux from these cells at the same level of that one from control oocytes. KCC2 expression reduces not only the intracellular chloride concentration but also the potassium concentration being this protein active in extruding $Cl^-$ and $K^+$ in a ratio of 1:1. In any case the loosing of potassium ions should be lower than that of chloride: was indeed estimated that, considering an intracellular chloride concentration of 50-60 mM for *X. laevis* oocytes, by these procedures is reduced of 40 mM and the potassium concentration is lowered from 120 mM to 80 mM (Kusano *et al.*, 1982): the relative decreasing is consequently of the 33% for potassium and of the 90% for chloride. Furthermore Na/K ATPase is continuously active in the stabilization of intracellular potassium concentration (Pacheco-Alvarez *et al.*, 2006) rendering the intracellular chloride concentration the main parameter modified by these approaches. Considering these evaluations the effect observed on the GABA efflux can be ascribed to the depletion of intracellular chloride concentration.

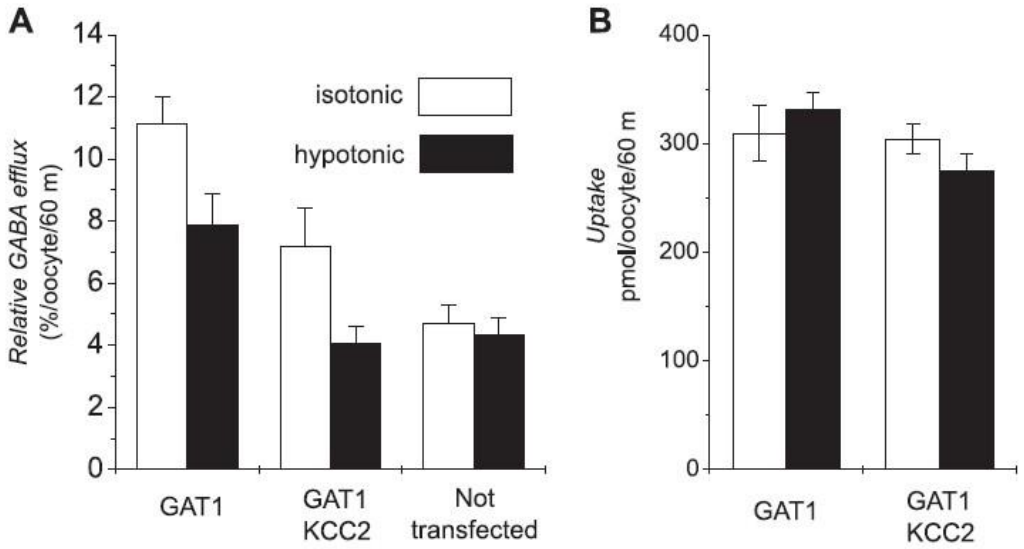


**Fig. 3***: Effect of internal chloride depletion on GABA efflux* (**A**): GABA efflux in Cl-depleted oocytes. Bars represent the GABA efflux expressed as percentage of the total injected radioactive GABA and are means SE of groups of 20–25 oocytes in triplicate from two different batches and transfected with GAT1 only or with GAT1 plus KCC2. (**B**): uptake of 0.1 mM GABA measured in oocytes transfected as indicated. In A and B, white bars are from oocytes kept in normal chloride, isotonic solution, while black bars are from oocytes incubated overnight in low-chloride hypotonic solution. Bars are means SE of groups of 8–10 in a representative experiment.

## 5.4 DISCUSSION

In chloride depleted oocytes no significant changes were observed in the amount of the GABA uptake compared with the control oocytes, indicating that when GABA is not present internally, no effect of chloride on the GAT1 activity can be detected. Data gathered indicate that high intracellular concentration of GABA, jointly to depolarizing condition of the plasma membrane, are conditions in which the neurotransmitter can be actively exported out from the cell. When a high concentration of GABA is present in the cytoplasm, GAT1 can operate in the reverse mode. The reverse transport is affected by the internal concentrations of $Cl^-$. The results of the chloride-depletion experiments, and particularly of those in which the chloride depletion was obtained by the coexpression of KCC2, might represent a good paradigm to study the physiological phenomena that occurs *in vivo*.

## 5.5 CONCLUDING NOTE

As mentioned the main analysis of this issue has been performed in the laboratory of Cellular and Molecular Physiology headed by Professor A. Peres from the University of Insubria, Varese, Italy. The results were published in (Bertram *et al.*, 2011; Cherubino *et al.*, 2012). Being this chapter just a little part of the whole project aimed to investigate the reverse transport of GABA through GAT1, following is reported a conclusion that Authors summarized for their work regarding the physiological implication of the described findings: "*our results suggest that younger neurons, with higher intracellular chloride concentration, may be more prone to generate GABA efflux, compared with adult neurons in which, thanks to the activity of KCC2, the internal chloride concentration has been lowered. Furthermore, any other conditions favoring higher intracellular chloride levels, such as underexpression of chloride exporters, or defects in osmoregulation or in ionic homeostasis, may be considered potentially relevant in affecting the balance between forward and reverse mode of neurotransmitter transport*".

## 5.6 MATERIALS AND METHODS

### 5.6.1 Oocytes harvesting, selection and injection

The experimental procedure for oocyte collection and treatment were already described (see chapter 2). To prepare the mRNA for oocyte injection, the cDNA encoding the rat GABA cotransporter GAT1, cloned into the pAMV-PA vector, was linearized by NotI digestion, while the cDNA encoding the human KCC2 cotransporter (kind gift of Prof. G. Gamba, Mexico City, Mexico, to Professor A. Peres), cloned into the pGEMHE vector, was linearized with NheI. Subsequently, the cRNAs were *in vitro* synthesized and capped exploiting the T7 RNA polymerase. All enzymes were purchased by Promega Italia (Milano, Italy). The oocytes were injected the day after with 50 nl of water containing 12.5

ng of cRNA coding for rat GAT1 (rGAT1) or, in some experiments, also with 12.5 ng of mRNA coding for the potassium/chloride symporter KCC2, using a manual microinjection system (Drummond). The oocytes were incubated at 18°C for 3–4 days in Barth's solution (for composition see chapter 2, *Materials and Methods* section).

### 5.6.2 GABA reverse transport measurements

Groups of 20-25 oocytes in triplicate, three days after cRNA injection, were injected with a solution containing 100 mM [$^3$H]-GABA in 98 mM NaCl or Na-gluconate (for experiments testing the effect of chloride depletion), 5 mM HEPES pH 7.6, 1 mM $MgCl_2$. Considering an average oocyte volume of about 1 µl and an injected volume of 50 nl/oocyte, a dilution of around 10 times is obtained allowing an estimation of a final concentration for GABA of 10 mM. After injection oocytes were kept on ice in Barth's solution (see chapter 2, *Materials and methods* section) or in the o/n preincubation solution (see next session) to recover after the cell damage due to injection. GABA efflux was induced incubating at RT for 60 minutes each group of oocyte in 500 µl of a solution with the following composition: 98 mM KCl, 1 mM $CaCl_2$, 5 mM HEPES pH 7.6; where indicated KCl was substituted by NaCl. The high extracellular potassium concentration induced the reverse transport depolarizing the oocyte and creating consequently the condition for GABA extrusion from the cell. The exported radioactivity was then counted by means of liquid scintillation counting on the whole volume of incubating solution.

### 5.6.3 Reduction of the intracellular chloride concentration

Three different methods were used to reduce the intracellular chloride concentration:

1. Oocytes were incubated o/n in a hypotonic chloride free solution (70 mM Na-gluconate, 2 mM K-gluconate, 10 mM Ca-gluconate, 1 mM Mg-gluconate e 5 mM HEPES pH 7.6). The extracellular calcium concentration was enhanced (compared to normal maintaining solution) to 10 mM to compensate the chelating effect of gluconate (Christoffersen and Skibsted, 1975).
2. Oocytes were co-injected with the cRNA coding for the cotransporter $K^+/Cl^-$ Cotranporter 2 (KCC2) that it extrudes potassium and chloride ions from the cell.
3. Oocytes expressing both GAT1 and KCC2 were incubated o/n in the hypotonic chloride free solution of method 1 (Pacheco-Alvarez *et al.*, 2006).

Non injected oocytes were used as a control. Data represent and are presented as percentage of the GABA injected into the oocytes extruded from the cells.

# Bibliography

# REFERENCES


1. Abramson J and Wright EM (2009) Structure and function of Na(+)-symporters with inverted repeats. *Curr Opin Struct Biol,* **19,** 425-432.

2. Altafaj X, Joux N, Ronjat M, and De WM (2006) Oocyte expression with injection of purified T7 RNA polymerase. *Methods Mol Biol,* **322,** 55-67.

3. Amara SG (2007) Chloride finds its place in the transport cycle. *Nat Struct Mol Biol,* **14,** 792-794.

4. Andrini O, Ghezzi C, Murer H, and Forster IC (2008) The leak mode of type II Na(+)-P(i) cotransporters. *Channels (Austin ),* **2,** 346-357.

5. Augood SJ, Herbison AE, and Emson PC (1995) Localization of GAT-1 GABA transporter mRNA in rat striatum: cellular coexpression with GAD67 mRNA, GAD67 immunoreactivity, and parvalbumin mRNA. *J Neurosci,* **15,** 865-874.

6. Ayres MD, Howard SC, Kuzio J, Lopez-Ferber M, and Possee RD (1994) The complete DNA sequence of *Autographa californica* nuclear polyhedrosis virus. *Virology,* **202,** 586-605.

7. Barnard EA, Miledi R, and Sumikawa K (1982) Translation of exogenous messenger RNA coding for nicotinic acetylcholine receptors produces functional receptors in *Xenopus* oocytes. *Proc R Soc Lond B Biol Sci,* **215,** 241-246.

8. Beckman ML, Bernstein EM, and Quick MW (1999) Multiple G protein-coupled receptors initiate protein kinase C redistribution of GABA transporters in hippocampal neurons. *J Neurosci,* **19,** RC9.

9. Ben-Ari Y (2002) Excitatory actions of gaba during development: the nature of the nurture. *Nat Rev Neurosci,* **3,** 728-739.

10. Ben-Ari Y, Cherubini E, Corradetti R, and Gaiarsa JL (1989) Giant synaptic potentials in immature rat CA3 hippocampal neurones. *J Physiol,* **416,** 303-325.

11. Ben-Yona A and Kanner BI (2009) Transmembrane domain 8 of the {gamma}-aminobutyric acid transporter GAT-1 lines a cytoplasmic accessibility pathway into its binding pocket. *J Biol Chem,* **284,** 9727-9732.

12. Bergeron MJ, Boggavarapu R, Meury M, Ucurum Z, Caron L, Isenring P, Hediger MA, and Fotiadis D (2011) Frog oocytes to unveil the structure and supramolecular organization of human transport proteins. *PLoS One,* **6,** e21901.

13. Bertram S, Cherubino F, Bossi E, Castagna M, and Peres A (2011) GABA reverse transport by the neuronal cotransporter GAT1: influence of internal chloride depletion. *Am J Physiol Cell Physiol,* **301,** C1064-C1073.

14. Bettè S, Castagna M, Bossi E, Peres A, and Sacchi VF (2008) The SLC6/NSS family members KAAT1 and CAATCH1 have weak chloride dependence. *Channels (Austin),* **2**.

15. Beuming T, Shi L, Javitch JA, and Weinstein H (2006) A comprehensive structure-based alignment of prokaryotic and eukaryotic neurotransmitter/$Na^+$ symporters (NSS) aids in the use of the LeuT structure to probe NSS structure and function. *Mol Pharmacol,* **70,** 1630-1642.

16. Boggavarapu R, Jeckelmann JM, Harder D, Schneider P, Ucurum Z, Hediger M, and Fotiadis D (2013) Expression, Purification and Low-Resolution Structure of Human Vitamin C Transporter SVCT1 (SLC23A1). *PLoS One,* **8,** e76427.

17. Bohmer C, Broer A, Munzinger M, Kowalczuk S, Rasko JE, Lang F, and Broer S (2005) Characterization of mouse amino acid transporter B0AT1 (SLC6A19). *Biochem J,* **389,** 745-751.

18. Borden LA, Smith KE, Hartig PR, Branchek TA, and Weinshank RL (1992) Molecular heterogeneity of the gamma-aminobutyric acid (GABA) transport system. Cloning of two novel high affinity GABA transporters from rat brain. *J Biol Chem,* **267,** 21098-21104.

19. Bossemeyer D (1994) The glycine-rich sequence of protein kinases: a multifunctional element. *Trends Biochem Sci,* **19,** 201-205.

20. Bossi E, Centinaio E, Castagna M, Giovannardi S, Vincenti S, Sacchi VF, and Peres A (1999a) Ion binding and permeation through the lepidopteran amino acid transporter KAAT1 expressed in Xenopus oocytes. *J Physiol,* **515 ( Pt 3),** 729-742.

21. Bossi E, Sacchi VF, and Peres A (1999b) Ionic selectivity of the coupled and uncoupled currents carried by the amino acid transporter KAAT1. *Pflugers Arch,* **438,** 788-796.

22. Bossi E, Soragna A, Miszner A, Giovannardi S, Frangione V, and Peres A (2007) Oligomeric structure of the neutral amino acid transporters KAAT1 and CAATCH1. *Am J Physiol Cell Physiol,* **292,** C1379-C1387.

23. Bossi E, Vincenti S, Sacchi VF, and Peres A (2000) Simultaneous measurements of ionic currents and leucine uptake at the amino acid cotransporter KAAT1 expressed in *Xenopus laevis* oocytes. *Biochim Biophys Acta,* **1495,** 34-39.

24. Boudker O and Verdon G (2010) Structural perspectives on secondary active transporters. *Trends Pharmacol Sci,* **31,** 418-426.

25. Boudko DY (2012) Molecular basis of essential amino acid transport from studies of insect nutrient amino acid transporters of the SLC6 family (NAT-SLC6). *J Insect Physiol,* **58,** 433-449.

26. Broer S (2006) The SLC6 orphans are forming a family of amino acid transporters. *Neurochem Int,* **48,** 559-567.

27. Broer S (2008) Amino acid transport across mammalian intestinal and renal epithelia. *Physiol Rev,* **88,** 249-286.

28. Broer S (2013) Diseases Associated with General Amino Acid Transporters of the Solute Carrier 6 Family (SLC6). *Curr Mol Pharmacol*.

29. Cai G, Salonikidis PS, Fei J, Schwarz W, Schulein R, Reutter W, and Fan H (2005) The role of N-glycosylation in the stability, trafficking and GABA-uptake of GABA-transporter 1. Terminal N-glycans facilitate efficient GABA-uptake activity of the GABA transporter. *FEBS J,* **272,** 1625-1638.

30. Camargo SM, Makrides V, Virkki LV, Forster IC, and Verrey F (2005) Steady-state kinetic characterization of the mouse B(0)AT1 sodium-dependent neutral amino acid transporter. *Pflugers Arch,* **451,** 338-348.

31. Cammack JN, Rakhilin SV, and Schwartz EA (1994) A GABA transporter operates asymmetrically and with variable stoichiometry. *Neuron,* **13,** 949-960.

32. Cammack JN and Schwartz EA (1996) Channel behavior in a gamma-aminobutyrate transporter. *Proc Natl Acad Sci U S A,* **93,** 723-727.

33. Castagna M, Bossi E, and Sacchi VF (2009) Molecular physiology of the insect K-activated amino acid transporter 1 (KAAT1) and cation-anion activated amino acid transporter/channel 1 (CAATCH1) in the light of the structure of the homologous protein LeuT. *Insect Mol Biol,* **18,** 265-279.

34. Castagna M, Shayakul C, Trotti D, Sacchi VF, Harvey WR, and Hediger MA (1998) Cloning and characterization of a potassium-coupled amino acid transporter. *Proc Natl Acad Sci U S A,* **95,** 5395-5400.

35. Castagna M, Soragna A, Mari SA, Santacroce M, Bettè S, Mandela PG, Rudnick G, Peres A, and Sacchi VF (2007) Interaction between lysine 102 and aspartate 338 in the insect amino acid cotransporter KAAT1. *Am J Physiol Cell Physiol,* **293,** C1286-C1295.

36. Cherubini E, Gaiarsa JL, and Ben-Ari Y (1991) GABA: an excitatory transmitter in early postnatal life. *Trends Neurosci,* **14,** 515-519.

37. Cherubino F, Bertram S, Bossi E, and Peres A (2012) Pre-steady-state and reverse transport currents in the GABA transporter GAT1. *Am J Physiol Cell Physiol,* **302,** C1096-C1108.

38. Chiu CS, Brickley S, Jensen K, Southwell A, Mckinney S, Cull-Candy S, Mody I, and Lester HA (2005) GABA transporter deficiency causes tremor, ataxia, nervousness, and increased GABA-induced tonic conductance in cerebellum. *J Neurosci,* **25,** 3234-3245.

39. Chiu CS, Jensen K, Sokolova I, Wang D, Li M, Deshpande P, Davidson N, Mody I, Quick MW, Quake SR, and Lester HA (2002) Number, density, and surface/cytoplasmic distribution of GABA transporters at presynaptic structures of knock-in mice carrying GABA transporter subtype 1-green fluorescent protein fusions. *J Neurosci,* **22,** 10251-10266.

40. Christoffersen CR and Skibsted LH (1975) Calcium ion activity in physiological salt solutions: influence of anions substituted for chloride. *Comp Biochem Physiol A Comp Physiol,* **52,** 317-322.

41. Clark JA and Amara SG (1994) Stable expression of a neuronal gamma-aminobutyric acid transporter, GAT-3, in mammalian cells demonstrates unique pharmacological properties and ion dependence. *Mol Pharmacol,* **46,** 550-557.

42. Claxton DP, Quick M, Shi L, de Carvalho FD, Weinstein H, Javitch JA, and McHaourab HS (2010) Ion/substrate-dependent conformational dynamics of a bacterial homolog of neurotransmitter:sodium symporters. *Nat Struct Mol Biol,* **17,** 822-829.

43. Conti F, Minelli A, and Melone M (2004) GABA transporters in the mammalian cerebral cortex: localization, development and pathological implications. *Brain Res Brain Res Rev,* **45,** 196-212.

44. Conti L, Palma E, Roseti C, Lauro C, Cipriani R, de GM, Aronica E, and Limatola C (2011) Anomalous levels of $Cl^-$ transporters cause a decrease of GABAergic inhibition in human peritumoral epileptic cortex. *Epilepsia,* **52,** 1635-1644.

45. Crisman TJ, Qu S, Kanner BI, and Forrest LR (2009) Inward-facing conformation of glutamate transporters as revealed by their inverted-topology structural repeats. *Proc Natl Acad Sci U S A,* **106,** 20752-20757.

46. Dascal N (1987) The use of *Xenopus* oocytes for the study of ion channels. *CRC Crit Rev Biochem,* **22,** 317-387.

47. De Felice LJ, Noskov S, and Schnetkamp PP (2008) Transporters in Channels. *Channels (Austin ),* **2,** 305-307.

48. Deisenhofer J, Epp O, Miki K, Huber R, and Michel H (1985) Structure of the protein subunits in the photosynthetic reaction centre of *Rhodopseudomonas viridis* at 3A resolution. *Nature,* **318,** 618-624.

49. Deken SL, Wang D, and Quick MW (2003) Plasma membrane GABA transporters reside on distinct vesicles and undergo rapid regulated recycling. *J Neurosci,* **23,** 1563-1568.

50. Dumont JN (1972) Oogenesis in *Xenopus laevis* (Daudin). I. Stages of oocyte development in laboratory maintained animals. *J Morphol,* **136,** 153-179.

51. Faham S, Watanabe A, Besserer GM, Cascio D, Specht A, Hirayama BA, Wright EM, and Abramson J (2008) The crystal structure of a sodium galactose transporter reveals mechanistic insights into $Na^+$/sugar symport. *Science,* **321,** 810-814.

52. Fang Y, Jayaram H, Shane T, Kolmakova-Partensky L, Wu F, Williams C, Xiong Y, and Miller C (2009) Structure of a prokaryotic virtual proton pump at 3.2 A resolution. *Nature,* **460,** 1040-1043.

53. Feldman DH, Harvey WR, and Stevens BR (2000) A novel electrogenic amino acid transporter is activated by $K^+$ or $Na^+$, is alkaline pH-dependent, and is $Cl^-$-independent. *J Biol Chem,* **275,** 24518-24526.

54. Focke PJ, Wang X, and Larsson HP (2013) Neurotransmitter transporters: structure meets function. *Structure,* **21,** 694-705.

55. Forrest LR (2013) Structural biology. (Pseudo-)symmetrical transport. *Science,* **339,** 399-401.

56. Forrest LR, Kramer R, and Ziegler C (2011) The structural basis of secondary active transport mechanisms. *Biochim Biophys Acta,* **1807,** 167-188.

57. Forrest LR and Rudnick G (2009) The rocking bundle: a mechanism for ion-coupled solute flux by symmetrical transporters. *Physiology (Bethesda ),* **24,** 377-386.

58. Forrest LR, Tavoulari S, Zhang YW, Rudnick G, and Honig B (2007) Identification of a chloride ion binding site in $Na^+/Cl^-$ -dependent transporters. *Proc Natl Acad Sci U S A,* **104,** 12761-12766.

59. Forrest LR, Zhang YW, Jacobs MT, Gesmonde J, Xie L, Honig BH, and Rudnick G (2008) Mechanism for alternating access in neurotransmitter transporters. *Proc Natl Acad Sci U S A,* **105,** 10338-10343.

60. Fotiadis D (2012) Atomic force microscopy for the study of membrane proteins. *Curr Opin Biotechnol,* **23,** 510-515.

61. Gao X, Lu F, Zhou L, Dang S, Sun L, Li X, Wang J, and Shi Y (2009) Structure and mechanism of an amino acid antiporter. *Science,* **324,** 1565-1568.

62. Geer BW (1966) Utilization of D-amino acids for growth by *Drosophila melanogaster* larvae. *J Nutr,* **90,** 31-39.

63. Giordana B, Sacchi VF, and Hanozet GM (1982) Intestinal amino acid absorption in lepidopteran larvae. *Biochim Biophys Acta,* **692,** 81-88.

64. Giovanola M, D'Antoni F, Santacroce M, Mari SA, Cherubino F, Bossi E, Sacchi VF, and Castagna M (2012) Role of a conserved glycine triplet in the NSS amino acid transporter KAAT1. *Biochim Biophys Acta,* **1818,** 1737-1744.

65. Guan L and Kaback HR (2006) Lessons from lactose permease. *Annu Rev Biophys Biomol Struct,* **35,** 67-91.

66. Guastella J, Nelson N, Nelson H, Czyzyk L, Keynan S, Miedel MC, Davidson N, Lester HA, and Kanner BI (1990) Cloning and expression of a rat brain GABA transporter. *Science,* **249,** 1303-1306.

67. Hahn MK and Blakely RD (2002) Monoamine transporter gene structure and polymorphisms in relation to psychiatric and other complex disorders. *Pharmacogenomics J,* **2,** 217-235.

68. Hahn MK and Blakely RD (2007) The functional impact of SLC6 transporter genetic variation. *Annu Rev Pharmacol Toxicol,* **47,** 401-441.

69. Harvey WR and Wieczorek H (1997) Animal plasma membrane energization by chemiosmotic $H^+$ V-ATPases. *J Exp Biol,* **200,** 203-216.

70. Hawtin RE, Arnold K, Ayres MD, Zanotto PM, Howard SC, Gooday GW, Chappell LH, Kitts PA, King LA, and Possee RD (1995) Identification and preliminary characterization of a chitinase gene in the *Autographa californica* nuclear polyhedrosis virus genome. *Virology,* **212,** 673-685.

71. Heinzelmann G, Bastug T, and Kuyucak S (2013) Mechanism and energetics of ligand release in the aspartate transporter GltPh. *J Phys Chem B,* **117,** 5486-5496.

72. Heller-Stilb B, van RC, Rascher K, Hartwig HG, Huth A, Seeliger MW, Warskulat U, and Haussinger D (2002) Disruption of the taurine transporter gene (TauT) leads to retinal degeneration in mice. *FASEB J,* **16,** 231-233.

73. Henry LK, Adkins EM, Han Q, and Blakely RD (2003) Serotonin and cocaine-sensitive inactivation of human serotonin transporters by methanethiosulfonates targeted to transmembrane domain I. *J Biol Chem,* **278,** 37052-37063.

74. Henry LK, Field JR, Adkins EM, Parnas ML, Vaughan RA, Zou MF, Newman AH, and Blakely RD (2006) Tyr-95 and Ile-172 in transmembrane segments 1 and 3 of human serotonin transporters interact to establish high affinity recognition of antidepressants. *J Biol Chem,* **281,** 2012-2023.

75. Hilgemann DW and Lu CC (1999) GAT1 (GABA:$Na^+$:$Cl^-$) cotransport function. Database reconstruction with an alternating access model. *J Gen Physiol,* **114,** 459-475.

76. Hong WC and Amara SG (2010) Membrane cholesterol modulates the outward facing conformation of the dopamine transporter and alters cocaine binding. *J Biol Chem,* **285,** 32616-32626.

77. Horton N and Quick MW (2001) Syntaxin 1A up-regulates GABA transporter expression by subcellular redistribution. *Mol Membr Biol,* **18,** 39-44.

78. Hu J and Quick MW (2008) Substrate-mediated regulation of gamma-aminobutyric acid transporter 1 in rat brain. *Neuropharmacology,* **54,** 309-318.

79. Ito K, Kidokoro K, Sezutsu H, Nohata J, Yamamoto K, Kobayashi I, Uchino K, Kalyebi A, Eguchi R, Hara W, Tamura T, Katsuma S, Shimada T, Mita K, and Kadono-Okuda K (2008) Deletion of a gene encoding an amino acid transporter in the midgut membrane causes resistance to a Bombyx parvo-like virus. *Proc Natl Acad Sci U S A,* **105,** 7523-7527.

80. Itouji A, Sakai N, Tanaka C, and Saito N (1996) Neuronal and glial localization of two GABA transporters (GAT1 and GAT3) in the rat cerebellum. *Brain Res Mol Brain Res,* **37,** 309-316.

81. Jardetzky O (1966) Simple allosteric model for membrane pumps. *Nature,* **211,** 969-970.

82. Jencks WP (1989) Utilization of binding energy and coupling rules for active transport and other coupled vectorial processes. *Methods Enzymol,* **171,** 145-164.

83. Kalayil S, Schulze S, and Kuhlbrandt W (2013) Arginine oscillation explains $Na^+$ independence in the substrate/product antiporter CaiT. *Proc Natl Acad Sci U S A.*

84. Kanner BI (2003) Transmembrane domain I of the gamma-aminobutyric acid transporter GAT-1 plays a crucial role in the transition between cation leak and transport modes. *J Biol Chem,* **278,** 3705-3712.

85. Kanner BI (2005) Molecular physiology: intimate contact enables transport. *Nature,* **437,** 203-205.

86. Kanner BI (2006) Structure and function of sodium-coupled GABA and glutamate transporters. *J Membr Biol,* **213,** 89-100.

87. Kanner BI and Zomot E (2008) Sodium-coupled neurotransmitter transporters. *Chem Rev,* **108,** 1654-1668.

88. Kantcheva AK, Quick M, Shi L, Winther AM, Stolzenberg S, Weinstein H, Javitch JA, and Nissen P (2013) Chloride binding site of neurotransmitter sodium symporters. *Proc Natl Acad Sci U S A,* **110,** 8489-8494.

89. Khafizov K, Perez C, Koshy C, Quick M, Fendler K, Ziegler C, and Forrest LR (2012) Investigation of the sodium-binding sites in the sodium-coupled betaine transporter BetP. *Proc Natl Acad Sci U S A,* **109,** E3035-E3044.

90. Kilic F and Rudnick G (2000) Oligomerization of serotonin transporter and its functional consequences. *Proc Natl Acad Sci U S A,* **97,** 3106-3111.

91. Klingenberg M (2005) When a common problem meets an ingenious mind. *EMBO Rep,* **6,** 797-800.

92. Kramer R (2009) Osmosensing and osmosignaling in *Corynebacterium glutamicum*. *Amino Acids,* **37,** 487-497.

93. Kramer R and Morbach S (2004) BetP of *Corynebacterium glutamicum*, a transporter with three different functions: betaine transport, osmosensing, and osmoregulation. *Biochim Biophys Acta,* **1658,** 31-36.

94. Krishnamurthy H and Gouaux E (2012) X-ray structures of LeuT in substrate-free outward-open and apo inward-open states. *Nature,* **481,** 469-474.

95. Krishnamurthy H, Piscitelli CL, and Gouaux E (2009) Unlocking the molecular secrets of sodium-coupled transporters. *Nature,* **459,** 347-355.

96. Krupka RM (1989) Role of substrate binding forces in exchange-only transport systems: I. Transition-state theory. *J Membr Biol,* **109,** 151-158.

97. Kusano K, Miledi R, and Stinnakre J (1982) Cholinergic and catecholaminergic receptors in the *Xenopus* oocyte membrane. *J Physiol,* **328,** 143-170.

98. Li LB, Chen N, Ramamoorthy S, Chi L, Cui XN, Wang LC, and Reith ME (2004) The role of N-glycosylation in function and surface trafficking of the human dopamine transporter. *J Biol Chem,* **279,** 21012-21020.

99. Liu QR, Lopez-Corcuera B, Mandiyan S, Nelson H, and Nelson N (1993) Molecular characterization of four pharmacologically distinct gamma-aminobutyric acid transporters in mouse brain [corrected]. *J Biol Chem,* **268,** 2106-2112.

100. Liu Y, Eckstein-Ludwig U, Fei J, and Schwarz W (1998) Effect of mutation of glycosylation sites on the Na+ dependence of steady-state and transient currents generated by the neuronal GABA transporter. *Biochim Biophys Acta,* **1415,** 246-254.

101. Liu Z, Stevens BR, Feldman DH, Hediger MA, and Harvey WR (2003) $K^+$ amino acid transporter KAAT1 mutant Y147F has increased transport activity and altered substrate selectivity. *J Exp Biol,* **206,** 245-254.

102. Lolkema JS and Slotboom DJ (2008) The major amino acid transporter superfamily has a similar core structure as Na+-galactose and $Na^+$-leucine transporters. *Mol Membr Biol,* **25,** 567-570.

103. Loo DD, Eskandari S, Boorer KJ, Sarkar HK, and Wright EM (2000) Role of $Cl^-$ in electrogenic $Na^+$-coupled cotransporters GAT1 and SGLT1. *J Biol Chem,* **275,** 37414-37422.

104. Loo DD, Hirayama BA, Meinild AK, Chandy G, Zeuthen T, and Wright EM (1999) Passive water and ion transport by cotransporters. *J Physiol,* **518 ( Pt 1),** 195-202.

105. Lopez-Corcuera B, Liu QR, Mandiyan S, Nelson H, and Nelson N (1992) Expression of a mouse brain cDNA encoding novel gamma-aminobutyric acid transporter. *J Biol Chem,* **267,** 17491-17493.

106. Lopez-Corcuera B, Nunez E, Martinez-Maza R, Geerlings A, and Aragon C (2001) Substrate-induced conformational changes of extracellular loop 1 in the glycine transporter GLYT2. *J Biol Chem,* **276,** 43463-43470.

107. LoTurco JJ, Owens DF, Heath MJ, Davis MB, and Kriegstein AR (1995) GABA and glutamate depolarize cortical progenitor cells and inhibit DNA synthesis. *Neuron,* **15,** 1287-1298.

108. Lu CC and Hilgemann DW (1999a) GAT1 ($GABA:Na^+:Cl^-$) cotransport function. Kinetic studies in giant Xenopus oocyte membrane patches. *J Gen Physiol,* **114,** 445-457.

109. Lu CC and Hilgemann DW (1999b) GAT1 ($GABA:Na^+:Cl^-$) cotransport function. Steady state studies in giant Xenopus oocyte membrane patches. *J Gen Physiol,* **114,** 429-444.

110. Ma D, Lu P, Yan C, Fan C, Yin P, Wang J, and Shi Y (2012) Structure and mechanism of a glutamate-GABA antiporter. *Nature,* **483,** 632-636.

111. MacAulay N, Zeuthen T, and Gether U (2002) Conformational basis for the Li(+)-induced leak current in the rat gamma-aminobutyric acid (GABA) transporter-1. *J Physiol,* **544,** 447-458.

112. Mager S, Cao Y, and Lester HA (1998) Measurement of transient currents from neurotransmitter transporters expressed in Xenopus oocytes. *Methods Enzymol,* **296,** 551-566.

113. Mager S, Kleinberger-Doron N, Keshet GI, Davidson N, Kanner BI, and Lester HA (1996) Ion binding and permeation at the GABA transporter GAT1. *J Neurosci,* **16,** 5405-5414.

114. Mager S, Naeve J, Quick M, Labarca C, Davidson N, and Lester HA (1993) Steady states, charge movements, and rates for a cloned GABA transporter expressed in *Xenopus* oocytes. *Neuron,* **10,** 177-188.

115. Mao Y, Mathewson L, Gesmonde J, Sato Y, Holy M, Sitte HH, and Rudnick G (2008) Involvement of serotonin transporter extracellular loop 1 in serotonin binding and transport. *Mol Membr Biol,* **25,** 115-127.

116. Margheritis E, Terova G, Cinquetti R, Peres A, and Bossi E (2013) Functional properties of a newly cloned fish ortholog of the neutral amino acid transporter BAT1 (SLC6A19). *Comp Biochem Physiol A Mol Integr Physiol,* **166,** 285-292.

117. Mari SA, Soragna A, Castagna M, Bossi E, Peres A, and Sacchi VF (2004) Aspartate 338 contributes to the cationic specificity and to driver-amino acid coupling in the insect cotransporter KAAT1. *Cell Mol Life Sci,* **61,** 243-256.

118. Mari SA, Soragna A, Castagna M, Santacroce M, Perego C, Bossi E, Peres A, and Sacchi VF (2006) Role of the conserved glutamine 291 in the rat gamma-aminobutyric acid transporter rGAT-1. *Cell Mol Life Sci,* **63,** 100-111.

119. Marsal J, Tigyi G, and Miledi R (1995) Incorporation of acetylcholine receptors and Cl-channels in *Xenopus* oocytes injected with *Torpedo* electroplaque membranes. *Proc Natl Acad Sci U S A,* **92,** 5224-5228.

120. Mathie A, Al-Moubarak E, and Veale EL (2010) Gating of two pore domain potassium channels. *J Physiol,* **588,** 3149-3156.

121. Meleshkevitch EA, Voronov DA, Miller MM, Penneda M, Fox JM, Metzler R, and Boudko DY (2013) A novel eukaryotic Na methionine selective symporter is essential for mosquito development. *Insect Biochem Mol Biol*.

122. Mertz JE and Gurdon JB (1977) Purified DNAs are transcribed after microinjection into *Xenopus* oocytes. *Proc Natl Acad Sci U S A,* **74,** 1502-1506.

123. Miller MM, Popova LB, Meleshkevitch EA, Tran PV, and Boudko DY (2008) The invertebrate B(0) system transporter, *D. melanogaster* NAT1, has unique D-amino acid affinity and mediates gut and brain functions. *Insect Biochem Mol Biol,* **38,** 923-931.

124. Miszner A, Peres A, Castagna M, Bettè S, Giovannardi S, Cherubino F, and Bossi E (2007) Structural and functional basis of amino acid specificity in the invertebrate cotransporter KAAT1. *J Physiol,* **581,** 899-913.

125. Mitchell P (1957) A general theory of membrane transport from studies of bacteria. *Nature,* **180,** 134-136.

126. Nelson H, Mandiyan S, and Nelson N (1990) Cloning of the human brain GABA transporter. *FEBS Lett,* **269,** 181-184.

127. Ochrombel I, Becker M, Kramer R, and Marin K (2011) Osmotic stress response in *C. glutamicum*: impact of channel- and transporter-mediated potassium accumulation. *Arch Microbiol,* **193,** 787-796.

128. Orsini F, Santacroce M, Arosio P, and Sacchi VF (2010) Observing *Xenopus laevis* oocyte plasma membrane by Atomic Force Microscopy. *Methods,* **51,** 106-113.

129. Ozaki N, Goldman D, Kaye WH, Plotnicov K, Greenberg BD, Lappalainen J, Rudnick G, and Murphy DL (2003) Serotonin transporter missense mutation associated with a complex neuropsychiatric phenotype. *Mol Psychiatry,* **8,** 895, 933-895, 936.

130. Pacheco-Alvarez D, Cristobal PS, Meade P, Moreno E, Vazquez N, Munoz E, Diaz A, Juarez ME, Gimenez I, and Gamba G (2006) The $Na^+$:$Cl^-$ cotransporter is activated and phosphorylated at the amino-terminal domain upon intracellular chloride depletion. *J Biol Chem,* **281,** 28755-28763.

131. Palmer LG (1987) Ion selectivity of epithelial Na channels. *J Membr Biol,* **96,** 97-106.

132. Penmatsa A and Gouaux E (2013) How LeuT shapes our understanding of the mechanisms of sodium-coupled neurotransmitter transporters. *J Physiol*.

133. Penmatsa A, Wang KH, and Gouaux E (2013) X-ray structure of dopamine transporter elucidates antidepressant mechanism. *Nature*.

134. Peres A and Bossi E (2000) Effects of pH on the uncoupled, coupled and pre-steady-state currents at the amino acid transporter KAAT1 expressed in *Xenopus* oocytes. *J Physiol,* **525 Pt 1,** 83-89.

135. Peres A, Giovannardi S, Bossi E, and Fesce R (2004) Electrophysiological insights into the mechanism of ion-coupled cotransporters. *News Physiol Sci,* **19,** 80-84.

136. Perez C, Khafizov K, Forrest LR, Kramer R, and Ziegler C (2011) The role of trimerization in the osmoregulated betaine transporter BetP. *EMBO Rep,* **12,** 804-810.

137. Perez C, Koshy C, Yildiz O, and Ziegler C (2012) Alternating-access mechanism in conformationally asymmetric trimers of the betaine transporter BetP. *Nature,* **490,** 126-130.

138. Perez-Siles G, Nunez E, Morreale A, Jimenez E, Leo-Macias A, Pita G, Cherubino F, Sangaletti R, Bossi E, Ortiz AR, Aragon C, and Lopez-Corcuera B (2011) An aspartate residue in the external vestibule of glycine transporter 2 (GLYT2) controls cation access and transport coupling. *Biochem J*.

139. Piscitelli CL, Krishnamurthy H, and Gouaux E (2010) Neurotransmitter/sodium symporter orthologue LeuT has a single high-affinity substrate site. *Nature,* **468,** 1129-1132.

140. Possee RD and Howard SC (1987) Analysis of the polyhedrin gene promoter of the *Autographa californica* nuclear polyhedrosis virus. *Nucleic Acids Res,* **15,** 10233-10248.

141. Preston GM, Carroll TP, Guggino WB, and Agre P (1992) Appearance of water channels in *Xenopus* oocytes expressing red cell CHIP28 protein. *Science,* **256,** 385-387.

142. Punta M, Forrest LR, Bigelow H, Kernytsky A, Liu J, and Rost B (2007) Membrane protein prediction methods. *Methods,* **41,** 460-474.

143. Quick M, Shi L, Zehnpfennig B, Weinstein H, and Javitch JA (2012) Experimental conditions can obscure the second high-affinity site in LeuT. *Nat Struct Mol Biol,* **19,** 207-211.

144. Quick M, Winther AM, Shi L, Nissen P, Weinstein H, and Javitch JA (2009) Binding of an octylglucoside detergent molecule in the second substrate (S2) site of LeuT establishes an inhibitor-bound conformation. *Proc Natl Acad Sci U S A,* **106,** 5563-5568.

145. Quick MW (2003) Regulating the conducting states of a mammalian serotonin transporter. *Neuron,* **40,** 537-549.

146. Quick MW, Hu J, Wang D, and Zhang HY (2004) Regulation of a gamma-aminobutyric acid transporter by reciprocal tyrosine and serine phosphorylation. *J Biol Chem,* **279,** 15961-15967.

147. Ressl S, Terwisscha van Scheltinga AC, Vonrhein C, Ott V, and Ziegler C (2009) Molecular basis of transport and regulation in the Na(+)/betaine symporter BetP. *Nature,* **458,** 47-52.

148. Reyes N, Ginter C, and Boudker O (2009) Transport mechanism of a bacterial homologue of glutamate transporters. *Nature,* **462,** 880-885.

149. Reyes N and Tavoulari S (2011) To be, or not to be two sites: that is the question about LeuT substrate binding. *J Gen Physiol,* **138,** 467-471.

150. Richerson GB and Wu Y (2003) Dynamic equilibrium of neurotransmitter transporters: not just for reuptake anymore. *J Neurophysiol,* **90,** 1363-1374.

151. Richerson GB and Wu Y (2004) Role of the GABA transporter in epilepsy. *Adv Exp Med Biol,* **548,** 76-91.

152. Risso S, Defelice LJ, and Blakely RD (1996) Sodium-dependent GABA-induced currents in GAT1-transfected HeLa cells. *J Physiol,* **490 ( Pt 3),** 691-702.

153. Rivera C, Voipio J, Payne JA, Ruusuvuori E, Lahtinen H, Lamsa K, Pirvola U, Saarma M, and Kaila K (1999) The $K^+/Cl^-$ co-transporter KCC2 renders GABA hyperpolarizing during neuronal maturation. *Nature,* **397,** 251-255.

154. Rohrmann GF (1986) Polyhedrin structure. *J Gen Virol,* **67 ( Pt 8),** 1499-1513.

155. Roux MJ and Supplisson S (2000) Neuronal and glial glycine transporters have different stoichiometries. *Neuron,* **25,** 373-383.

156. Rudnick G (2006) Structure/function relationships in serotonin transporter: new insights from the structure of a bacterial transporter. *Handb Exp Pharmacol,* 59-73.

157. Rudnick G (2011) Cytoplasmic permeation pathway of neurotransmitter transporters. *Biochemistry,* **50,** 7462-7475.

158. Salomons GS, van Dooren SJ, Verhoeven NM, Cecil KM, Ball WS, deGrauw TJ, and Jakobs C (2001) X-linked creatine-transporter gene (SLC6A8) defect: a new creatine-deficiency syndrome. *Am J Hum Genet,* **68,** 1497-1500.

159. Sanna E, Motzo C, Murgia A, Amato F, Deserra T, and Biggio G (1996) Expression of native GABA A receptors in *Xenopus* oocytes injected with rat brain synaptosomes. *J Neurochem,* **67,** 2212-2214.

160. Santacroce M, Castagna M, and Sacchi VF (2010) Passive water permeability of some wild type and mutagenized amino acid cotransporters of the SLC6/NSS family expressed in *Xenopus laevis* oocytes. *Comp Biochem Physiol A Mol Integr Physiol,* **156,** 509-517.

161. Santacroce M, Daniele F, Cremona A, Scaccabarozzi D, Castagna M, and Orsini F (2013) Imaging of *Xenopus laevis* Oocyte Plasma Membrane in Physiological-Like Conditions by Atomic Force Microscopy. *Microsc Microanal,* 1-6.

162. Sato Y, Zhang YW, ndroutsellis-Theotokis A, and Rudnick G (2004) Analysis of transmembrane domain 2 of rat serotonin transporter by cysteine scanning mutagenesis. *J Biol Chem,* **279,** 22926-22933.

163. Schmid JA, Just H, and Sitte HH (2001a) Impact of oligomerization on the function of the human serotonin transporter. *Biochem Soc Trans,* **29,** 732-736.

164. Schmid JA, Scholze P, Kudlacek O, Freissmuth M, Singer EA, and Sitte HH (2001b) Oligomerization of the human serotonin transporter and of the rat GABA transporter 1 visualized by fluorescence resonance energy transfer microscopy in living cells. *J Biol Chem,* **276,** 3805-3810.

165. Scholze P, Freissmuth M, and Sitte HH (2002) Mutations within an intramembrane leucine heptad repeat disrupt oligomer formation of the rat GABA transporter 1. *J Biol Chem,* **277,** 43682-43690.

166. Schulze S, Koster S, Geldmacher U, Terwisscha van Scheltinga AC, and Kuhlbrandt W (2010) Structural basis of Na(+)-independent and cooperative substrate/product antiport in CaiT. *Nature,* **467,** 233-236.

167. Schweikhard ES and Ziegler CM (2012) Amino acid secondary transporters: toward a common transport mechanism. *Curr Top Membr,* **70,** 1-28.

168. Shaikh SA, Li J, Enkavi G, Wen PC, Huang Z, and Tajkhorshid E (2013) Visualizing functional motions of membrane transporters with molecular dynamics simulations. *Biochemistry,* **52,** 569-587.

169. Shannon JR, Flattem NL, Jordan J, Jacob G, Black BK, Biaggioni I, Blakely RD, and Robertson D (2000) Orthostatic intolerance and tachycardia associated with norepinephrine-transporter deficiency. *N Engl J Med,* **342,** 541-549.

170. Shi L, Quick M, Zhao Y, Weinstein H, and Javitch JA (2008) The mechanism of a neurotransmitter:sodium symporter: inward release of $Na^+$ and substrate is triggered by substrate in a second binding site. *Mol Cell,* **30,** 667-677.

171. Sigel E and Minier F (2005) The *Xenopus* oocyte: system for the study of functional expression and modulation of proteins. *Mol Nutr Food Res,* **49,** 228-234.

172. Singh SK, Piscitelli CL, Yamashita A, and Gouaux E (2008) A competitive inhibitor traps LeuT in an open-to-out conformation. *Science,* **322,** 1655-1661.

173. Singh SK, Yamashita A, and Gouaux E (2007) Antidepressant binding site in a bacterial homologue of neurotransmitter transporters. *Nature,* **448,** 952-956.

174. Sitte HH, Singer EA, and Scholze P (2002) Bi-directional transport of GABA in human embryonic kidney (HEK-293) cells stably expressing the rat GABA transporter GAT-1. *Br J Pharmacol,* **135,** 93-102.

175. Smith GE, Summers MD, and Fraser MJ (1983) Production of human beta interferon in insect cells infected with a baculovirus expression vector. *Mol Cell Biol,* **3,** 2156-2165.

176. Soragna A, Bossi E, Giovannardi S, Pisani R, and Peres A (2005) Functionally independent subunits in the oligomeric structure of the GABA cotransporter rGAT1. *Cell Mol Life Sci,* **62,** 2877-2885.

177. Soragna A, Mari SA, Pisani R, Peres A, Castagna M, Sacchi VF, and Bossi E (2004) Structural domains involved in substrate selectivity in two neutral amino acid transporters. *Am J Physiol Cell Physiol,* **287,** C754-C761.

178. Sorkina T, Doolen S, Galperin E, Zahniser NR, and Sorkin A (2003) Oligomerization of dopamine transporters visualized in living cells by fluorescence resonance energy transfer microscopy. *J Biol Chem,* **278,** 28274-28283.

179. Sutcliffe JS, Delahanty RJ, Prasad HC, McCauley JL, Han Q, Jiang L, Li C, Folstein SE, and Blakely RD (2005) Allelic heterogeneity at the serotonin transporter locus (SLC6A4) confers susceptibility to autism and rigid-compulsive behaviors. *Am J Hum Genet,* **77,** 265-279.

180. Tian J, Thomsen GH, Gong H, and Lennarz WJ (1997) *Xenopus* Cdc6 confers sperm binding competence to oocytes without inducing their maturation. *Proc Natl Acad Sci U S A,* **94,** 10729-10734.

181. Vincenti S, Castagna M, Peres A, and Sacchi VF (2000) Substrate selectivity and pH dependence of KAAT1 expressed in *Xenopus laevis* oocytes. *J Membr Biol,* **174,** 213-224.

182. Volkman LE and Summers MD (1977) *Autographa californica* nuclear polyhedrosis virus: comparative infectivity of the occluded, alkali-liberated, and nonoccluded forms. *J Invertebr Pathol,* **30,** 102-103.

183. Wagner CA, Friedrich B, Setiawan I, Lang F, and Broer S (2000) The use of *Xenopus laevis* oocytes for the functional characterization of heterologously expressed membrane proteins. *Cell Physiol Biochem,* **10,** 1-12.

184. Wagner S, Castel M, Gainer H, and Yarom Y (1997) GABA in the mammalian suprachiasmatic nucleus and its role in diurnal rhythmicity. *Nature,* **387,** 598-603.

185. Wagner S, Sagiv N, and Yarom Y (2001) GABA-induced current and circadian regulation of chloride in neurones of the rat suprachiasmatic nucleus. *J Physiol,* **537,** 853-869.

186. Waight AB, Love J, and Wang DN (2010) Structure and mechanism of a pentameric formate channel. *Nat Struct Mol Biol,* **17,** 31-37.

187. Wang D, Deken SL, Whitworth TL, and Quick MW (2003) Syntaxin 1A inhibits GABA flux, efflux, and exchange mediated by the rat brain GABA transporter GAT1. *Mol Pharmacol,* **64,** 905-913.

188. Wang D and Quick MW (2005) Trafficking of the plasma membrane gamma-aminobutyric acid transporter GAT1. Size and rates of an acutely recycling pool. *J Biol Chem,* **280,** 18703-18709.

189. Wang H, Goehring A, Wang KH, Penmatsa A, Ressler R, and Gouaux E (2013) Structural basis for action by diverse antidepressants on biogenic amine transporters. *Nature,* **503,** 141-145.

190. Weyand S, Shimamura T, Beckstein O, Sansom MS, Iwata S, Henderson PJ, and Cameron AD (2011) The alternating access mechanism of transport as observed in the sodium-hydantoin transporter Mhp1. *J Synchrotron Radiat,* **18,** 20-23.

191. Weyand S, Shimamura T, Yajima S, Suzuki S, Mirza O, Krusong K, Carpenter EP, Rutherford NG, Hadden JM, O'Reilly J, Ma P, Saidijam M, Patching SG, Hope RJ, Norbertczak HT, Roach PC, Iwata S, Henderson PJ, and Cameron AD (2008) Structure and molecular mechanism of a nucleobase-cation-symport-1 family transporter. *Science,* **322,** 709-713.

192. White SH (2009) Biophysical dissection of membrane proteins. *Nature,* **459,** 344-346.

193. Woo NS, Lu J, England R, McClellan R, Dufour S, Mount DB, Deutch AY, Lovinger DM, and Delpire E (2002) Hyperexcitability and epilepsy associated with disruption of the mouse neuronal-specific K-Cl cotransporter gene. *Hippocampus,* **12,** 258-268.

194. Wu Y, Wang W, Diez-Sampedro A, and Richerson GB (2007) Nonvesicular inhibitory neurotransmission via reversal of the GABA transporter GAT-1. *Neuron,* **56,** 851-865.

195. Wu Y, Wang W, and Richerson GB (2006) The transmembrane sodium gradient influences ambient GABA concentration by altering the equilibrium of GABA transporters. *J Neurophysiol,* **96,** 2425-2436.

196. Yamashita A, Singh SK, Kawate T, Jin Y, and Gouaux E (2005) Crystal structure of a bacterial homologue of Na(+)/Cl(-)-dependent neurotransmitter transporters. *Nature,* **437,** 215-223.

197. Yan XX and Ribak CE (1998) Developmental expression of gamma-aminobutyric acid transporters (GAT-1 and GAT-3) in the rat cerebellum: evidence for a transient presence of GAT-1 in Purkinje cells. *Brain Res Dev Brain Res,* **111,** 253-269.

198. Yernool D, Boudker O, Jin Y, and Gouaux E (2004) Structure of a glutamate transporter homologue from Pyrococcus horikoshii. *Nature,* **431,** 811-818.

199. Yuste R and Katz LC (1991) Control of postsynaptic $Ca^{2+}$ influx in developing neocortex by excitatory and inhibitory neurotransmitters. *Neuron,* **6,** 333-344.

200. Zerangue N, Schwappach B, Jan YN, and Jan LY (1999) A new ER trafficking signal regulates the subunit stoichiometry of plasma membrane K(ATP) channels. *Neuron,* **22,** 537-548.

201. Zhou Y, Bennett ER, and Kanner BI (2004) The aqueous accessibility in the external half of transmembrane domain I of the GABA transporter GAT-1 Is modulated by its ligands. *J Biol Chem,* **279,** 13800-13808.

202. Zhou Y and Kanner BI (2005) Transporter-associated currents in the gamma-aminobutyric acid transporter GAT-1 are conditionally impaired by mutations of a conserved glycine residue. *J Biol Chem,* **280,** 20316-20324.

203. Zhou Y, Zomot E, and Kanner BI (2006) Identification of a lithium interaction site in the gamma-aminobutyric acid (GABA) transporter GAT-1. *J Biol Chem,* **281,** 22092-22099.

204. Zhou Z, Zhen J, Karpowich NK, Goetz RM, Law CJ, Reith ME, and Wang DN (2007) LeuT-desipramine structure reveals how antidepressants block neurotransmitter reuptake. *Science,* **317,** 1390-1393.

205. Zhou Z, Zhen J, Karpowich NK, Law CJ, Reith ME, and Wang DN (2009) Antidepressant specificity of serotonin transporter suggested by three LeuT-SSRI structures. *Nat Struct Mol Biol,* **16,** 652-657.

206. Ziegler C, Bremer E, and Kramer R (2010) The BCCT family of carriers: from physiology to crystal structure. *Mol Microbiol,* **78,** 13-34.

207. Zomot E, Bendahan A, Quick M, Zhao Y, Javitch JA, and Kanner BI (2007) Mechanism of chloride interaction with neurotransmitter:sodium symporters. *Nature,* **449,** 726-730.

# Appendix

## Publications

**2012**

1. Article
   Giovanola M, D'Antoni F, Santacroce M, Mari SA, Cherubino F, Bossi E, Sacchi VF, Castagna M.
   *Role of a conserved glycine triplet in the NSS amino acid transporter KAAT1.*
   Biochim Biophys Acta. 2012 Jul;1818(7):1737-44.

2. Abstract National Congress of the Italian Physiological Society (Verona, 2012)
   M. Giovanola, M. Santacroce, V.F. Sacchi, M. Castagna.
   *Molecular determinants of chloride dependence of the SLC6 amino acid transporter KAAT1*
   Acta physiologica.206:Suppl.692(2012)

**2011**

1. Abstract National Congress of the Italian Physiological Society (Sorrento, 2011)
   F. D'Antoni, M. Giovanola, M. Santacroce, S.A. Mari, E. Bossi, V.F. Sacchi, M. Castagna
   *The role of the highly conserved Glycines (85-87) in the function of the neutral amino acid transporter KAAT1*
   Acta physiologica.203:Suppl.688(2011)

**2010**

1. Abstract National Congress of the Italian Physiological Society (Varese, 2010)
   M. Castagna, M. Santacroce, M. Giovanola, E. Bossi, S.A Mari, F. Cherubino, R. Sangaletti, V.F. Sacchi
   *Defining the role of a highly conserved domain in SLC6//NSS family of transporters: the insect homologue KAAT1 as a tool.*
   Acta physiologica.200:Supplement 681(2010)

## Communications to national or international congresses

**2013**

1. 7th Annual meeting of Young Researcher in Physiology of the Italian Physiological Society, Anacapri (NA), Italy, *oral presentation*
2. 64th Annual National Congress of the Italian Physiological Society, Portonovo (AN), Italy, *poster*
3. 6th SBF35 Symposium Transmembrane Transporters in Health and Disease, Vienna, *poster*

**2012**

1. 63rd Annual National Congress of the Italian Physiological Society, Verona, Italy, *poster*
2. 3rd International Workshop on Expression, Structure and Function of Membrane Proteins Florence, Italy, *poster*

**2011**

1. 62nd Annual National Congress of the Italian Physiological Society, Sorrento, Italy, *poster*
2. 5th Annual meeting of Young Researcher in Physiology of the Italian Physiological Society, Sestri Levante (GE), Italy, *poster*
3. 4th SBF35 Symposium Transmembrane Transporters in Health and Disease, Vienna, *poster*

**2010**

1. 61st Annual National Congress of the Italian Physiological Society, Varese, Italy, *poster*

## International Schools

**2011**

International School of Biophysics "A. Borsellino", 41st Course: Channels and Transporters, Erice (TP), Italy

## Visiting scientist

Visiting Ph.D. student (March-October 2012) in the laboratory of Professor Christine Ziegler at the Department of Structural Biology of Max Planck Institute of Biophysics, Max-von-Laue-Straße 3, D-60438 Frankfürt am Main, Germany.

## Teaching and tutoring activities

1. Taught three sessions of Physiology Laboratory for students of Pharmaceutical Biotechnologies at the School of Pharmacy, *Università degli Studi di Milano* (Academic years from 2010-2011 to 2012-2013).

2. Provided scientific tutoring for graduating student in Pharmaceutical Biotechnologies at the Department of Pharmacological and Biomolecular Sciences, *Università degli Studi di Milano.*

3. Assistant supervisor of two Bachelor degree thesis in Pharmaceutical Biotechnologies:

   - *Structure/function analysis of KAAT1 Na2 sodium binding site.*
     (Thesis in Italian; Academic Year 2012-2013);
   - *Functional expression in Xenopus oocytes of the transporter Nramp1 and Nramp2 from Dictyostelium discoideum.*
     (Thesis in Italian; Academic Year 2012-2013).

## Attended lectures and seminars

**2013**

**Omega-3 PUFA alter lipid raft organization in colon and breast cancer cells** (Dr. P. Corsetto), 01/25/2013, Department of Pharmacological and Biomolecular Sciences, *Università degli Studi di Milano.*

**Critical and time-dependent role of the GPR17 receptor during oligodendrocyte maturation: implications for demyelinating diseases** (Dr. M. Fumagalli), 03/22/2013, Department of Pharmacological and Biomolecular Sciences, *Università degli Studi di Milano.*

**Malaria acute respiratory distress syndrome (MA-ARDS): modification of the lipid profile, antioxidant defenses and cytokine content in different tissues** (Dr. D. Scaccabarozzi) 07/12/2013, Department of Pharmacological and Biomolecular Sciences, *Università degli Studi di Milano.*

**Synaptic availability of NMDA receptors: from physiological mechanisms to pathology** (Dr. J. Stanic), 09/18/2013, Department of Pharmacological and Biomolecular Sciences, *Università degli Studi di Milano.*

2012

**Probiotics and probiogenomics** (dr. M. Ventura), 01/20/2012, *Università degli Studi di Milano.*

**Deciphering and re-designing interaction specificity among signaling proteins** (Prof. Dr. M. Kosloff), 03/13/2012, Max Planck Institute of Biophysics, Frankfürt am Main, Germany.

**Role of the Sec61 translocon during polytopic membrane protein folding** (Prof. Dr. W. R. Skach, 04/11/2012, Max Planck Institute of Biophysics, Frankfürt am Main, Germany.

**Structural determinants of TRPV channel activation and desensitization** (Prof. R. Gaudet), 04/26/2012, Max Planck Institute of Biophysics, Frankfürt am Main, Germany.

**Molecular function and cellular regulation of cocaine-sensitive neurotransmitter transporters** (Prof. Dr. Ulrik Gether), 05/09/2012, Max Planck Institute of Biophysics, Frankfürt am Main, Germany.

**Dissecting molecular mechanism of glutamate transporter using a bacterial homologue** (Prof. Dr. Joe Mindell), 05/10/2012, Max Planck Institute of Biophysics, Frankfürt am Main, Germany.

**Diffraction before destruction: imaging macromolecules with x-rays laser** (Prof. Dr. H. Chapam), 05/23/2012, Max Planck Institute of Biophysics, Frankfürt am Main, Germany.

**Multi-scale simulation of processes in membrane proteins and biomembranes: methods and applications** (Prof. Dr. Qiang Cui), 08/30/2012, Max Planck Institute of Biophysics, Frankfürt am Main, Germany

2011

**Cellular biology of Epithelia**, 05/26/2011, Symposium at *Università degli Studi di Milano.*

**Thermoregulation and fever**, 05/31/2011, International short course at *Università degli Studi di Milano.*

**Electrophysiological techniques: applications in both basic and clinical research**, 07/06/2011, *Università degli Insubria.*

**Integrating synaptic plasticity into the hippocampal circuit** (prof. S. Siegelbaum), 10/05/2011, *Università degli Studi di Milano.*

**Novel approaches in the immunotherapy of tumors** (dr. M. Rescigno), 11/29/2011, *Università degli Studi di Milano.*